EFFECTS OF SYSTEM FILTRATION CHARACTERISTICS ON TRIBOLOGICAL WEAR OF ROTATING ELEMENTS

By

ING-TSANN HONG

Bachelor of Science
National Central University
Chungli, Taiwan
1974

Master of Science
Oklahoma State University
Stillwater, Oklahoma
1980

Submitted to the faculty of the Graduate College
of the Oklahoma State University
in partial fulfillment of the requirements
for the degree of
DOCTOR OF PHILOSOPHY
December, 1983

Thesis
1983D
H772e
Cop. 2

OKLAHOMA STATE UNIVERSITY LIBRARY

EFFECTS OF SYSTEM FILTRATION CHARACTERISTICS

ON TRIBOLOGICAL WEAR OF

ROTATING ELEMENTS

Thesis Approved:

Thesis Adviser

Dean of the Graduate College

1193238

© Copyright

by

Ing-Tsann Hong

December, 1983

PREFACE

The author wishes to express his deepest appreciation to his major adviser and graduate committee chairman, Dr. E. C. Fitch, for his guidance, patience, and understanding throughout the graduate program and dissertation.

Appreciation is also extended to other members of my advisory committee for their advice and encouragement; to Dr. L. Broemeling, Dr. C. E. Price, Dr. B. Kaftanoglu, and Dr. R. Taylor.

Gratitude is expressed to the 15 companies who supported and sponsored the Technology Development Project entitled "An Updated Multipass Filtration Theory". Special thanks to the American Committee Program of the Filtration Society for their donation of a research grant in supporting this dissertation. Their encouragement was valuable to this research.

I have had the unique opportunity to work with an outstanding group of colleagues in the Fluid Power Research Center. I wish to thank them for their willing cooperation and assistance in this study. Especially, Mr. T. Ito and Mr. I. Kalial deserve thanks for their assistance in the experimental verification phase. Thanks are also to Robert Hagar for his professional assistance in providing the drafting and artwork for this thesis.

Special gratitude is expressed to Mrs. Jane and Miss Janie Remnsnider for their patience, editing, proofreading, and encouragement during the preparation of this manuscript. Thanks are also expressed to Mrs. Evelyn

Norvelle for her careful typing.

My sincerest appreciation is expressed to my parents and other family members, without whose support and understanding this undertaking would have been impossible.

Most of all, I thank my wife, Li Jane, and son Andrew, for their understanding, encouragement and many sacrifices.

TABLE OF CONTENTS

LIST OF TABLES

LIST OF FIGURES

NOMENCLATURE

a	filter characteristic process constant
c	radial clearance
d_c	cutting depth
d_i	indentation depth
dp	particle size
ds	side length of prism square
e	eccentricity of the shaft
$f_f(x)$	density function of filter pore size distribution
$f_p(x)$	density function of particle size distribution
h	film thickness
h max	maximum film thickness
h min	minimum film thickness
l	sliding distance
Ndp	particle concentration of size dp
p	local pressure within the fluid film
s	filter time scaling constant
sp	particle size scaling constant
w	total abrasive wear rate
w_{dp}	wear rate caused by particle of size dp
w_e	external load
x	coordinate
y	coordinate perpendicular to x

E	particle separation efficiency
F	external force on a single particle
F_c	cutting force of a single particle
L	diagonal length of prism square
L_j	journal length
N	rotation speed
Nc,dp	the inversely cumulative concentration of particle size greater than dp
Nd	cumulative particle concentration of size greater than the dp at downstream of filter
No,dp	initial value of Nc,dp
Nu	cumulative particle concentration of size greater than dp at upstream of filter
Q	flow rate pass through the bearing
R	journal radius
S	Sommerfeld number
S_t	material tension yield stress
T	filter characteristic time constant
U	surface velocity
$W(t)$	accumulative wear rate at time t
α	particle inclination angle relative to moving surface
β	Beta filtration ratio
β'	Beta Prime filtration ratio
γ	rake angle
ε	eccentricity ratio
η	absolute viscosity of lubricant
θ	rotation angle
μ	coefficient of friction

σ_{ii}	principle stress along direction i
σ_{ij}	shear stress parallel to plane ij
τ_h	material shear yield stress of harder surface
τ_s	material shear yield stress of softer surface

CHAPTER I

INTRODUCTION

A rotating element is a general term that can be applied to a bearing in which the relative motion between the bearing surfaces is rotation. Thus a rotating element can be either a journal bearing or a thrust bearing or a combination of both. The formation of oil pressure in the bearing can be through hydrostatic or hydrodynamic action. This research will concentrate on a journal form of rotating element bearing in which only hydrodynamic action occurs.

Essentially, a rotating element consists of two components: the journal, which is the inner cylindrical member, and the bearing, which is the surrounding shell. By means of the rotating action and an eccentricity, the journal usually transfers the load to the bearing. This mechanism plays a vital role in industrial application. Within almost all mechanical systems there exists a journal bearing of some form.

Wear is the phenomenon of undesired material removal. It may occur both mechanically (abrasion, adhesion, fatigue) and chemically (corrosion). Excluding the chemical process, wear can be stated as the progressive loss of material from the operating surface of a body occurring as a result of relative motion at the surface (1). Consequentially, wear is unavoidable whenever there is a relative motion between two surfaces in contact. In order to reduce the damage caused by wear, lubricants are normally introduced to separate critical surfaces and hence prevent direct contact.

In most applications, the surfaces between a rotating journal and the bearing are separated by a hydrodynamic fluid film which is generated and maintained by the viscous drag of the mating surfaces. The degree of protection depends on the bearing characteristic number, namely the Sommerfeld number, which is a function of the fluid viscosity, rotation speed, load, pressure and geometry. Theoretically, a properly designed journal bearing assembly provides a fluid film thick enough to protect the surfaces under normal operating conditions. As a result, no short time mechanical induced wear occurs under steady state because of this thick film. However, wear can occur on the start/stop condition. Furthermore, if the lubricating oils contain abrasive particles with size compatible to the critical film thickness, wear can be induced. Thus, machine performance degradation follows.

The demand for improved machine longevity performance indicated by operating accuracy, reliability, and service life has made designers become more aware of the damage caused by entrained contaminants between precision moving surfaces. To reduce tribological failures resulting from such damage, filters are used in the system to remove damaging particles from circulating fluid and thus, protect components from contaminant abrasion.

Throughout industry, system designers and users have overlooked the significance of having proper filtration to avoid either overdesigning or underdesigning a critical component. They have, however, recognized the impossibility of achieving absolute removal of all particles from the fluid and become resigned to some contaminant level. However, designers realize that some filters are more efficient than others. However, designers usually depend on their individual experience to size

a filter for the system. Such "know-how" assessment normally cannot provide an effective and accurate way to control system contamination level to meet specific cleanliness requirements. Inevitable failures still continue due to their 'ad hoc' practice. The reason for these failures stem from the fact that there is insufficient knowledge concerning the filtration phenomena available at present.

It can be seen from the above that the performance of tribological elements depends not only on the lubrication mechanism but also on the filtration process. Thus, for a system designer, an understanding of the tribo-filtration phenomenon, namely, lubrication, wear, and filtration, will allow an adequate design to ensure the function of a system. On the other hand, the user will benefit from this knowledge by having the ability to correctly select the tribological elements required to prolong existing system reliability and service life. Accordingly, there has been great interest expressed in an investigation of the combination phenomena of both the degree of filtration that a specific filter may provide and the relative severity of wear reflected by critical elements protected by the filter.

This dissertation presents the theoretical development of an updated filtration model, called the "Beta Prime" and a reclamation wear model. In addition, the hydrodynamic lubrication mechanism of a journal bearing is comprehensively investigated. Based on the above rationales, a tribo-filtration performance model is formulated to predict the wear behavior of rotating elements in terms of system filtration characteristics. Experimental work has been conducted to validate the developed models.

The remainder of this dissertation presents and discusses the

results of the entire research program. Chapter II reviews previous related investigations in the area of lubrication, wear, and filtration. The theoretical development of the tribo-filtration model is presented in Chapter III. Chapters IV, V, and VI illustrate the experimental verification of the developed models. Chapter VII delineates the application of results obtained from this research and recommends further studies. Finally, Chapter VIII provides a summary and conclusions of this study. The Appendix contains the development and application of the Monte Carlo method used for simulating the filtration and tribo-filtration process.

CHAPTER II

PREVIOUS INVESTIGATIONS

The performance degradation of an operating machine due to the effects of entrained abrasive particles in the lubrication system has been recognized by machine operators and system designers for a long time. The realization of this problem has over the past two decades brought about a considerable amount of research in the areas of lubrication, wear, and filtration. A thorough search of the previous literature has revealed that many investigations have been conducted related to the disciplines of lubrication, wear, and filtration. However, very little research on tribo-filtration phenomenon is addressed in the literature.

This chapter reviews the previous research relating to tribology and filtration. It forms the theoretical basis of developing the tribo-filtration model in Chapter III.

Lubrication

The use of lubricants to reduce the friction of rotating bearings is not new. It, at least, dates back to when ancient Egyptians greased the chariot wheels and axles with tallow. However, the scientific studies of lubrication began in the ninteenth century. Historically, at the beginning of the ninteenth century, the investigation of lubrication was based on the knowledge of friction processes. Nevertheless, it moved into the development of fluid film lubrication in the middle of the last century.

Dowson (2) indicated that two major reasons influenced this transition: a new source of lubricant, mineral oil which almost entirely replaced the animal and vegetable oils and the energetic growth of the machine age in general and the railway in particular. This transition stimulated the studies of lubrication.

The discovery and development of fluid film lubrication brought a widespread use of bearings in industrial application. The function of a bearing is to promote smooth relative motion at a low friction between solid surfaces (3). The journal and bearing are separated with a fluid film, thus, reducing the damage due to surface contact.

It is well known that the continuous fluid film separating the bearing surfaces can be generated and maintained either hydrodynamically or hydrostatically. In the hydrodynamic lubrication mode, the fluid film is created by the viscous drag of the surfaces themselves. In contrast, to the self-acting case, a hydrostatic bearing is externally pressurized. The film is generated by an external pressure source that forces the lubricant between bearing surfaces.

Most early work on lubrication study was devoted to journal bearings. In 1883, Petrov (4) initiated the first theoretical approach to show how the friction of a bearing could be related to fluid viscosity. He indicated that the fluid lubricating characteristic under constant temperature was generated by viscosity rather than density. This innovative finding brought the research of lubrication into a new discipline. Petrov applied Newton's law of viscosity to the hydrodynamic principle of a rotating concentric journal, and found that the friction force between bearing surfaces could be formulated in terms of viscosity, surface velocity of the journal, and the mean effective film thickness. Petrov's

equation is still valid today for light load bearings.

About the same time, Mr. Beauchamp Tower (5) in England was independently investigating the friction mechanism of the journal of a railway car wheel, and accidently discovered the hydrodynamic pressure characteristics in oil films in the journal bearing. The achievement of Tower's work set both the experimental and conceptual basis for analyzing the lubrication mechanism of a journal bearing.

After analyzing Tower's experimental results, Professor Osborn Reynolds applied the principles of fluid mechanics and found that the results can be well explained. In 1886, Reynolds (6) formulated a mathematical foundation to analyze the function of hydrodynamic lubrication. This was the now well known Reynolds equation. This equation will be discussed in Chapter III.

The Reynolds equation indicates that there are three major parameters which contribute to the generation of a sufficient pressure to carry the load. These parameters are the wedge, stretch, and squeeze effects. As a result of the pressure formation, the bearing surfaces are separated and hydrodynamic lubrication is achieved.

At the beginning of the twentieth century, Stribeck (9) carried out many experiments in studying the effects of operating variables on the friction and lubrication of bearings. At the same time (1904), Sommerfeld (10) using a subtle substitution solved the Reynolds equation and compared the theoretical results with the experimental results obtained by Stribeck. This work correlated the coefficient of friction of a given bearing with fluid viscosity, journal rotation speed and load. A graphical representation of the Stribeck curve is illustrated in Figure 1. It should be noted that there are three lubrication regimes that can be distinguished, based

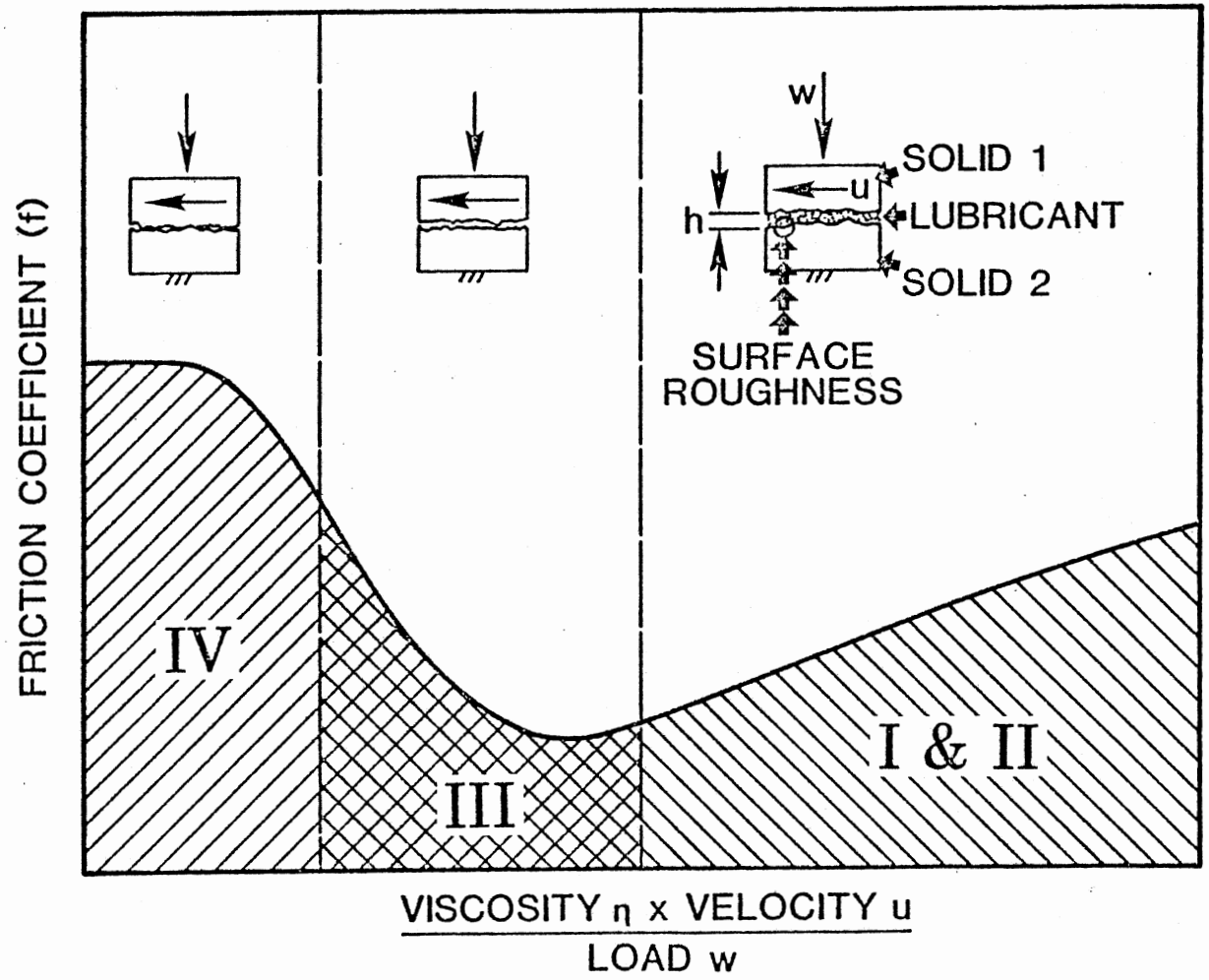

Figure 1. Stribeck Curve and Lubrication Regimes

on the fluid film thickness, h, and the bearing surface roughness, r. They are

1. Hydrodynamic lubrication ($h \gg r$)
2. Mixed lubrication ($h = r$)
3. Boundary lubrication ($h \sim 0$)

Hydrodynamic lubrication is maintained as long as the continuous fluid film thickness is much larger than the surface roughness. Normally, hydrodynamic lubrication exists if the film thickness ratio, the ratio of film thickness to surface roughness, is greater than five. In engineering practice the upper limit of 100 for this ratio is seldom exceeded. Thus the film thickness ratio of hydrodynamic action ranges from 5 to 100 (11, 12). Within this range, oil film pressure is formed and load supported. Theoretically, no wear can take place in this regime. This characteristic is of tribological significance in the investigation of the tribo-filtration phenomenon.

In the boundary lubrication regime, the fluid film thickness basically does not exist. There is direct contact between solid surfaces. Obviously, the wear process is governed by the chemical nature at the surface interface and the lubricant, and the surface property of the bearing.

Mixed lubrication clearly exists between the hydrodynamic lubrication and boundary lubrication. The load is partially supported by the oil film pressure and partially by the contact of surfaces. The lubrication mechanism is extremely complicated in this regime.

It is surprising that there are no major papers published regarding new principles for lubrication since Reynolds developed the fluid film equation. For almost one century, the general trend in lubrication study appears to be a search for an effective numerical method to solve the

Reynolds equation for specific problems of interest. Especially, as in the past three decades, due to the fact that the use of computers has become widespread.

Up to this point, theoretically, the wear of a rotating element can be well controlled through the application of the hydrodynamic theory. Regardless of applying the surface separation mechanisms, wear still takes place between bearing surfaces. The question to be answered is why?

Excluding the chemical influence and surface fatigue, the wear process in the hydrodynamic lubricating condition changes from surface to surface contact to abrasion caused by the external entrained abrasive particles.

After World War II, the new trend in machine design was to improve the accuracy and reliability of an operating system. This led to a reduction in film thickness. By virtue of this abrasive wear between precision surfaces, once trivial, became important. The reason for this particulate matter which originally passed between the bearing surfaces now interacted with them. This process has received increasing attention from most tribologists since the 1960's. The next section will review some related research regarding abrasive wear.

Wear

Wear is the process of unwanted material removal. The study of wear behavior has been a practical interest for several decades. However, the systematic investigation of wear phenomena did not receive much attention from tribologists until the end of World War II.

To have a better understanding of wear process, researchers classified wear into many categories. Nevertheless, due to the inherently complex

process of wear, no common classification exists up until now. From the standpoint of wear mechanism, normally, at least four wear mechanisms can be summarized as follows (7, 15, 16, 17):

1. Adhesive wear
2. Abrasive wear
3. Corrosive wear
4. Fatigue wear

Adhesive wear occurs if there is solid surface to surface contact. Material is transferred from one surface to another during relative motion. This wear behavior mainly depends on the material characteristic of contacting surfaces, surface roughness, and fluid lubricity.

Abrasive wear is caused by the plowing action of a hard particle or asperity abrading on a softer surface. Normally, it includes two mechanisms: two-body abrasion and three-body abrasion. In two-body abrasive wear, a rough hard surface slides against a softer surface. In three-body type, abrasion is caused by the entrained abrasive particles sliding between rubbing surfaces. The particle may embed on the softer surface and functions as a cutting tool to abrade the harder surface.

Corrosive wear is the process in which a chemical reaction with the environment predominates. It depends on the environmental parameters and the chemical property of lubricant.

According to the fatigue theory of wear, failure takes place due to the cyclic stress variation. In the past, fatigue has been considered as a minor mechanism to cause wear. However, recently it has become a significant factor in explaining the wear process; especially, if the wear material is elastic, or the reaction force is cyclic.

In addition to the above classification of wear mechanism, wear can

also be classified, according to the lubrication condition, as an unlubricated wear process or a lubricated wear process. In the unlubricated process, the wearing surface is not wetted by oils or other lubricating fluids. In the latter case there are lubricating fluids between the surfaces that have relative motion. The tribological wear behavior of a hydrodynamically lubricated rotating element, the subject studied in this research, falls into the category of the lubricated, three-body, abrasive wear.

At present, no consistent theory of lubricated wear has been developed. The reason stems from the fact that the introduction of a lubricant into the tribological systems dramatically complicates the analysis of wear mechanism. The operating condition, fluid property, and environmental factors have to be considered. Furthermore, the three-body wear process, normally, encompasses both the indentation and abrasion mechanism; further complicating a theoretical analysis. As a result, there is a general reluctance of tribologists to devote themselves to the investigation of a lubricated, three-body wear. However, the lubricated, three-body wear is one of the major wear mechanisms in engineering practice. Therefore, it is of prime importance to investigate this process.

Although the mechanism of the lubricated wear and unlubricated wear is different, some of the basic principles are applicable to both cases. Consequently, it is believed that a brief review of the relevent subjects on the unlubricated wear would provide a strong background in developing the lubricated wear model.

Both the two-body and the three-body abrasive wear in an unlubricated condition have been investigated by many researchers (18, 19, 20, 21, 22). From these findings, it was realized that the abrasive wear depends on a

great number of variables. However, from the standpoint of contaminant control, the component hardness, abrasive particle size, and contaminant concentration are the major factors in governing the wear process.

Primarily, the study of the abrasion mechanism was initiated by examining the wear behavior of a solid surface sliding on emery paper. The main objective was to investigate the wear resistance of metal to the abrasive particles. Khrushchov (23) found a direct relationship between wear resistance and hardness of metal. He indicated that for a given steel which has been heat treated, the slope of the wear resistance to the hardness was lower than that for pure metals. Recently, Murray (24) postulated that the relationship between abrasion resistance and metal hardness was not linear. The discrepancy was claimed to be due to the effect of the attack angle of contacting abrasive particles.

The effect of particle size on wear rate has received more attention as compared to any other factor. This is probably due to it presenting a physical approach for the calculation of the wear rate relating to known operating conditions. Normally, the wear models were developed by assuming either a conical (19, 22, 25) or a wedge (26, 27) shape particle. The experimental results showed that the wear increases with the particle size up to some critical diameters, in general, in the region from 50 micrometers to 80 micrometers, and then either slowly increases with the particle size or remaining constant. Rabinowicz (25) stated that the critical diameter effects are due to the interference between the abrasive process and the adhesive wear process. However, Larsen-Badse (28) postulates that this phenomenon is caused by the specimen size, since different lengths of an abrasive particle have a different effect on the deterioration with different grit size.

It would seem logical that with more abrasive particles in the system, a higher wear rate would be obtained, because the component surface has a higher probability of damage by the particles. This implies that wear increases with contaminant concentration (29, 30, 31). Normally, the wear rate is proportional to the concentration until some saturation point is reached. The saturation phenomena is understandable since a rolling effect occurs at a high concnetration level. This effect is discussed in Chapter IV.

Abrasion with lubricated systems has received very little attention in the literature. In 1951, Roach (32) conducted a bearing wear test with abrasive particles in the lubricants. The bearing operated with a constant rotating radial load under the hydrodynamic condition. From the test result, he found taht the bearing wear rate increases linearly with abrasive particle size and particle concentration of the lubrication system. In 1965, Broeder and Heijnekamp (33) reported a similar result as Roach's work regarding the particle size. However, different from Roach's results, they found that the wear was not distributed uniformly around the bearing circumference but there was more wear at locations of smaller oil-film thickness. Ronen (34) extended Broeder and Heijnekamp's work under dynamic loading conditions. Experimental tests were conducted with both clean oils and contaminated oils. It was found that wear increased dramatically in the contaminated case. Furthermore, the wear tended to occur at the smaller oil film thickness. Recently, an investigation was carried out by the Fluid Power Research Center on the wear rate of lubricated piston-ring assembly by abrasive particles in the oils (27). The wear phenomenon was studied by the Ferrography wear analysis technique. The result showed that maximum wear is obtained if the particle

size is compatible to the minimum oil-film thickness. This manifested the significant relationship between the particle size and the minimum oil-film thickness on the lubricated wear investigation.

In addition to the abrasion mechanism, the concept of fatigue has been viewed by some investigators (35, 36). It is postulated that surface fracture arises from a considerable number of impacts on a single point by contaminants. The fatigue failure usually occurs in the Elastic Hydrodynamic (EHD) lubrication condition. The wear is not obviously revealed during a short testing time. Normally, it requires more than 100 million cycles to produce the failure of a lubricated bearing (35, 36).

Filtration

It has been recognized that the abrasive particles are harmful to the bearing surfaces. Particulate contaminants may be generated by the operation of the system or entrained into the system from the dirty environment. In order to avoid system malfunction due to contamination damage, the abrasive particles should be removed from the system.

In the past, changing the lubricating oil after a certain operation period was believed to be the best way to provide a clean operating condition; thus, it might protect the bearing from abrasive damage. However, there is no guarantee that the "new" oil provides a cleaner operating condition. A "new fluid" cleanliness survey including forty-three samples was conducted by the Fluid Power Research Center at Oklahoma State University, and it was found that the contamination levels observed were as high as 22,000 particles per milliliter greater than the 10 micrometers, and gravimetric levels of 218 mg/liter can be expected in the new fluids(37).

Apparently, using filters to remove contaminants is a necessity.

Filters utilize mechanical screens or porous media to remove or retain particulate contaminants from circulating fluid. Apparently, a filter not only has to remove particles from the system but also allows the fluid to pass through. As a matter of fact, no filter can completely separate particles from circulating fluid. Consequently, there is a compromise between the degree of particle separation and the designed flow rate. In other words, as long as there is flow passing through the filter, there is an opportunity for particles to pass through it. Therefore, a very basic question in filtration is how efficiently can a filter remove particles from the system. This stimulated researchers to study the rationales in assessing filter performance.

In general, two approaches have been made in trying to evaluate filter performance. They are from the standpoint of either component design aspect or system contamination control. In the area of component design, it is centered on the study of particle capture mechanism regarding the internal structure of filter media. However, a filter is treated as a control element in the system contamination control approach.

Sieving mechanism and surface force effects are two major parameters pertaining to the study of particle capture mechanism. In the past, filters were considered as a two-dimensional sieve. Particle capture is determined by means of the geometrical relationship between particle size and filter pore size. Normally, a particle is retained by the filter if the dimension of the particle is larger than that of a sieve hole. It is evident that the sieving mechanism is governed by the functions of particle size distribution and the filter pore size distribution. Therefore, the application of a statistical method has been widely used in studying the sieving process. Tucker (38) used wire cloth filter media with a normal

distribution for the capillary size distribution and, experimentally, verified that the related filter efficiency had the same distribution of the capillary size. Further, he reported that the efficiency curve changed for a multiple layer filter even if the filter had the same medium as a single layer filter. The efficiency curve was correlated as the function of the transmission factor with a power of n, while n is the number of layers of media. Similar results were found by Rosenfeld (39). He indicated that the pore size distribution of a single layer filter bears the Gaussian shape and that the greater the number of layers the nearer the pore size distribution to a logarithmic Gaussian curve. No mathematical expression was made in his report.

Stuntz (40) extended Tucker's work and he comprehensively studied the development of the mathematical model for the filtration process of a hydraulic system. Sieving was the only mechanism of particle capture considered in his study. Both the particle size and filter pore size were treated stochastically. Filter efficiency was represented in terms of particle size and filter pore size distributions. He employed both the numerical integration and Monte Carlo simulation techniques to analyze the formulate model. Results revealed that errors existed between simulation results and experimental data. He pointed out that the major discrepancy caused by the model was idealized by the use of regular geometric shapes and considered the capture only by sieving. However, this is not the case in the actual application. Despite the error, Stuntz's work was very instructive in the study of sieving mechanism.

In contrast to the approach of Tucker's and Stuntz's methods in analyzing the sieving mechanism, English (41), based on the principle of mass conservation in a close system, developed a model to illustrate the

efficiency of the filter. The model is a first order system. Filter performance is designated in terms of the residue on the sieve at any instant. The model was experimentally verified. However, it required a great number of parameters before using the model.

Surface force is another important consideration in filter design. The mechanisms which may contribute to surface force are categorized as (37, 39, 40):

1. Direct Interception
2. Inertial Impaction
3. Brownian Diffusion
4. Gravity
5. Hydrodynamic Effects.

These factors have been detailed in many investigations (42, 43, 44). Particle retention is mainly due to the interference of forces between particles and filter media. One of the commonalty of this approach, is that the developed filter models are usually very complicated and incorporated with a lot of unknown quantities. They restricted the study of filtration in the state-of-the-art. No direct application can be easily obtained.

In order to reduce the void between theoretical developments and practical applications, many efforts have been made around the world in trying to evaluate filter performance effectively. One of the earliest available hydraulic filter test specifications is MIL-F-5504 (October, 1958). It specified two important filter assessment methods: the bubble point test method and the nominal filter rating method.

The bubble point test determines the pressure needed to force a bubble through the pores of a submerged filter. Theoretically, the pressure

differential across a capillary is inversely proportional to the size of the hole. Therefore, the comparison between pore size of filters can be observed.

In the "nominal" rating, the filter is supposed to catch 98 percent of all incidental particles greater than the rating. Test dust used is the full distribution of AC Fine Test Dust. However, the nominal rating does not specify the upper limit of the size of the particle which could be passed.

In March, 1960, the MIL-F-8815 was specified which established an "absolute" rating system. This method specifies a filter in terms of the minimum size of spherical particles that the filter can capture. However, actual test results reveal that no filter can absolutely retain all particles greater than a given size and pass the test. Figure 2 illustrates the discrepancy between the actual filter performance and the ideal performance.

To help minimize the mentioned discrepancies and to improve the filter assessing technique, an innovative rating method, called the Beta filtration ratio, was introduced by the Fluid Power Research Center at Oklahoma State University in the early 1970's. The Beta filtration ratio is defined as the number of particles greater than a given size in the influent fluid to the number of particles greater than the same size in the effluent fluid during the operating process. The Beta method provides a simple figure of merit in which to rate the particle separation capacity. Due to its effectiveness, the Beta has been accepted as an International Standard Organization (ISO) standard.

Recently, many complaints have been voiced by designers and users about higher than expected contamination levels caused by improper

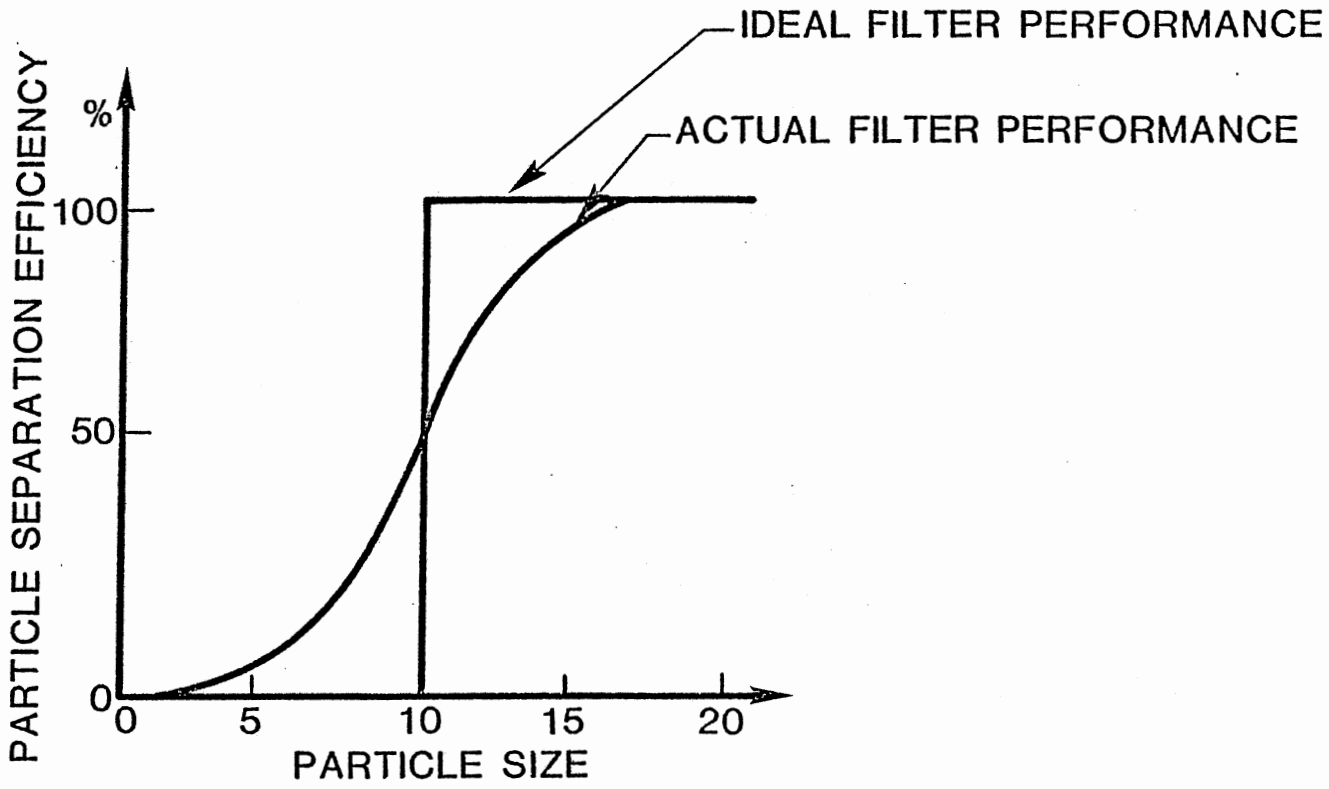

Figure 2. Filter Performance Characteristic Curves

location of filters. The new trend in modern machine design indicates that both pressure line and suction line filters are not adequate. Instead, the off-line filter design is more effective. Many advantages can be obtained, subjected to the system's efficiency, reliability and service life, through the use of off-line type filtration process. This new process usually includes low flow and high beta type filters. Currently, a great deal of research has been done at the FPRC in evaluating the performance of these two types of filters. Experimental efforts to utilize the current contamination control theory have been disappointing. One of the major reasons stems from the Beta theory being derived from a "dynamic" basis. Due to the complex function of the filtration process, the downstream particle concentration does not maintain at a relative ratio to the upstream particle concentration throughout the entire process. Any attempts to obtain a high sensitivity ratio for a high beta filter encounter the problem of ratio instability. Despite the success of Beta in dealing with the commonly used filters, it is necessary to update the beta theory so that it may encompass a general scheme for assessing filters.

The previous work of the author and that of the other investigators has established the need for the development of the tribo-filtration model. Details of the theoretical development are illustrated in the following chapter.

CHAPTER III

DEVELOPMENT OF THEORETICAL MODELS

In chapter II, literature relevant to this subject was surveyed. It was realized that in order to achieve the investigation of the tribo-filtration phenomena, three major disciplines are involved: lubrication, wear, and filtration. This chapter presents the theoretical models of these three parameters bringing them together to formulate the tribo-filtration model.

Hydrodynamic Lubrication Model

It is well known that a converging, wedge-shaped film is a major cause of generating an oil pressure to separate bearing surfaces. The physical process of the wedge effect can be gained by considering the simple pad bearing in Figure 3. The tilting pad is stationary and with an inlet gap h_1 larger than the outlet gap h_0. The loaded surface of the pad moves at a velocity U. The gap between the pad and the moving surface is flooded with a viscous incompressible lubricant. Assume that initially the velocity distribution at the inlet is linear with a null velocity at the pad surface and a velocity of U at the moving surface. It is also assumed that the velocity distribution at outlet follows the linear relationship. Since h_1 is larger than h_0 there would be an excess flow in the system. This is against the principle of continuity of flow. As a result, a pressure is generated to overcome the work of the excess flow. This

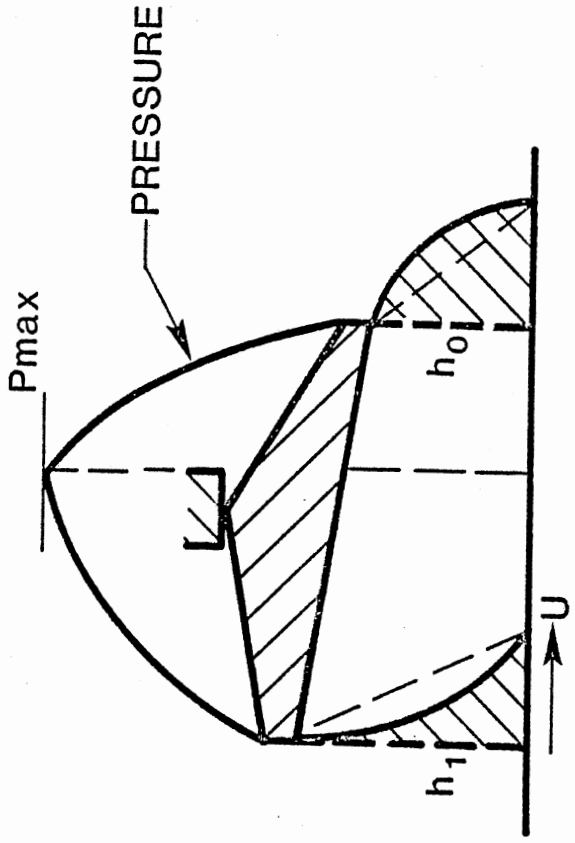

Figure 3. Physical Process of Wedge Effect

provides the theoretical basis of hydrodynamic lubrication.

Excluding the stretch and squeeze effects, the hydrodynamic lubrication characteristics can be well described by the Reynolds equation which takes the following form:

$$\frac{\partial}{\partial x}\left(h^3 \frac{\partial p}{\partial x}\right) + \frac{\partial}{\partial y}\left(h^3 \frac{\partial p}{\partial y}\right) = 6\, U\, \eta \frac{dh}{dx} \qquad (3.1)$$

where x = coordinate

y = coordinate perpendicular to x

h = film thickness

P = local pressure within the film

U = surface velocity in x direction

η = absolute viscosity of lubricant

A journal bearing behaves in an angular motion rather than a linear motion. Further, the film shape of a journal bearing is more involved than that of a pad bearing. Thus, before employing the Reynolds equation, Equation (3.1), to analyze a journal bearing performance, proper coordinate transformations regarding the reference coordinates and the film thickness must be made.

Figure 4 illustrates the geometry of a journal bearing. Consider the journal of radius R rotates in the bearing of radius R_0, and the shaft has an eccentricity of e. From the geometric relationship of R, R_0, and e as shown in Figure 4, an approximate expression of film thickness at rotation angle θ is:

$$h = c + e \cdot \cos\theta \qquad (3.2)$$

Where h = fluid film thickness

c = radial clearance

e = eccentricity of the shaft

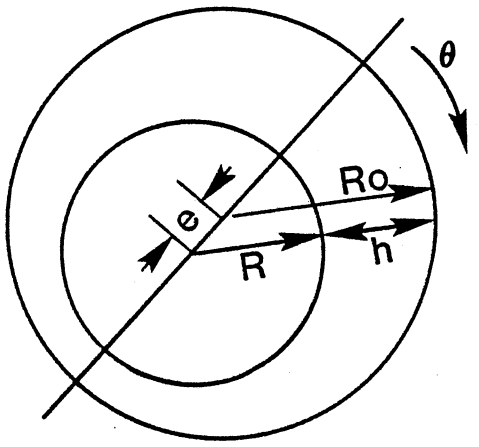

Figure 4. Geometry of Approximate Oil Film Thickness Relation

θ = rotation angle

Define an eccentricity ratio, ε, as

$$\varepsilon = e / c \tag{3.3}$$

then, Equation (3.2) becomes

$$h = c\cdot(1 + \varepsilon\cdot\cos\ ) \tag{3.4}$$

Furthermore, x, the coordinate in the direction of motion is correlated by the journal radius, R, and the rotating angle, θ, as

$$x = R\cdot\theta \tag{3.5}$$

Substituting Equations (3.4) and (3.5) into Equation (3.1), gives the Reynolds equation for a finite journal bearing (13),

$$\frac{\partial}{\partial\theta}\left((1+\varepsilon\cdot\cos\theta)^3\frac{\partial p^*}{\partial\theta}\right) + \left(\frac{R}{L}\right)^2\frac{\partial}{\partial y^*}\left((1+\varepsilon\cdot\cos\theta)^3\frac{\partial p^*}{\partial y^*}\right) = -\varepsilon\cdot\sin\theta \tag{3.6}$$

where

$y^* = Ly$

$p^* = pc^2 / 6\pi UR$

L = journal length

p = local pressure

c = radial clearance

η = fluid viscosity

R = journal radius

Equation (3.6) can only be solved analytically for special cases. In general, it is solved numerically to calculate the pressure distribution between the bearing surfaces. The mathematical precedure has been detailed in many texts related to the lubrication engineering, for example in Reference 13. The solution for the local pressure is then applied to correlate the external load characteristic to bearing parameters and

operating conditions. The bearing load can be expressed as

$$W_f = 6U\eta(\frac{R}{c})^2 L ((\int\int p^*\cdot\cos\theta d\theta dy)^2 + (\int\int p^*\cdot\sin\theta d\theta dy)^2)^{\frac{1}{2}} \quad (3.7)$$

Where W_f is the load.

It can be shown that in formulating the load equation a parametric group is derived that involves bearing characteristics. This parametric group; known as the Sommerfeld number, is represented as

$$S = (R/c)^2 \cdot (N\eta/p) \quad (3.8)$$

where N is the rotating speed.

Thus, Equation (3.7) is rewritten as

$$S = ((\int\int p^*\cdot\cos\theta d\theta dy)^2 + (\int\int p^*\cdot\sin\theta d\theta dy)^2)^{\frac{1}{2}} / 6\pi \quad (3.9)$$

Normally, Equation (3.9) is illustrated graphically to signify the relationship between the Sommerfeld number and the eccentricity ratio of the journal. Figure 5 shows a typical S - ε graph of a 180^o journal bearing.

The S - ε bearing characteristic curve is of physical significance in calculating the dimension of fluid film thickness. It is obvious that by giving a bearing characteristic number, one can obtain the related eccentricity ratio. Therefore, the film thickness can be calculated from Equation (3.4).

From the standpoint of tribological wear, the extremities of the fluid film thickness are of more significance because these values determine the severity of contaminated wear. The maximum thickness specifies the upper size of a particle that can entrain into the bearing surface and it may cause wear. On the other hand the minimum thickness determines the lowest size of a particle that may cause wear. These two parameters can be directly derived from Equation (3.4), and are shown as:

$$h \text{ max} = c(1 + \varepsilon) \quad (3.10)$$

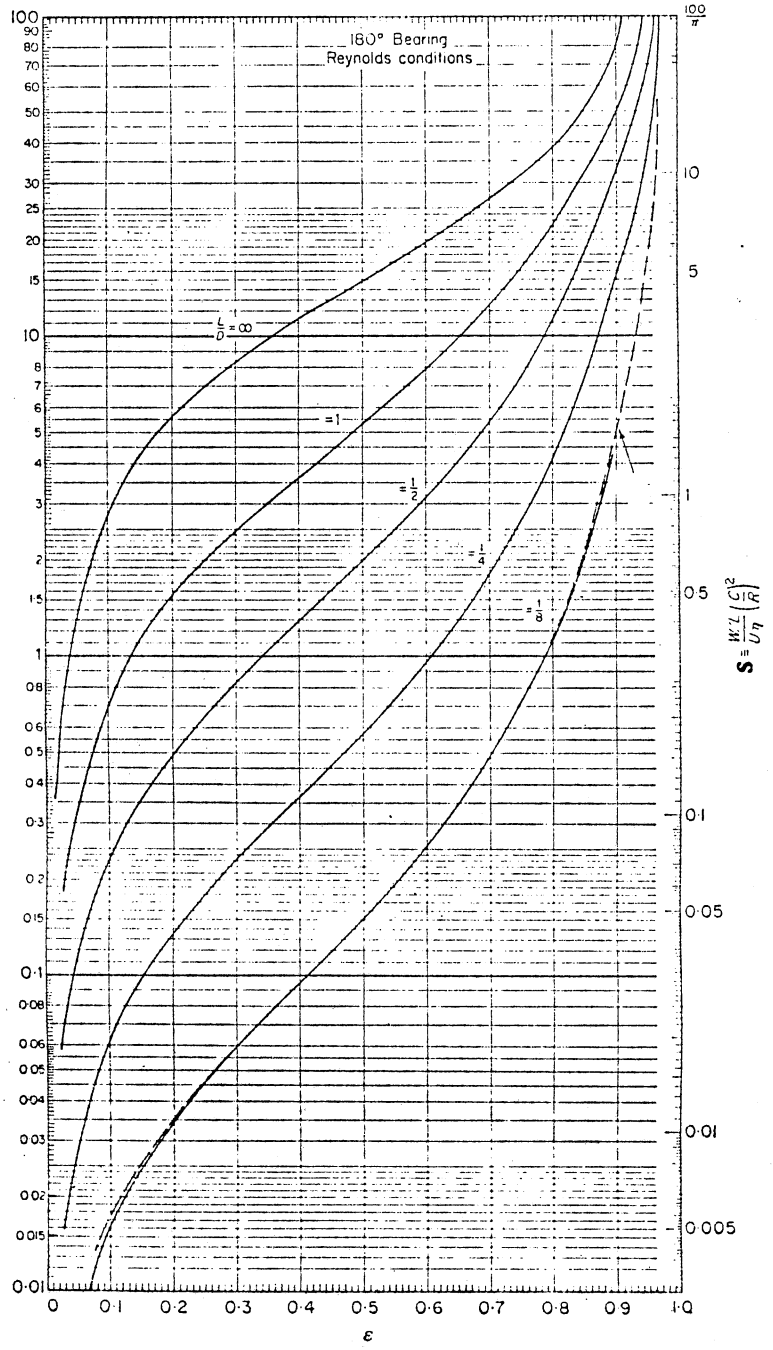

Figure 5. S - ε Graph of 180° Journal Bearing

and

$$h_{min} = c(1 - \varepsilon) \tag{3.11}$$

where h_{max} = the maximum oil film thickness

h_{min} = the minimum oil film thickness

c = radial clearance

ε = eccentricity ratio

Equations (3.10), and (3.11) provide the required information in sizing a filter to reduce component damage from the abrasive wear. They will be part of the major considerations in the development of the tribo-filtration model.

Tribological Wear Model

To evaluate the influence of the system filtration characteristics on component wear performance, the contaminant sensitivities of the rotating elements must first be determined. In the tribological systems, contaminant induced wear is caused by particles entrained into the lubricant between surfaces in relative motion. The tribological wear investigated in this research is intended to signify the component wear behavior regarding the interferences between the entrained abrasive particle properties and fluid lubrication condition.

As noted in Chapter II, abrasion and fatigue are the two major mechanisms normally postulated in investigating the contaminated induced wear. Abrasion is the predominant wear mechanism imposed on the associated moving surfaces if the abrasive particles are hard enough to cut the wearing surfaces. On the other hand, the fatigue mechanism fails the surfaces if the entrained particles perform indentation but not cutting, or the loading pressure is cyclic. Generally, the fatigue wear occurs

after a great number of rotation cycles.

In design practice, the hardness of a journal is harder than that of a bearing. Therefore, this material combination provides a suitable environment for the abrasive particle to embed on the softer material surface and abrade the harder surface. As a result, abrasion becomes the predominant contribution to wear the bearing surfaces.

In this investigation, Air Cleaner Fine Test Dust (ACFTD) was employed as the abrasive particle. The advantages of using ACFTD are that the properties of ACFTD are inherently close to that of silica which is the major solid contaminant existing in a lubricating system and its particle size and concentration can be precisely controlled. Accordingly, it provides a realistic approach to simulating a contaminanted environment.

The shape of the abrasive particle is one of the major parameters in the development of a wear model. There are many shape models that have been postulated to represent the shape of an abrasive particle (25, 26, 45). For instance, a cone, ellipsoid, spheroid, or square prism. ACFTD was examined under the scanning electronic microscope (SEM) to determine the shape of an ACFTD. Figure 6 illustrates the result observed. Apparently, the shape of an ACFTD is irregular, nevertheless, it is close to that of a square prism.

Kroeker (46) defined the shape of an ACFTD as a square prism with a 1.25 length ratio of the longest side to the square side. The longest side of a particle has been universally adopted as the standard size for a particle (37). For example, a particle of 10 micrometers in the Kroeker's model indicates the particle has the longest side of 10 micrometers and the square side of 8 micrometers. This quantitative description of an ACFTD has been successfully adopted by Inoue (27) to develop a three-body

Figure 6. Shape of ACFTD Observed Under SEM, 1000X

abrasive cutting wear model. Consequently, throughout this analysis, contaminants are assumed to have the same physical and geometrical properties as that of ACFTD.

As mentioned previously, a lubricated, three-body abrasive wear mechanism consists of a multi-process: lubricating, indenting, and cutting. In the following analysis of abrasive wear, it is assumed that the oil film is thick enough to provide an ideal hydrodynamic lubrication. Further, only particles with size between the range of the minimum and maximum film thickness may cause the wear. In addition, the particle is hard enough to indent and cut metal surfaces.

The mechanism of cutting has been comprehensively studied in the early 1950's (47, 48, 49). Because the behavior of cutting and abrasion is similar, the cutting theories have been widely applied to abrasion analysis. However, it is noted that the function of tool cutting is merely a two-body abrasion. This theory cannot simply apply in analyzing the contaminated induced wear system. Recently, Inoue (27) observed that the abrasive process can be advanced to analyze the three-body cutting mechanism by using the conventional cutting model (50) incorporated with the wedge indentation model (51).

In Inoue's wear model, the cutting rake angle was specified to be null and the model was not explicitly expressed in terms of wear. However, in the abrasion process, particle attitude is in a random manner. The rake angle is not always null. To improve these shortcomings and give an explicit expression of the wear model, the following analysis is developed to extend the abrasion model in a more realistic form.

Figure 7 schematically presents the three-body cutting process. The abrasive particle embedded in the softer surface and abraded the harder

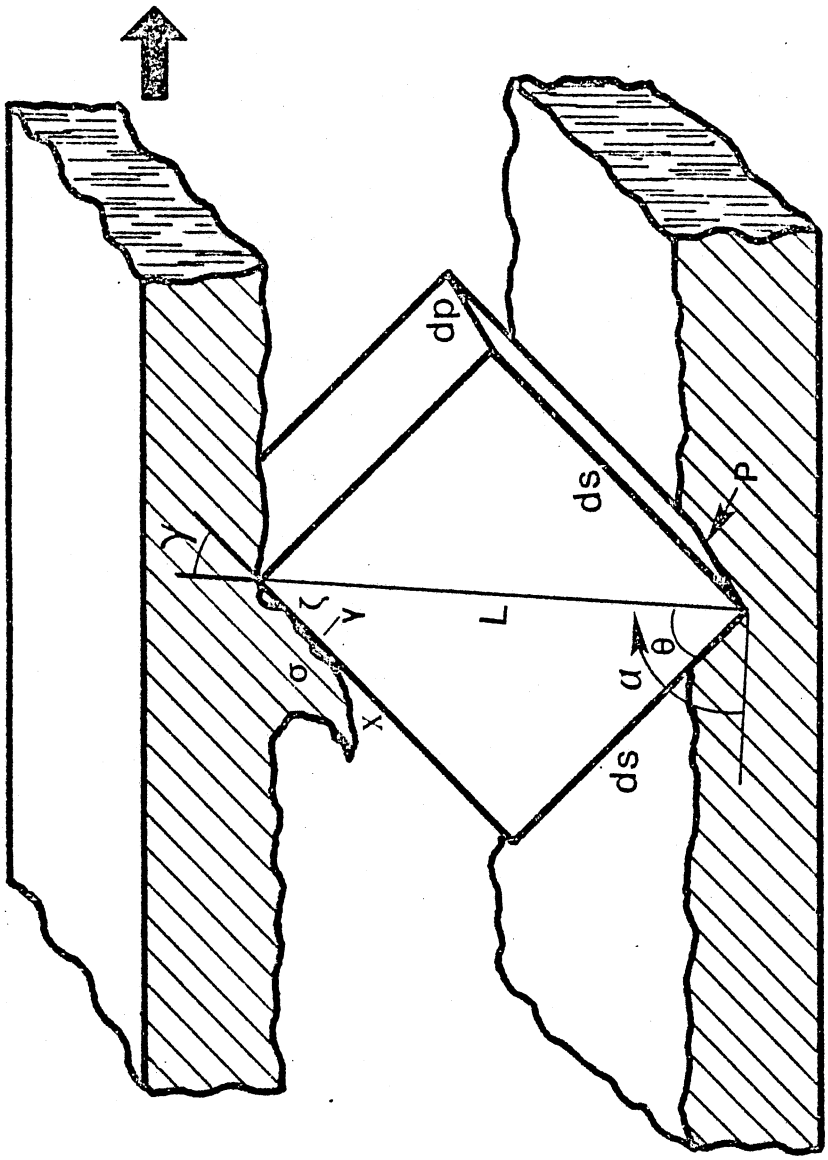

Figure 7. Three-Body Wear Model

surface. Assume that the square side surface of the particle is perpendicular to the moving direction, according to the low energy principle. And the harder surface is abrades orthogonally by the longer side of the particle. Note that the rake angle, γ, is included.

Applying Ernst and Merchant's (50) cutting theory, the cutting force can be formulated as

$$F_c = 2\tau_h \cdot d_p \cdot d_c \cdot \cot\ (0.25\pi + 0.5\ \gamma + \ 0.5\ \tan^{-1}(\mu)) \qquad (3.12)$$

where F_c = cutting force

τ_h = material shear yield stress of harder surface

d_p = entrained particle size

d_c = cutting depth

γ = rake angle

μ = coefficient of friction

Using the geometric relationship shown in Figure 7 the rake angle, γ , is expressed in terms of the inclination angle, α , as

$$\gamma = \alpha\ - 0.25\,\pi \qquad (3.13)$$

Consider now, the indentation process. This is the breakthrough in rationale from the conventional two-body or three-body cutting wear to lubricated abrasive wear. Based on Grunzweig's (44) wedge indentation model, Inoue (27) correlated the indenting pressure, p, with the coefficient of friction, μ, for a rectangular angle indentor as

$$p = (3.154 + 4.051\ \mu - 1.457\mu^2 - 12\mu^3)\cdot\tau_s \qquad (3.14)$$

where τ_s is the shear yield stress of the material being indented.

In considering force equilibrium between cutting force and indenting force, the following relationships are derived:

$$F_c \cdot \sec\ \alpha = p \cdot d_i \cdot d_p \cdot (\sin\theta \cdot \csc(\alpha-\theta)\ - \cos\theta \cdot \sec(\alpha-\theta)) \qquad (3.15)$$

$$F_c \cdot \csc\alpha = F \cdot \cos(\alpha - 0.5\pi) \tag{3.16}$$

where F = external force on a single particle

d_i = indenting depth

α = inclination angle relative to moving surface

θ = diagonal angle in square surface.

Let $\delta = \tan^{-1}(\cot(\alpha - \theta))$ (3.17)

then, Equation (3.15) and (3.16) can be written as

$$F_c \cdot \sec\alpha = p \cdot d_i \cdot d_p \cdot \sin(\alpha - \delta) \tag{3.18}$$

and

$$F_c = 0.5\ F \cdot \sin(2\alpha) \tag{3.19}$$

Referring to Figure 7, it is seen that

$$d_s = L \cdot \sin\alpha - d_c - d_i \tag{3.20}$$

and

$$\theta = \tan^{-1}(d_s / L) \tag{3.21}$$

where d_s = side length of prism square equals to 0.8 d_p

L = diagonal length of prism square

Solving Equation (3.15) and (3.20) simultaneously yields

$$d_c = \frac{1.13 \sin\alpha - 0.8}{1+\left(\frac{\tau_h}{\tau_s}\right)\frac{2\cot(0.5\alpha+0.125\pi-0.5\tan^{-1}(\mu))\cdot\sec\alpha}{(3.154+4.051\mu-1.457\mu^2-12\mu^3)\cdot\sin(\theta-\delta)}}\ d_p \tag{3.22}$$

Thus, the cutting depth depends on the compnent's material properties (τ_h, τ_s), particle size (d_p), particle orientation (α), and fluid properties (μ). Written briefly,

$$d_c = f_c\ (\tau_h, \tau_s, \alpha, \mu)\ d_p \tag{3.23}$$

From Equation (3.22) and Equation (3.23), the expression of function f_c is obvious.

The indenting depth, d_i, can be obtained by substituting Equation (3.23) into Equation (3.20).

$$d_i = f_i (\tau_h, \tau_s, \alpha , \mu) \cdot d_p \tag{3.24}$$

where $f_i = 1.13 \sin\alpha - 0.8 - f_c$.

Substituting Equation (3.24) into Equation (3.18), and then combining Equation (3.18) and Equation (3.19) together yields

$$F = 2 \sec(2\alpha) \cdot \sin\alpha \cdot p \cdot f_i \cdot \sin(\theta - \delta) \cdot d_p^2 \tag{3.25}$$

Equation (3.25) is a highly nonlinear equation. It can not be solved analytically and must be solved numerically in order to determine the inclination angle, α, subjected to a given external force for an individual particle of size d_p. In turn, the calculated value of the inclination angle is substituted into Equations (3.23) and (3.24) to calculate the cutting depth and indenting depth.

In many cases, the material properties are expressed in terms of the tensile yield stress rather than the shear yield stress. The conversion can be achieved by employing the von Mises yield criterion which is expressed as

$$(\sigma_{xx} - \sigma_{yy})^2 + (\sigma_{yy} - \sigma_{zz})^2 + (\sigma_{zz} - \sigma_{xx})^2 + 6(\sigma_{xy}^2 + \sigma_{yz}^2 + \sigma_{zx}^2) = 2 S_t^2 \tag{3.26}$$

where σ_{ii} = principle stress along direction i

σ_{ij} = shear stress parallel to plane ij

S_t = material tension yield stress

Consider the cutting process, Figure 7. Let the y-axis be normal to the shear stress plane, and assume that there is no strain in the Z direction, thus,

$$\sigma_{yy} = \sigma_h \tag{3.27}$$

$$\sigma_{xy} = \tau_h \tag{3.28}$$

$$\mu = \tau_h / \sigma_h \tag{3.29}$$

and the other stress terms are zero.

Substituting Equation (3.27), (3.28) and (3.29) into Equation (3.26) gives:

$$\tau_h = (1 + 3\mu^2)^{-\frac{1}{2}} \cdot \mu S_t \tag{3.30}$$

A similar procedure can be followed to convert the shear stress of the indented material into the tensile stress. At first step of this investigation it is assumed that the shear stress plane is parralel to the wedge surface and the coefficient of friction between the ACFTD to both wearing surfaces is indentical, then the shear stress term in Equation (3.22) can be replaced by the tensile stress.

It is of interest in applying the derived cutting depth, Equation (3.28), to formulate the tribological wear model. Referring to Figure 8, it is obvious that the cutting wear rate caused by particle of size d_p is

$$W_{dp} = d_c \cdot d_p \cdot n_{dp} \cdot Q \cdot \ell \tag{3.31}$$

where W_{dp} = wear rate caused by particle of size d_p

d_c = cutting depth

d_p = particle size

ℓ = sliding distance

n_{dp} = particle concentration of size d_p

Q = flow rate pass through the bearing

Equation (3.31) gives the wear rate in terms of volume loss per unit time.

Consider the case where the material is homogeneous and that the operating conditions are constant during a test. By virtue of this, the function f_c in Equation (3.23) is a constant. Let it be k_c, then

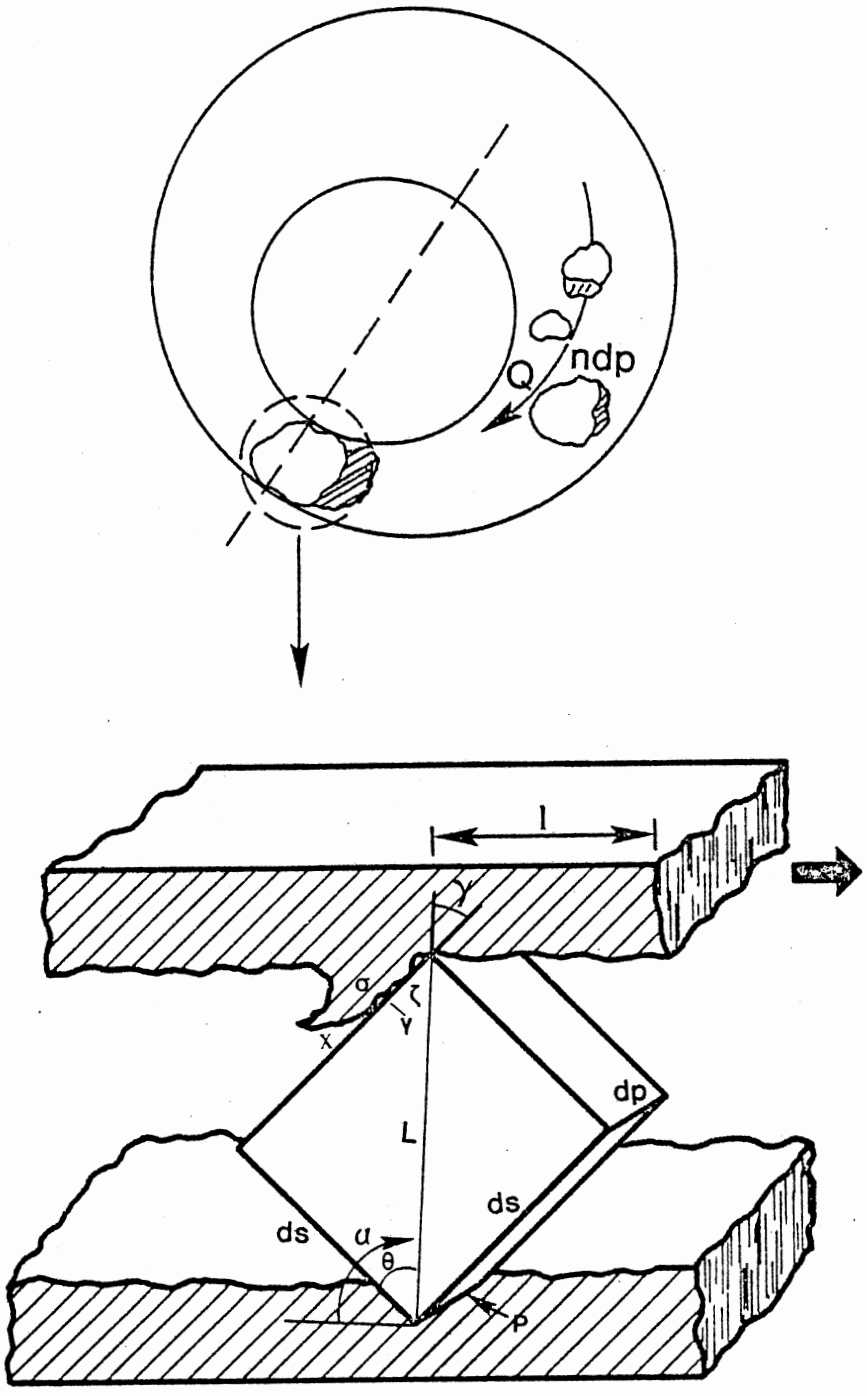

Figure 8. Illustration of Accumulative Wear

$$d_c = k_c \cdot d_p \tag{3.32}$$

Therefore,

$$W_{dp} = k_d \cdot N_{dp} \cdot d_p^{\,2} \tag{3.33}$$

where $k_d = k_c \cdot \ell \cdot Q$

Equation (3.33) indicates that the abrasive wear rate is proportional to the particle concentration and the square of particle size. As a result, the total abrasive wear rate of a journal bearing under hydrodynamic condition is

$$W = \int_{h\ min}^{h\ max} k_d \cdot n(x) \cdot x^2\ dx \tag{3.34}$$

where w = total abrasive wear rate

n(x) = particle concentration with size x

x = particle size

h min = minimum oil film thickness

h max = maximum oil film thickness

Beta Prime Filtration Model

In Chapter II, it was noted that the Beta filtration ratio is derived from the instantaneaous values of the upstream and downstream particle concentrations. This may introduce the problem of ratio instability. Consequently, it is conceived that if the reference concentration is a constant value instead of a time variant upstream concentration level, the instability problem can be avoided. Based on this concept the Beta Prime rating method is formulated. The "Prime" being used to signify the difference of the reference upstream particle concentration level used. In the Beta Prime system, a constant initial particle concentration level is used to formulated the filtration ratio. The new Beta Prime theory is

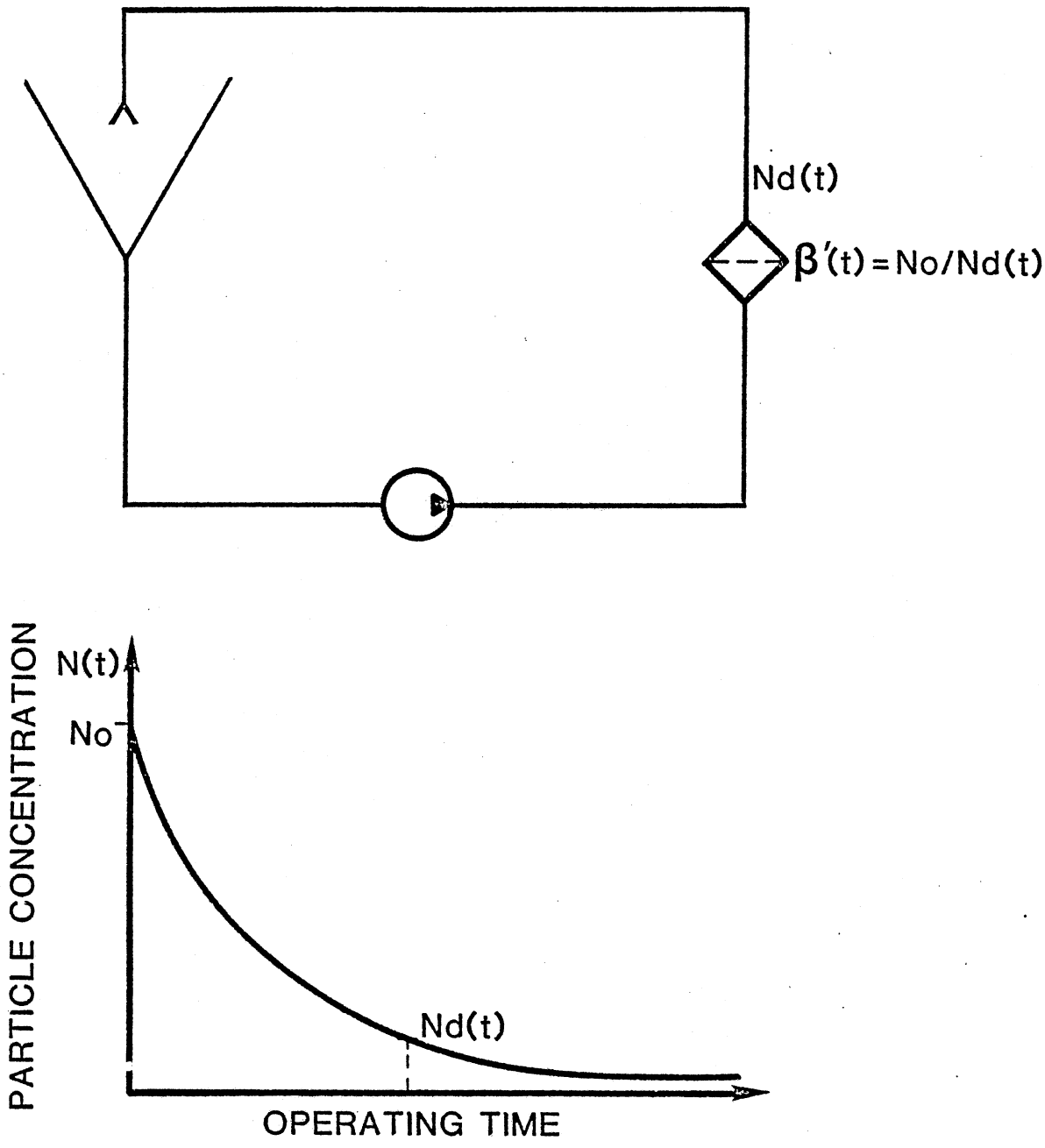

Figure 9. Concept of Draw Down Test

derived from a "drawdown" basis and uses the schematic shown in Figure 9.

In the filtration ratio approach, both the Beta and Beta Prime methods, in fact, are dealing with the probability that a given particle may pass the filter. Hence, if initially there are $N_{dp}(0)$ particles greater than size d_p in the system, and there are $N_{dp}(t)$ particle greater than the same size in the downstream of the filter at time, t; then the cumulative probability that particles of a size greater than d_p may pass the filter is

$$B_{dp}(t) = N_{dp}(t) \; / \; N_{dp}(0) \tag{3.35}$$

On the other hand, the cumulative probability of particles being captured and retained by the filter is

$$R_{dp}(t) = 1 - B_{dp}(t) \tag{3.36}$$

Obviously, the density function of a capture can be expressed as

$$r_{dp}(t) = - \frac{d}{dt} \left(B_{dp}(t)\right) \tag{3.37}$$

Hence, the rate of capture is

$$C_{dp}(t) = r_{dp}(t) \; / \; B_{dp}(t) \tag{3.38}$$

Rearrange Equations (3.37) and (3.38), and integrate

$$\int C_{dp}(t) \, dt = - \ln B_{dp}(t) \tag{3.39}$$

Statistically, the left hand side term of Equation (3.39) represents the cumulative probability of the capture rate. Figure 10 depicts the relationships between the various quantities appearing in the above analysis. Physically, the cumulative capture rate depends on the filtration mechanism. It may be affected by many factors, for example, caking, blocking, particle desorption, etc. This phenomenon has been investigated in a variety of fields. A general model can be concluded and is illustrated as

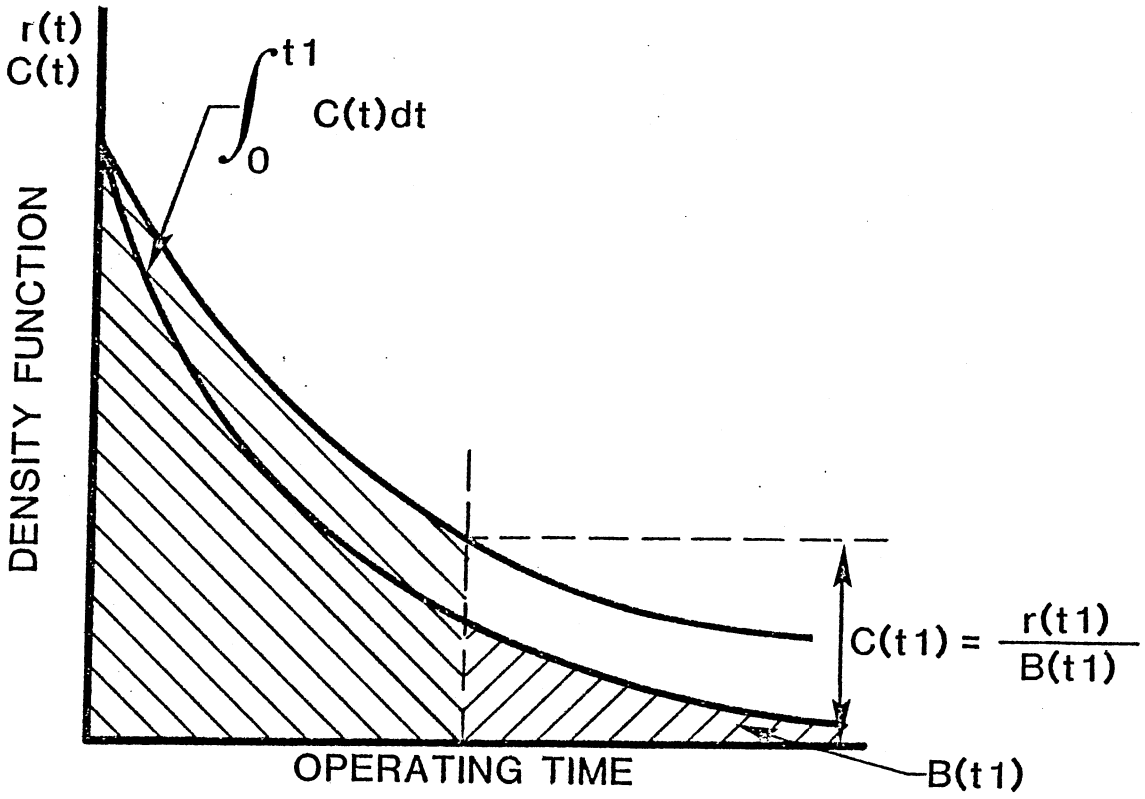

Figure 10. Schematic of Cumulative Rate of Capture

$$\int C_{dp}(t)\,dt = \left(\frac{t}{s \cdot T}\right)^{a} \tag{3.40}$$

where a = the characteristic process constant

T = the characteristic time constant

s = the time scaling constant

And the characteristic time constant is a function of fluid volume, V, and fluid flow rate, Q,

$$T = V / Q \tag{3.41}$$

Thus, substitute Equation (3.40) into Equation (3.39) gives

$$B_{dp}(t) = e^{-\left(\frac{t}{s \cdot T}\right)^{a}} \tag{3.42}$$

and

$$F_{dp}(t) = 1 - e^{-\left(\frac{t}{s \cdot T}\right)^{a}} \tag{3.43}$$

Apparently, Equations (3.42) and (3.43) bear the Weibull distribution characteristics.

Suppose that particles are perfectly mixed in the fluids, and all fluids pass through the filter once during a complete circulating time. Thus, the value of the Beta Prime is

$$\beta'_{dp}(t) = \frac{1}{B_{dp}(t)} \tag{3.44}$$

It is well known that the Weibull function can be expressed as a linear equation by doing the following transformation

$$Y = a \cdot X + b \tag{3.45}$$

where $Y = \ln(\ln(\beta'_{dp}(t))$

$X = \ln(t / T)$

$$b = - a \ln s$$

Equation (3.45) indicates that if any three of the parameters $\beta'_{dp}(t)$, a, T, and s are known, then the remaining one can be obtained. In practice, the value of the characteristic time constant, T, is predetermined. Furthermore, the characteristic process constant, a, and the time scaling constant, s, can be determined from the effort of the drawdown test for a given filter. Accordingly, the filtration ratio, Beta Prime, can be determined with respect to the operating time, t. It would be more convenient if a reference Beta Prime is selected at a specific time. Then, the Beta Prime may contribute two major advantages in filter assessment: the higher the Beta Prime value the better the filter separation performance (how good), and the higher the characteristic process constant value the faster the system reaches its stable concentration level (how fast). Therefore, filter performance can be specified uniquely, Figure 11.

The Tribo-filtration Model

From the previous analysis, it is realized that both the filtration characteristics and wear behavior are expressed in terms of particle size and particle concentration. Intuitively, the wear rate can be directly correlated with the filtration ratio. However, this is not the case. It should be noted that the inversely cumulative particle concentration is used in the Beta Prime system while the individual particle concentration is applied to derive the wear model. Statistically, these two parameters can be correlated to each other by using the discrete distribution concept, such that the number of particle size, dp, might be defined as the difference between two consequential inversely cumulative values, namely,

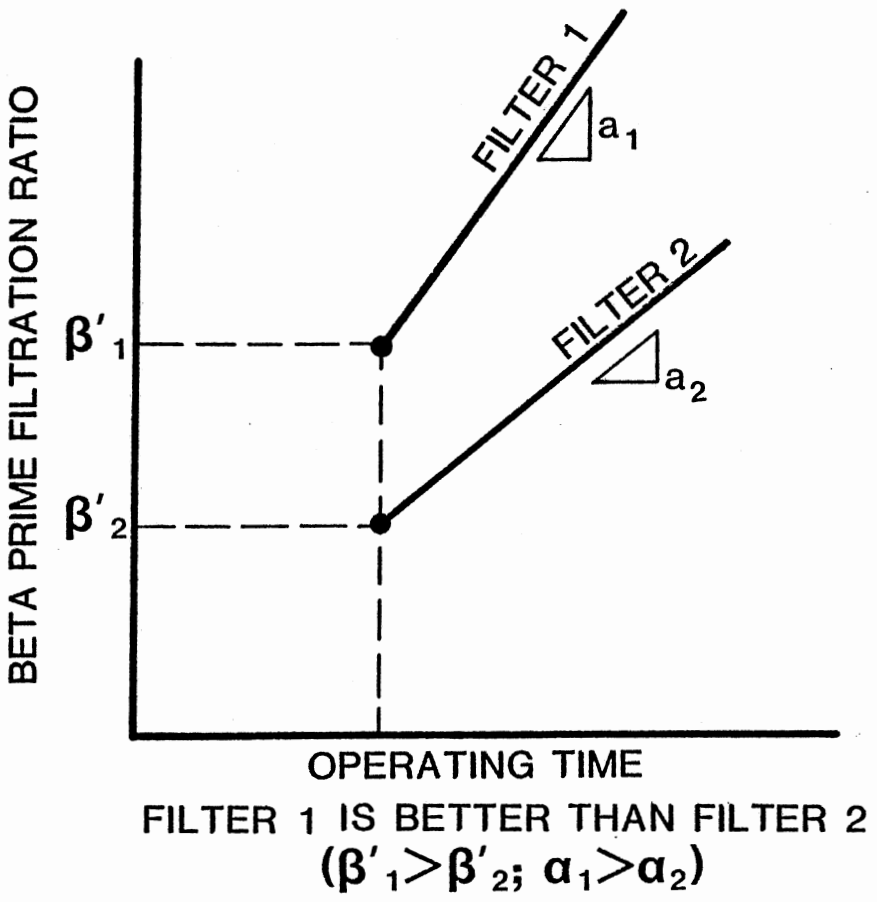

Figure 11. Characteristic Curves of Filter on the Beta Prime Graph

$$n_{dp} = N_{c,dp} - N_{c,\ dp+1} \tag{3.46}$$

where n_{dp} = the number of particle of size d_p

$N_{c,dp}$ = the inversely cumulative concentration of particle size greater than d_p

Therefore, from Equation (3.33), the total accumulative wear rate, W(t), which concerns all the particle sizes at time t is

$$W(t) = \sum_{t=0}^{t} \sum_{dp=0}^{\infty} (N_{c,dp}(t) - N_{c,dp+1}(t)) \cdot f(dp) \tag{3.47}$$

where $f(dp) = k_d \cdot d_p^{\ 2}$

Applying the Beta Prime definition, it gives

$$W(t) = \sum_{t=0}^{t} \sum_{dp=0}^{\infty} \left(\frac{N_{0,dp}}{\beta'_{dp}(t)} - \frac{N_{0,dp+1}}{\beta'_{dp+1}(t)}\right) \cdot f(dp) \tag{3.48}$$

where $N_{0,dp}$ = the initial value of $N_{c,dp}$

β'_{dp} = the Beta Prime filtration ratio of size d_p

In most applications, the value of Beta Prime for a given filter is specified at a reference point, for example, the Beta Prime value of particle size of 10 micrometers. Therefore, in any attempts to use Equation (3.48) difficulties arise from using Beta Prime value for other than the reference value. It is desirable to express Equation (3.48) in terms of the reference Beta Prime.

In the discussion of filter capture mechanism, it indicates that the only opportunity for the particle to pass through the filter is when the particle size is less than the filter pore size, Figure 12. Hence, the probability that the particle of a size greater than d_p being captured is

$$E_{dp} = \int_0^{dp} \int_x^{\infty} f_p(x) \cdot f_f(y)\ dy\ dx \ / \int_x^{\infty} f_p(x)\ dx \tag{3.49}$$

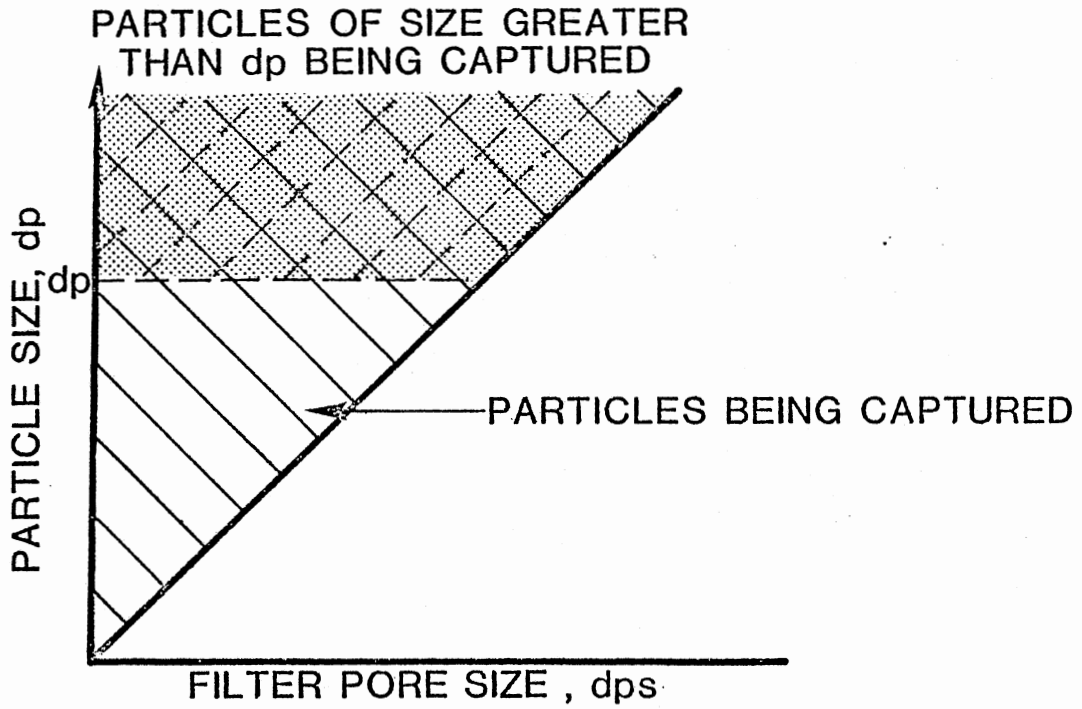

Figure 12. Schematic of Capture Function

where $f_p(x)$ = density function of particle size distribution

$f_f(x)$ = density function of filter pore size distribution

Supose that $f_p(x)$ and $f_f(x)$ are two independent density functions; namely, the change of particle size distribution does not affect the filter pore size distribution such that Equation (3.49) is simplified as

$$E_{dp} = \int_0^{dp} f_f(y)\, dy \tag{3.50}$$

Equation (3.50) states that the overall filter separation efficiency of particle size d_p is the cumulative probability of filter pore size distribution up to d_p. Even more significant is that generally the pore size distribution of industrial filters (except for the wire-cloth type media) obeys the Log-normal model (37, 38, 40, 41). Furthermore, a Log-normal distribution can be correlated to the Weibull distribution with a slope of two or slightly less (52). As this is an initial investigation into this field, it could seem reasonable to assume that the slope is two , then by giving the reference Beta Prime value, the scaling constant is obtained. This provides a feasible approach to correlate any Beta Prime to the reference Beta Prime value for a given filter. Equation (3.50) is rewritten as

$$E_{dp} = 1 - e^{-(d_p/s_p)^2} \tag{3.51}$$

where s_p is the particle size scaling constant.

By applying the Beta Prime definition and doing mathematical manipulations, any Beta Prime value is represented in terms of the reference Beta Prime value, β'_{dr}, as

$$\beta'_{dp} = \beta'_{dr} \cdot e^{(dp^2 - dr^2)/s_p^2} \tag{3.52}$$

In practice, the distribution of the test dust is known; thus the initial particle concentration of different sizes can be determined by using the reference value. For example, the ACFTD particle size distribution standardized by the ISO shows

$$N_{0,dx} = 10^{(3.246 - 1.086\ (\log(dx))^2)} \tag{3.53}$$

Thus,

$$N_{0,dp} = N_{0,dr}\ 10^{1.086((\log(dr))^2 - (\log(dp))^2)} \tag{3.54}$$

Therefore, Equation (3.48) represents the tribo-filtration performance with respect to the wear rate and the reference filtration parameters only. It can be seen that the higher the Beta Prime value, namely, the better the filter, the lower the wear rate of the elements.

CHAPTER IV

EXPERIMENTAL EVALUATION OF TRIBOLOGICAL WEAR MODEL

General Considerations

In order to evaluate the tribological wear model, Equation (3.34), developed in Chapter III, a large number of experimental tests were performed and are reported in this chapter. From Broeder (33) and Ronen (34), it is realized that a very high intensity of wear occurs at locations of minimum oil film thickness. Therefore, as an initial step into this area of investigation, Equation (3.34) can be expressed as

$$W = Kd \cdot h^2 \text{ min} \cdot N(h \text{ min}) \tag{4.1}$$

where W = total wear rate

Kd = proportional coefficient of particle property

h min = minimum oil film thickness

$N(h \text{ min})$ = particle concentration with size h min.

Furthermore, if the test is conducted under a constant oil film thickness condition, then

$$W = K_f \cdot N(h \text{ min}) \tag{4.2}$$

where $K_f = K_d \cdot h^2_{min}$

In other words, the wear severity of a rotating element is proportional to the concentration of entrained abrasive particles, subject to a given fluid film thickness. Hydrodynamic lubrication condition must be established before conducting any abrasive wear tests. Thus, the purpose of

tests carried out in this chapter was to expose journal bearings to conditions which would provide data pertaining to the journal bearings' sensitivity to particulate contaminant entrained in the lubricating fluid.

A number of test methods have been developed and several adopted for evaluating the lubricating and wear property of lubricants, for instance, the Falex wear test, Four Ball tests, etc. However, almost no standardized procedures are available regarding the test of contaminant induced wear in a lubricating system. Probably one of the most commonly used methods for detecting and estimating harmful substances that may be found in lubricants is the Plastic Plate Abrasion test, standardized as ASTM D - 1404. Nevertheless, this test restricts its use to lubricating greases only, it is not applicable to other kinds of lubricants.

Due to the lack of effective methods for assessing the contaminate induced wear in a lubricating system, and an increasing demand for such technique being voiced by industry, a bench test entitled the Gamma Falex System was proposed by the FPRC in 1980. The Gamma Falex System is modified from the Falex System (ASTM D 2670-67). Major improvements on the tester include providing a fluid circulation system, a temperature controller, and a contamination control system, Figure 13.

The fluid circulation system is used to remove wear debris from the wearing surface. System bulk temperature is controlled by the temperature controller, thus ensuring a constant fluid viscosity during the test. The contamination control system consists of a filter circuit to provide the desired contamination environment that enables the investigation of the contaminant induced wear to be possible. By doing so, the Gamma Falex System therefore operates under well controlled conditions. As a result of these modifications, the accuracy of the test increased.

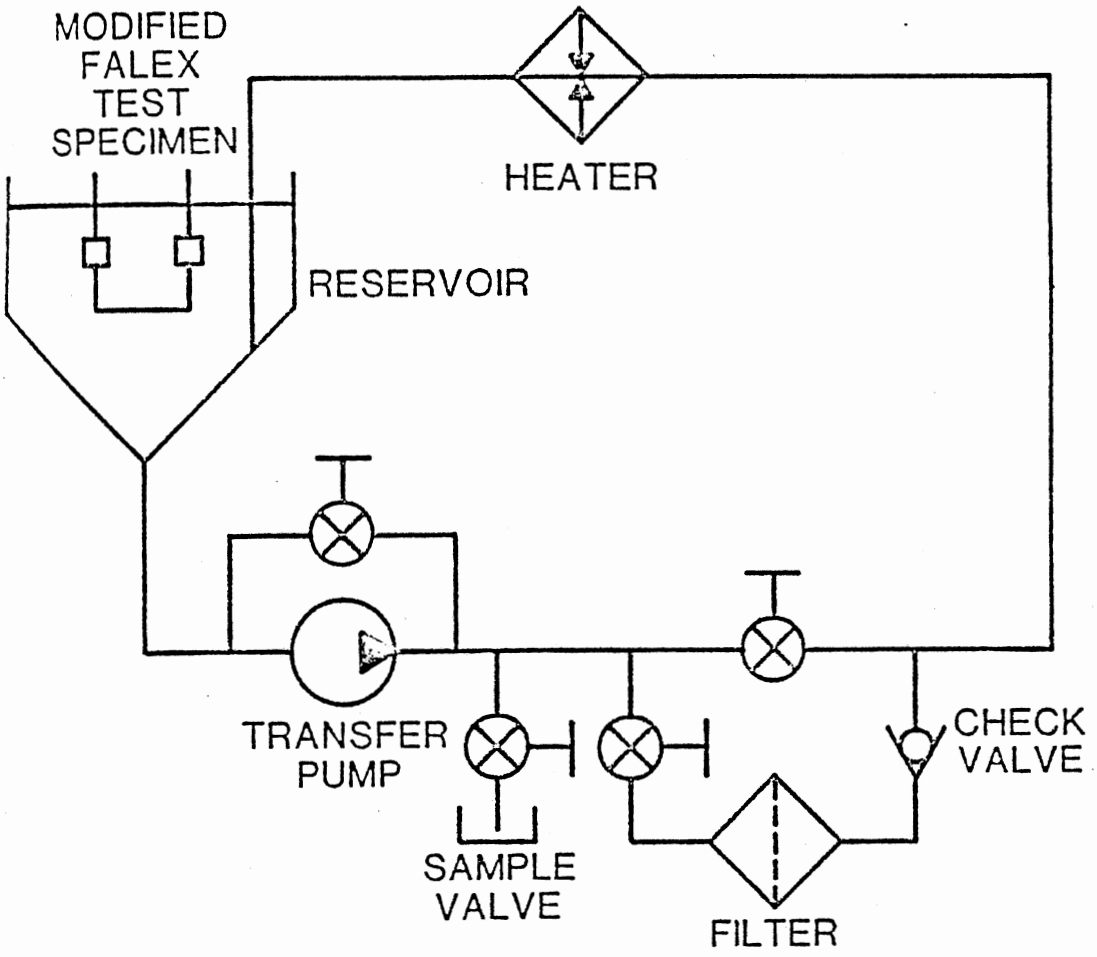

Figure 13. Schematic of Gamma Falex System

The basic operating principle of the Gamma Falex System is the same as that of the Falex system. It includes a steel journal and bearing loaded by a spring-gage micrometer. The journal is driven by a fixed speed motor at 290 rpm. The bearings are stationary and forced against the journal. The loading mechanism functions as a nut cracker. The spring force is loaded at the open end of the jaw to produce a high load pressure at the pivot point, where the bearings are located, near the end of the jaw. Normally, the bearings are v-shape blocks. Figure 14 illustrates the journal - bearing assembly of the Gamma Falex System.

The primary function of the Gamma Falex System was to detect the protection characteristic of a lubricant. As in the Falex System, the Gamma Falex System operates under boundary lubrication conditions. It is well known that adhesive wear is predominant under boundary lubrication, due to direct surface to surface contact. Wear takes place whenever there is a relative motion between bearing surfaces. Accordingly, it reduced the diameter of the journal. This changes the loading condition. Consequently, the system requires a way to detect the load change and to correlate it into a wear parameter. The device employed in the Gamma Falex System to accomplish this task is a ratchet mechanism which provides the required load to the bearing. The wear is measured by the number of teeth advanced to maintain the jaw load during the prescribed time.

During the past two years, a great number of tests have been carried out at the FPRC to qualify the performance of the Gamma Falex tests. The repeatability of the tester has been recognized after conducting a total number of 47 tests with four different fluids. The result shows that 86 percent of the tests fall within the normal distribution with a standard deviation of 0.043 (27).

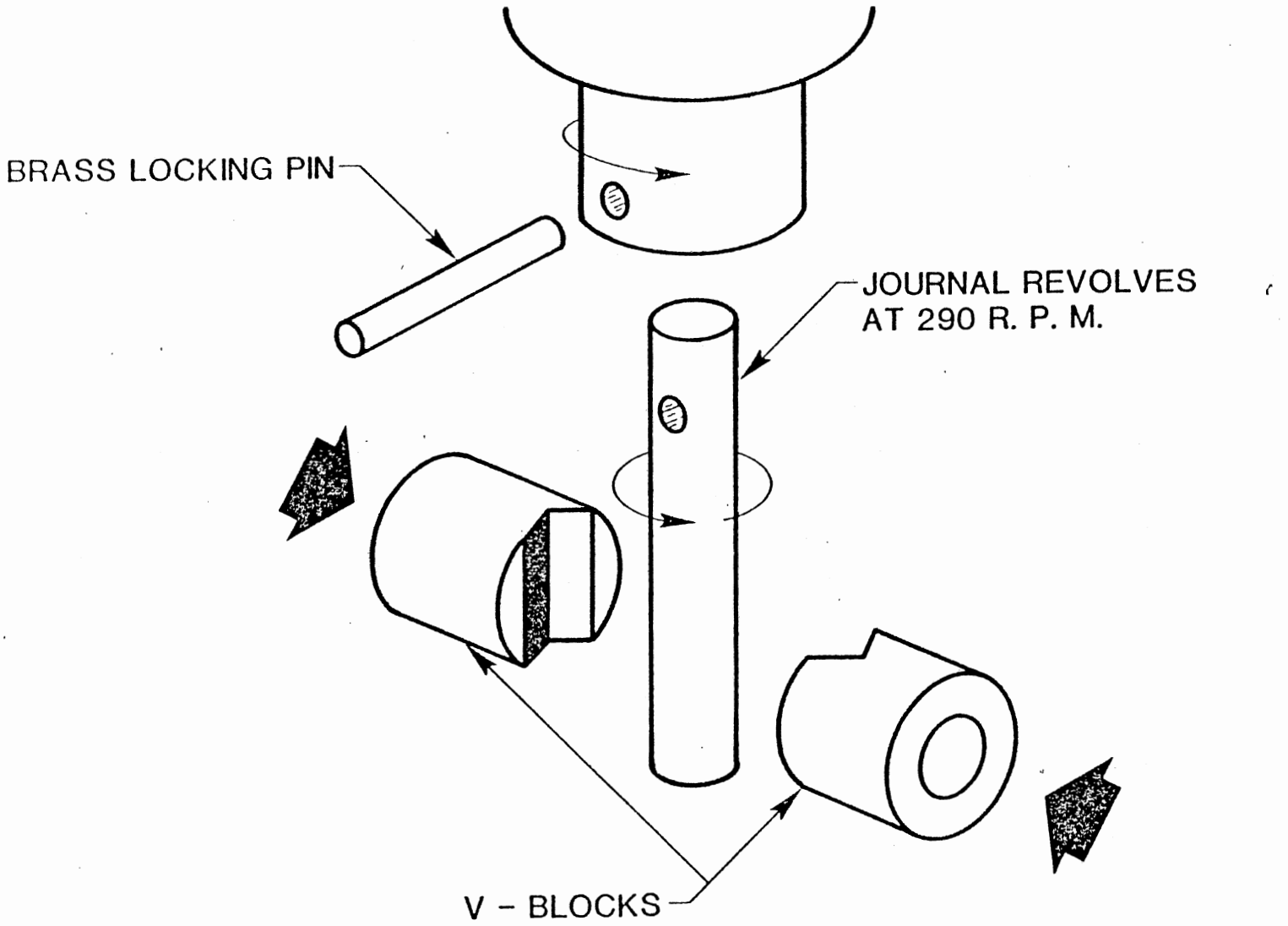

Figure 14. Test Specimens of Gamma Falex Wear Tester

Due to the high test repeatability obtained, Inoue (27) attempted to advance the Gamma Falex System from doing fluid lubricity tests to contaminated wear tests. Realizing the importance of the rotating speed might significantly affect the lubrication condition of the bearings, Inoue replaced the conventional fixed speed motor on the Gamma Falex System by a variable speed hydraulic motor. As a result, the rotating speed of the journal can be controlled. Normally, any rotating speed under 2500 rpm can be achieved. This improvement broadens the application of the Gamma Falex System in tribological wear research.

Figure 15 presents a typical result of the Gamma Falex test obtained by varying the rotating speed of the journal. The bearing was loaded at 100 lbs.. The wear behavior was monitored in a specific time interval at the journal rotating speed of 580, 1160, and 2320 rpm, respectively. The results revealed that a wear rate of 0.5, 0.35, and 0.77 were obtained at 580, 1160, and 2320 rpm respectively (27). The wear rate is designated by the wear reading, namely the teeth advanced, divided by the test time at the prescribed rotating speed. It was found that the wear rate at 1160 rpm was less than that at 580 rpm. He claimed the decrease of the wear rate was due to the increase of the film thickness at high speed. However, this was not the case. A higher wear rate at 580 rpm than that of the wear rate at 1160 rpm was due not exactly to the effect of an increasing film thickness at 1160 rpm. This may have been due to experimental error. This is evident by examing the Sommerfeld number for the stated operating conditions. Assume the lubrication condition of the v-shape journal bearing assembly has the same configuration as the 120 degree bearing. This is a gross overestimation as the bearing in actual function operates under line contact. Also, assume the radial clearance

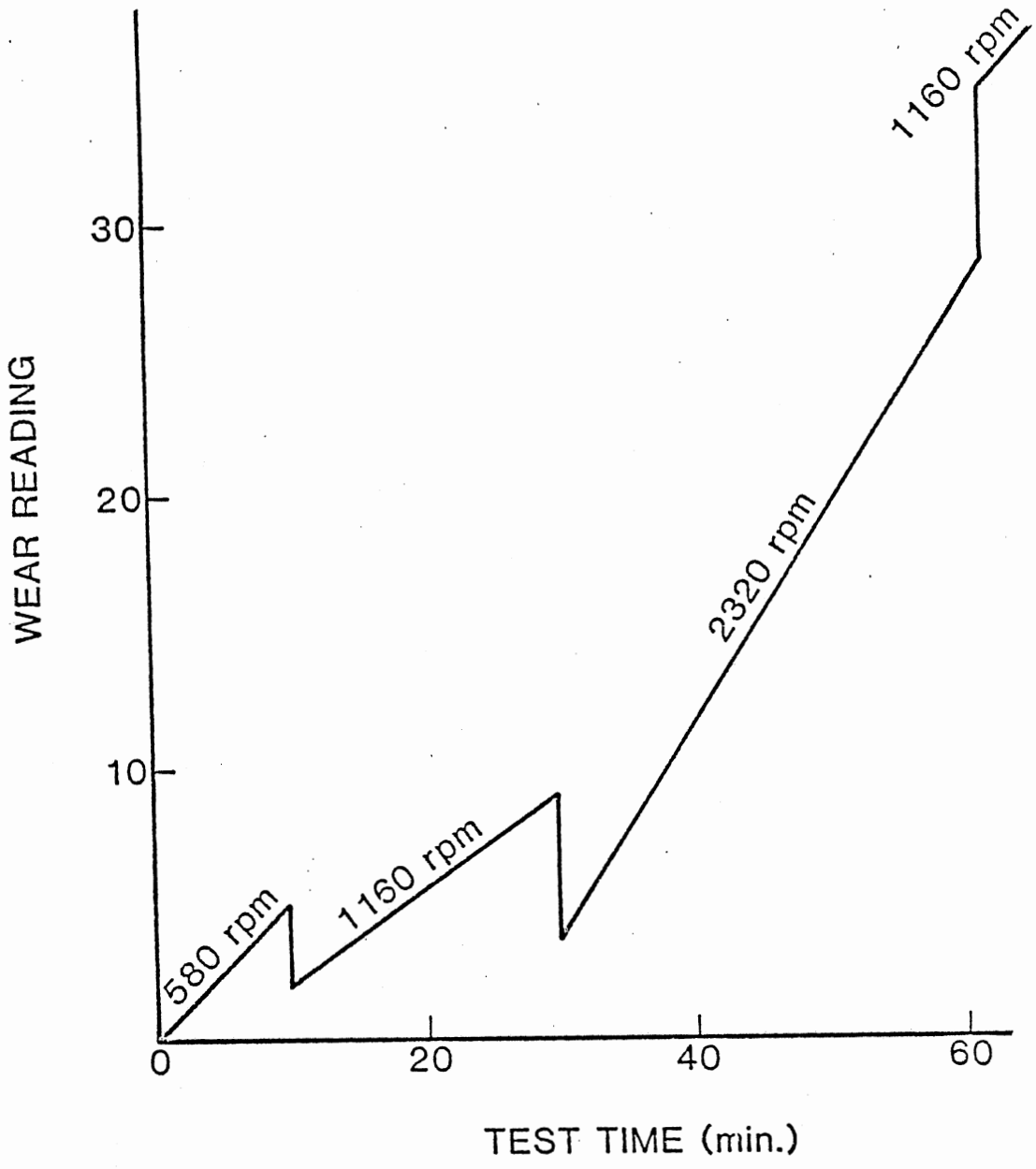

Figure 15. A Typical Result of Gamma Falex Test (27).

is 0.001 inches. Then, the calculated Sommerfeld number under a 100 lbs load at 1160 rpm is 0.0012. At this value of Sommerfeld number the journal is by all practical means operating fully eccentric. In other words, the bearing operated under full surface contact conditions when loaded with a 100 lbs load and rotated at a speed of 1160 rpm.

It is of interest in investigating the lubrication mode at different rotating speeds. Theoretically, no wear occurs at 0 rpm. By examining the wear rate - rotating speed data set obtained at 0, 290, 580, 1160, and 2320 rpm, it is found that a linear relationship exists among these data set. Excluding the data obtained at 580 rpm, four data points at 0, 290, 1160, and 2320 rpm were employed and correlated with each other by means of linear square curve fitting technique. The wear rate - rotating speed characteristic curve obeys the following equation.

$$W = 0.0003 \cdot U + 0.0035 \tag{4.3}$$

where W = wear rate, ratchets advanced per minute

U = rotating speed, rpm

The coefficient of correlation is as high as 0.9977. This strongly reveals that the linear relationship exists between wear rates and the journal rotating speeds under the operating condition; that the bearing is laoded at 100 lbs and the journal rotates at a speed less than 2320 rpm and the working fluid is MIL-L-2104. This linear property is plotted along with the test data and is shown in Figure 16.

It is a commonly accepted principle that the adhesive wear rate, W, is proportional to the sliding distance, L (16).

$$W \propto L \tag{4.4}$$

Mathematically, the sliding distance of a rotating journal bearing is expressed as

$$L = 2\pi RUt \tag{4.5}$$

L = sliding distance

R = radius of the journal

U = rotating speed

Comparing Equations (4.3), (4.4), and (4.5), it is found that Equation (4.3) indicates the wear behavior under previously stated conditions is a typical adhesive wear. In other words, the improvement made on changing rotating speed, did not allow the journal bearing to transcend from boundary lubrication into hydrodynamic lubrication.

It is well known that the effect of abrasive particles is not significant as long as the bearing is operating in the boundary lubrication condition. This is because under the boundary lubrication condition, the clearance between bearing surfaces is too small to allow the abrasive particles to entrain into it. In contrast to this, the abrasive wear is predominant in the hydrodynamic condition. Thus, in order to achieve the hydrodynamic condition, the currently used Gamma Falex System requires further modifications.

The reason for the failure in achieving the hydrodynamic lubrication, stems from the fact that the rotating speed is not the only parameter that affects bearing lubricating conditions. In Chapter II, it has already been mentioned that the lubrication characteristic of bearings is controlled by the bearing characteristic number which is a function of unit load, rotating speed, fluid viscosity, and surface roughness. This characteristic is well described by the Stribeck curve, Figure 1. It is seen that there are two operating parameters, the unit load and the rotating speed, which depend on the mechanical design of the operating system.

The other parameter is the fluid viscosity which is the physical property of the test fluid. This can simply be controlled by the

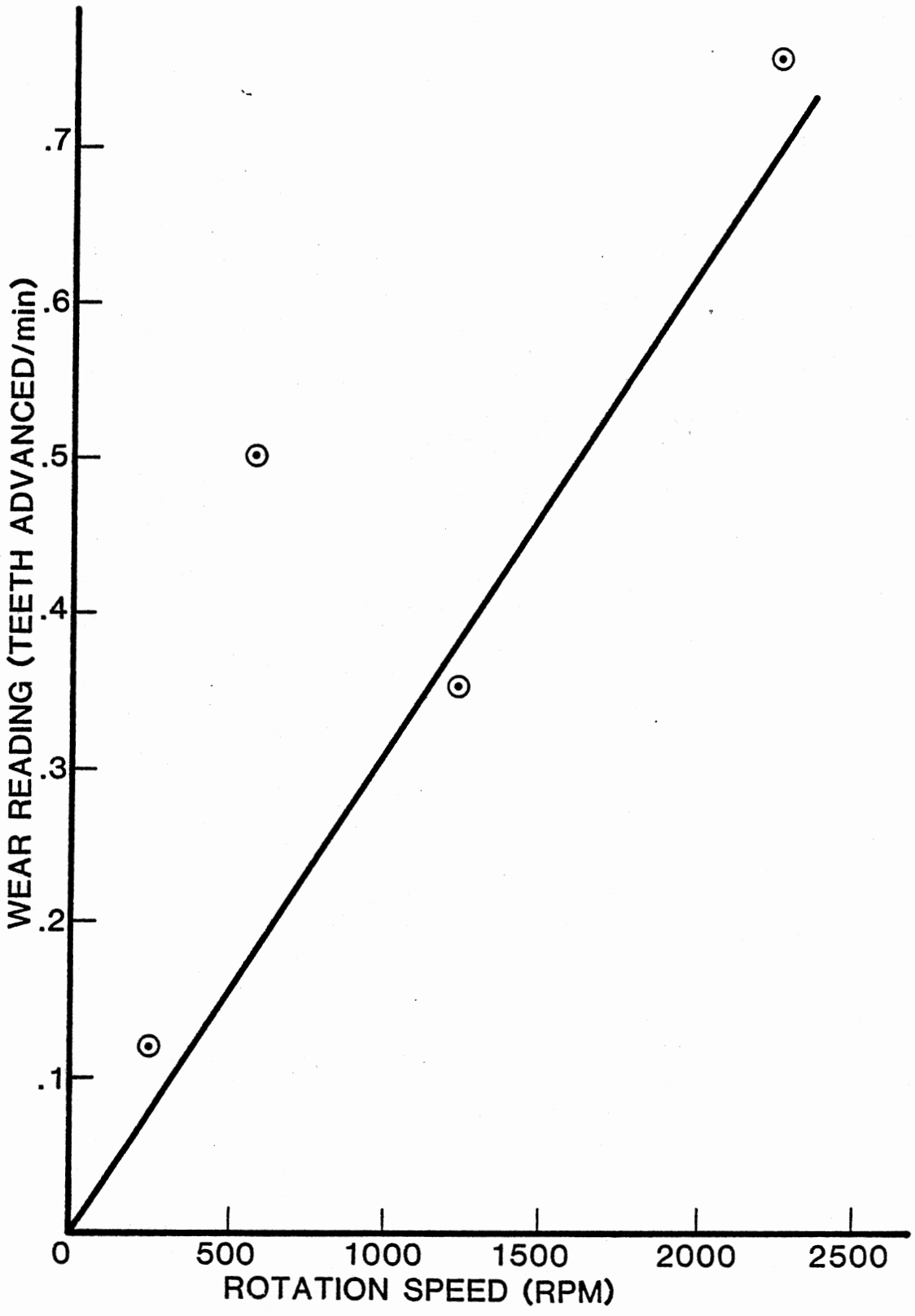

Figure 16. Gamma Falex Test Data with Variable Speed

temperature controller as stated previously. Further, the information of the component surface roughness is required. This parameter is determined by the manufacturing process and the material used. Accordingly, in order to achieve the hydrodynamic lubrication, parameters that may affect the value of the bearing characteristic number should be taken into account rather than just considering a single parameter only. Since fluid viscosity and surface roughness can be specified by external devices other than the Gamma Falex System, no technical improvement on these two parameters were made in this study. Therefore, special attention was paid to the modification of the loading mechanism so that it could be compatible with the rotating speed, thus a satisfactory bearing lubrication condition can be predicted and maintained.

The highest journal rotating speed that the currently used Gamma Falex System can achieve is 2400 rpm. This speed is fairly representative of most applications of a mechanical system because the rotating speed of most mechanical elements is under 4000 rpm except in some special applications. On the other hand, it would be impractical to modify the Gamma Falex System by increasing the rotating speed to a much higher value since it would require redesigning most of the physical structure. Consequently, there was a necessity to modify the loading mechanism.

From the discussion in Chapter II and Chapter III, it is realized that a high rotation speed and light load pressure system, means the bearing will operate in the hydrodynamic mode of lubrication. This is shown in the Stribeck curve. In practice, there are two approaches used to reduce the loading pressure on the bearing. They are by increasing the bearing surface or by reducing the external load. Of course, it is also possible to do both of them simultaneously.

Figure 17 illustrates the loading mechanism of the Gamma Falex System. It is found that the bearing is loaded by a spring force and the magnitude of the force is detected by a micrometer dial gauge according to the displacement of the spring. Based on Hook's Law, for a linear spring, the spring force is proportional to its displacement. As a result, if two springs have different stiffness but are compressed by the same amount of length, then the spring forces are different. This enables one to reduce the external load imposed on the bearing by replacing a heavier spring with a lighter spring. The load reduction factor is proportional to the ratio of the stiffness coefficient of springs.

It is noted that the bearing used in the Gamma Falex System has a v-shape. From the standpoint of bearing design, a v-shape bearing has a very poor contact area because there are only four "lines" contacted between the journal and the bearing. Theoretically, a line contact results in an infinitive contact pressure between journal and bearing at the specific lines due to the contact area being infinitively small. Accordingly, with a v-shape bearing hydrodynamic lubrication can only be achieved if the load is infinitely small. Furthermore, once the wear occurs, the bearing configuration changes. The schematic illustration of these two shortcomings in using the V-block in hydrodynamic design is shown in Figure 18. All these drawbacks made the study of hydrodynamic lubricant very cumbersome. As a result, a 120° journal bearing was selected as the test specimen. The reason is that it avoids a direct side to side contact and there is a great number of technical data available for such a bearing configuration. In addition, the ratio of bearing length to diameter, namely L/D, is equal to two. This selection was intended to keep the modified journal bearing with the same dimension as the conventional Gamma

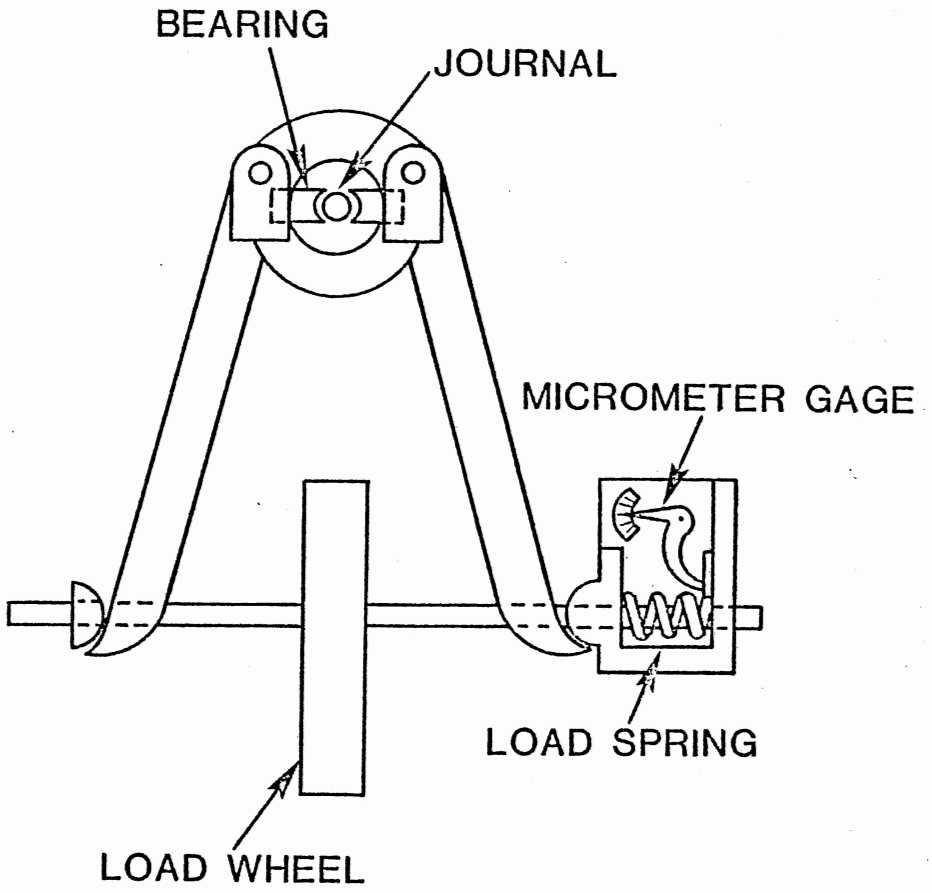

Figure 17. Loading Mechanism of Gamma Falex System

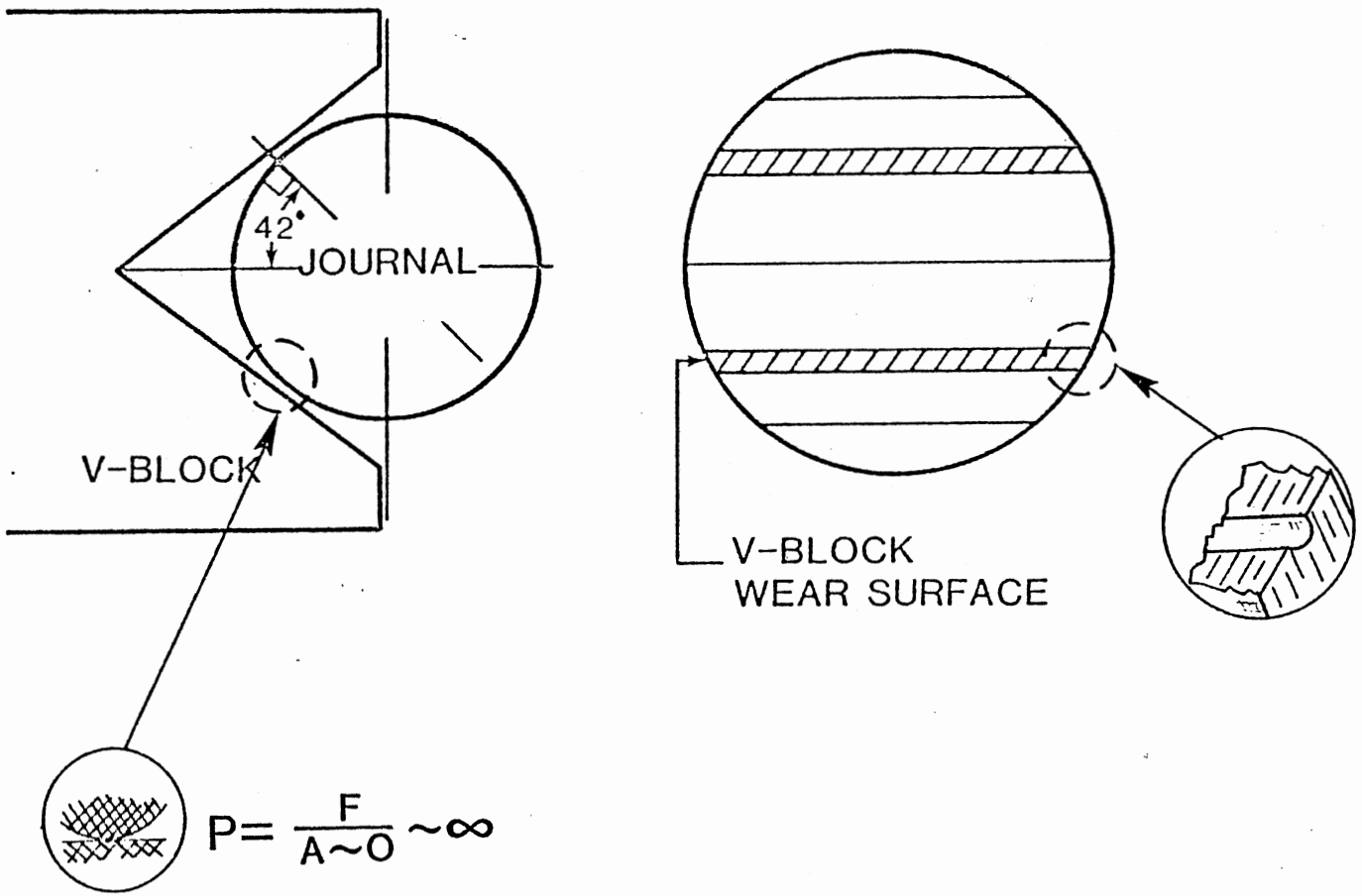

Figure 18. Shortcomings of Using V-Block in Gamma System

Falex System. Thus, no physical structure of the system needs to be modified.

The advantages of the new version of the Gamma Falex System, named the Gamma System, are delineated as follows:

1. It provides a light loading mechanism, such that the test load can be accurately controlled and allow hydrodynamic lubrication.
2. It provides a formalized load acting area.
3. It maintains the geometric configuration of the bearing during the test.
4. It maintains the same mechanical dimension as the previous Falex System that reduces the effort in modifying the system.
5. The 120° bearing configuration avoids a direct side to side contact as a 180° bearing. This implies that the function, valid for the Falex System, is still valid for the Gamma System.
6. There is a considerable amount of technical data available for a 120° bearing, thus the operating conditions can be theoretically determined without the need for numerical solution of the relevant Reynolds equation.
7. It provides hydrodynamic lubrication under proper operating conditions, thus, the wear severity of a journal bearing caused by abrasive particles in the lubricant can be explicity revealed.

Intuitively, after making the change of the loading system and the bearing configuration, the Gamma System is now more than adequate for the detection of abrasive wear in hydrodynamic lubricating. However, care must be taken before using the Gamma System in monitoring abrasive wear behavior. It is noted that the wear mechanism changes from adhesion to abrasion when the lubrication mode changes from boundary to hydrodynamic, if the

lubricant is contaminated by the entrained particulates. Tribologically, adhesive wear is caused by a surface to surface contact. Accordingly, wear takes place over the entire bearing surface. Therefore, a "surface" clearance is formed between the bearing surfaces. Thus, the Falex machine detects this difference and converts it into wear parameter, namely, the ratchets advanced to compensate the surface clearance. In contrast to this, abrasion causes a "local" cutting wear rather than a surface wear. Although the cutting process occurs, the dimension of surface profile remains as before. The conventional Falex wear monitor is insensitive to such local wear. This phenomena is illustrated in Figure 19. Therefore, a new technique used to detect abrasive wear is required.

There are many ways to designate wear rate, for instance, by weight loss, volume loss, area changed, amount of wear debris, etc. Also, a large number of wear monitoring techniques are available. However, the most direct technique is by means of the weight loss. Namely, the wear index is designated by the weight difference of the tribological component before and after the test. This method was employed in this study.

The Gamma System utilizes the same loading mechanism as the Gamma Falex System but with lighter load spring and different bearing configuration. However, the abrasive wear severity is detected by the weight loss from the component instead of the reading of the rachet advanced.

Development of Experimental Facility

The Gamma System consists of a loading system, a lubricant circulation system, a contaminant circulation system, a temperature control system, and a journal bearing assembly with the lubrication reservoir. Figure 20 shows a schematic diagram of the Gamma System. In addition, it

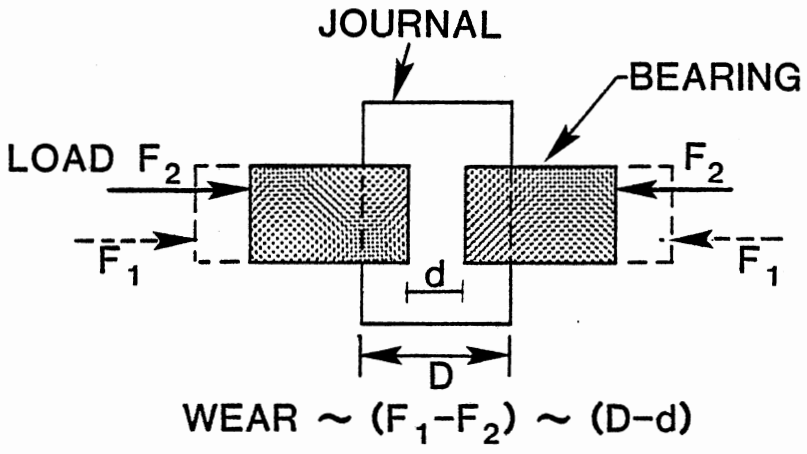

(a) WEAR PROCESS UNDER SURFACE CONTACT ACTION

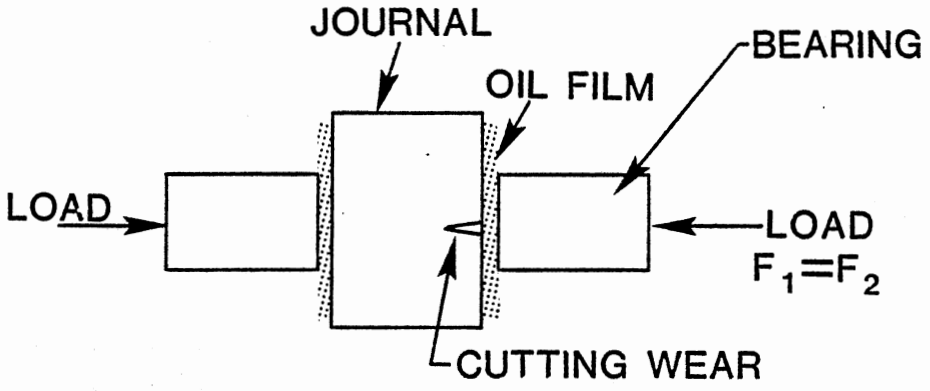

(b) WEAR PROCESS UNDER HYDRODYNAMIC ACTION

Figure 19. Wear Process Under Surface Contact and Hydrodynamic Lubrication

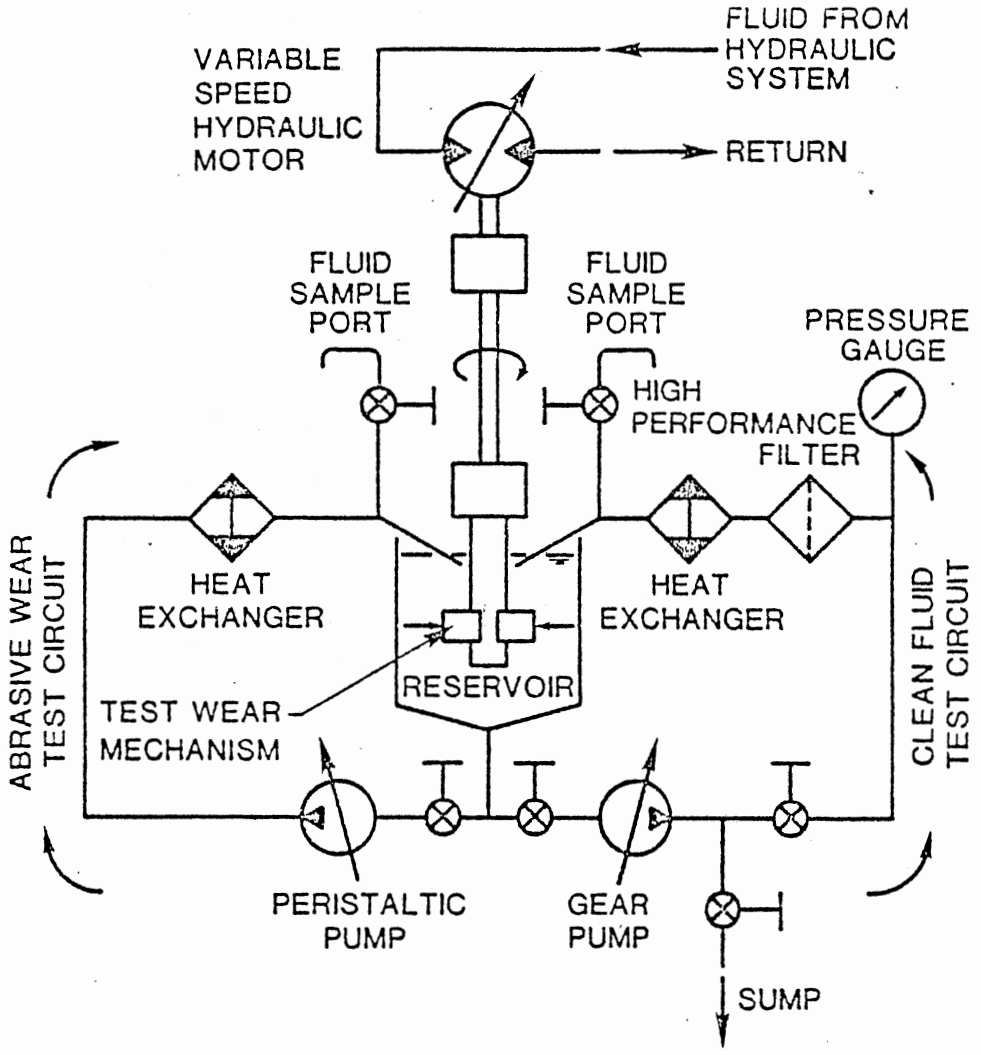

Figure 20. Schematic of Gamma System

also requires a balance with a resolution of 10 micrograms or better to monitor the weight loss of test specimen.

The loading system imposes the desired load condition on the bearing. The system is composed of a set of loading arms, a spring-gage micrometer to control the loading condition and a ratchet to constrain the distance between the loading arms.

The lubrication system serves to circulate lubricant and wash off the wear debris generated on the wearing surface. In addition, it consists of a gear pump and a filter. Thus, it also can be used to clean-up the system.

The contaminant circulation system includes a peristaltic pump to circulate the injected contaminant during the contamination tests.

The temperature control system maintains the operating bulk temperature at the specific condition by means of a heater and an air cooler. This system ensures fluid viscosity constant during the test.

The journal bearing assembly has a journal which is driven by an external variable speed hydraulic motor. The rotating speed varies within the range of 0 to 2400 rpm. In addition, it has two bearings which are stationary and loaded by the jaws.

The material of the journal is AISI 3135 steel, Rockwell hardness numbers 87 to 91 on the B-Scale. The bearing is brass, Rockwell hardness number 70 on the B-Scale. The choice of a steel-brass combination for journal bearing assembly is primarily that it is a common pairing of materials in industrial applications. The material properties and geometrical dimension of the journal and bearing are tabulated in Table I. Figure 21 illustrates the geometrical configuration and dimension of the bearing.

Generally, the operating conditions listed in Table II are followed

TABLE I

THE JOURNAL BEARING ASSEMBLY
SPECIFICATION

Description	Journal	Bearing
Material	AISI 3135 steel	Free Cutting Brass
Hardness	87 - 91 HRB	70 HRB
Radius	0.1245 ins.	0.1255 ins.
Surface Roughness	5 ~ 10 μins. (0.13 ~ 0.25 μm)	50 ~ 100 uins (1.3 ~ 2.5 μm)

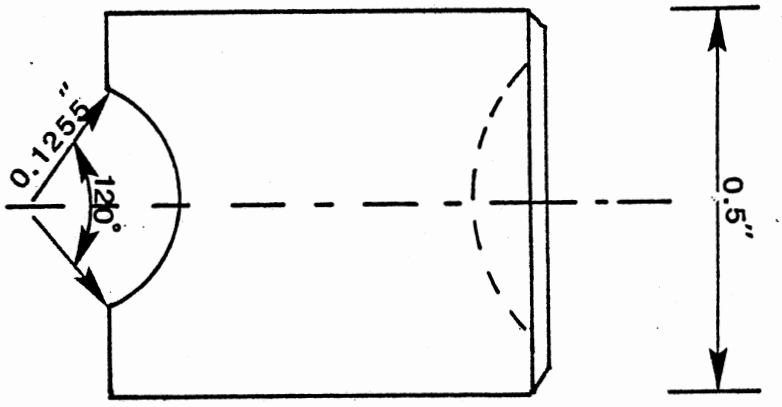

BEARING

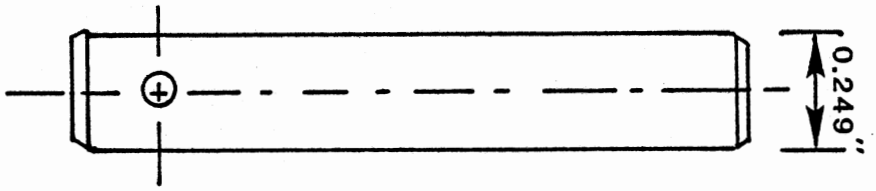

JOURNAL

Figure 21. Test Specimens of Gamma System

TABLE II

THE OPERATION PARAMETERS
OF THE GAMMA MACHINE

Parameter	Specification	Unit
Rotation Speed	$2{,}400 \pm 10$	RPM
Operating Temperature	40 ± 2	^{o}C
Load	$0.5 \cdot (\text{viscosity}/2\text{x}10^{-6}\text{reyns})$	LBS
Break-in Speed	500	RPM
Break-in Period	5	Minutes
Test Time	30	Minutes
Contaminant	ACFTD	Full Distribution

throughout the entire test except when otherwise specified. From the data shown in Tables I and II, the required loading condition can be determined. Before doing the actual parameter calculation, two auxiliary figures are required: Figures 22 and 23 (7, 14). Figure 22 gives the required film thickness to achieve hydrodynamic lubrication. Figure 23 is used to determine the required load to ensure and maintain hydrodynamic lubrication. Figure 23 is obtained from the work of Raimondi and Boyn (14) who numerically solved the Reynolds equation for the finite journal bearings of a variety of bearing angles and L/D ratio. This figure graphically represents the relationship between the minimum film thickness to the bearing characteristic number and journal eccentricity ratio.

From Figure 22, it was found that a film thickness ratio greater than five is required to achieve the hydrodynamic lubrication. This has been discussed in Chapter II. The average surface roughness of the journal is 0.5 micrometers, and 0.71 micrometers for the bearing after break-in. Thus, the total average surface roughness is 1.21 micrometers. This implies that the hydrodynamic lubrication occurs as long as the minimum fluid film is thicker than 6.05 micrometers.

Suppose that a fluid film thickness of 15 micrometers is of interest, and the working fluid is MIL-H-5606 with a viscosity of 14.3 centistokes at 40 degrees centigrade then, the required load is calculated as follows.

Equation (3.10) correlates the minimum fluid film thickness, h min, with the radial clearance, c, and eccentricity ratio, ε. This equation can be rewritten as

$$\varepsilon = 1 - (h \text{ min} / c) \qquad (4.6)$$

From Table I it is known that the radial clearance is 25.4

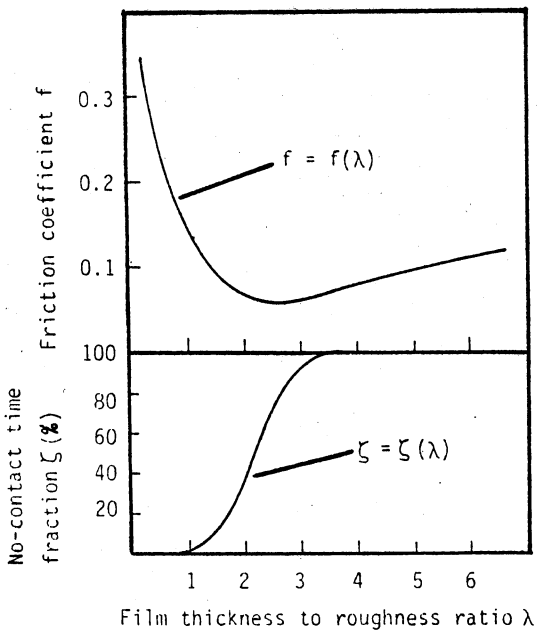

Figure 22. Stribeck Curve and No-contact Time Fraction

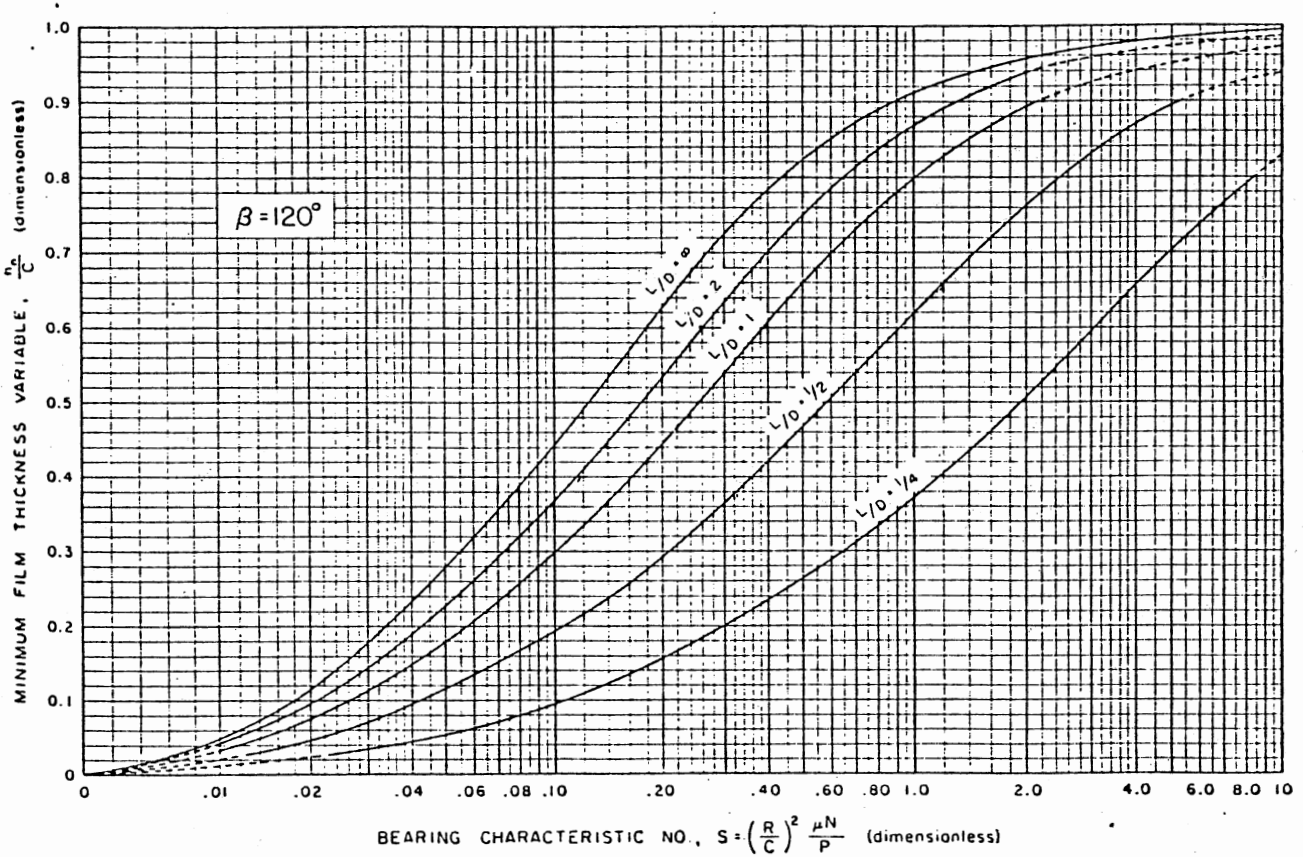

Figure 23. S - ε Graph of 120° Journal Bearing

micrometers. Thus the eccentricity ratio is 0.41. This implies a bearing characteristic number of .26 in Figure 23.

Rearrange Equation (3.7), and express the load in terms of the bearing characteristic number as

$$W_f = \left(\frac{R}{C}\right)^2 \frac{\eta NA}{S} \tag{4.7}$$

where W_f = Load

R = Journal radius

C = radial clearance

η = viscosity

N = rotation speed

A = projected bearing area

S = Sommerfeld number

From Equation (4.7), the required load is obtained. In this case, it has a value of 0.527 lbs.. This indicates that the Gamma Falex System was totally overloaded at 100 lbs. Thus, it is not surprising that a satisfactory hydrodynamic lubrication condition could not be achieved in the previous work.

For convenience of setting the test gauge, a 0.5 lb force is set to load the bearing if the working fluid is MIL-H-5606. By a reversed calculation as shown above, the minimum film thickness under such conditions is 13.2 micrometers.

There are four springs of different stiffness constants available for the Gamma System. The specification and its related load range are shown in Table III. It is seen that spring D meets the requirement to provide a light spring load to achieve hydrodynamic lubrication.

TABLE III

THE STIFFNESS OF LOAD SPRINGS

Spring	Spring Constant(LBS/IN)	Load Range(LBS)
A	500	50 - 800
B	60	6 - 96
C	15	1.5 - 24
D	2.5	0.25 - 4.0

Qualifying Experimental Facility

A number of tests were carried out to qualify the performance of the developed Gamma System. For the foregoing discussion, it is realized that the entire purpose of this chapter is to develop a facility which may establish hydrodynamic lubrication and allow the investigation of the abrasive wear in the journal bearing. As a result, the qualifying test of the Gamma System is divided into three major parts: (1) to ensure the formation of a hydrodynamic lubrication condition, (2) to ensure the system is able to monitor abrasive wear and (3) ensure repeatability.

To accurately investigate the abrasive wear of the journal bearing, a break-in test prior to doing any abrasive wear test is a necessity. This is due to the fact that any new components exhibit a high wear rate during initial running, namely, the break-in period. It is caused by a surface to surface contact. After the break-in period, the bearing surface has been smoothed. And then a low wear rate period occurs until the tertiary failure period, Figure 24. For practical reasons, it is recommended to perform the wear test after conducting the break-in test. Therefore, it is necessary to determine the break-in period and the operating condition to conduct the break-in test.

Three sets of journal bearings were tested for this purpose. The surface roughness of the bearings were measured at the beginning, and the test was then conducted under a low speed condition, usually at 500 rpm. The surface roughness of the bearings was examined every two minutes for six minutes. The break-in period is set at the time that the surface roughness value remains reasonably constant. In other words, it reaches the steady state value. Test results of the break-in test are tabulated in Table IV and illustrated graphically in Figure 25. It is seen that

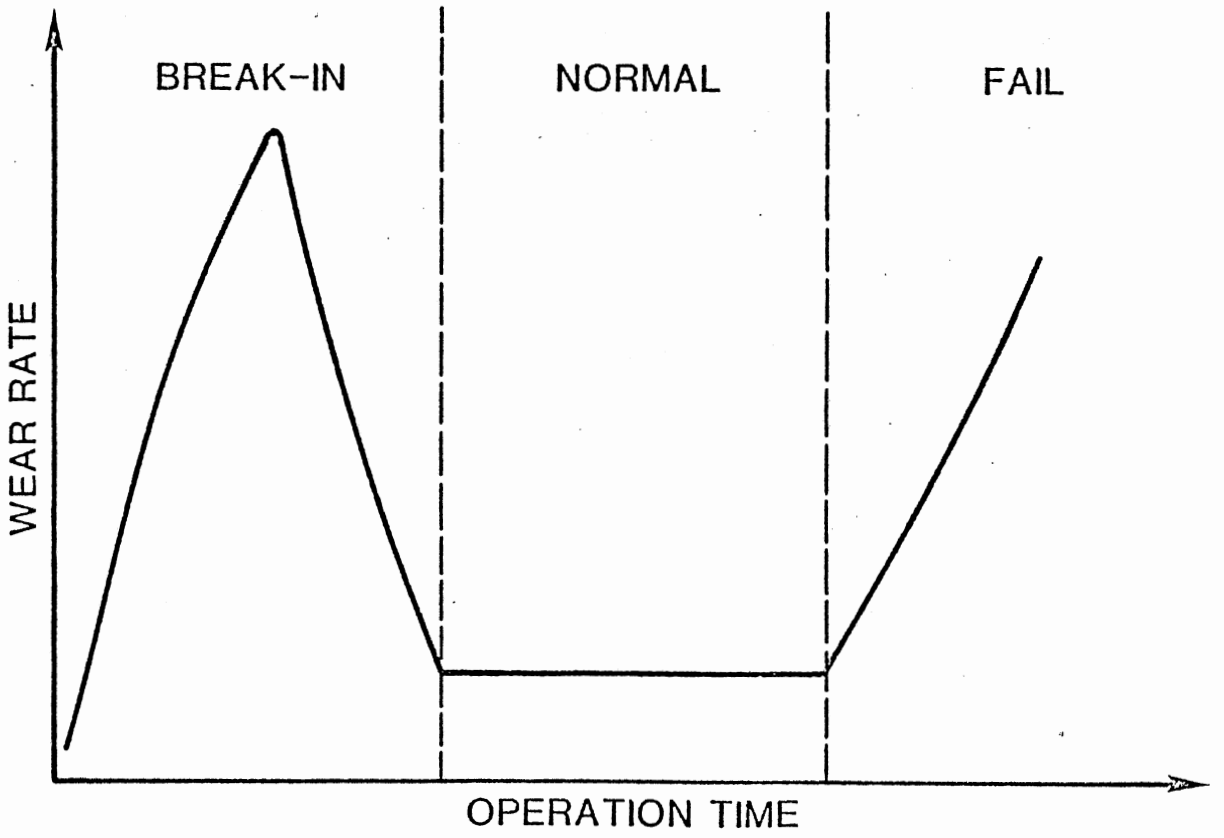

Figure 24. Component Wear Modes

TABLE IV

BEARING BREAK-IN TEST RESULT

Bearing ID NO	Test Time (min) 0	2	4	6
A1	1.20*	0.37	0.78	0.66
B1	1.12	0.84	0.71	0.58
A2	2.19	1.04	0.63	0.69
B2	1.26	0.45	0.56	0.75
A3	1.02	0.93	0.77	0.66
B3	1.35	1.14	0.83	0.92
Average	1.35	0.8	0.71	0.71

*Surface roughness, μm

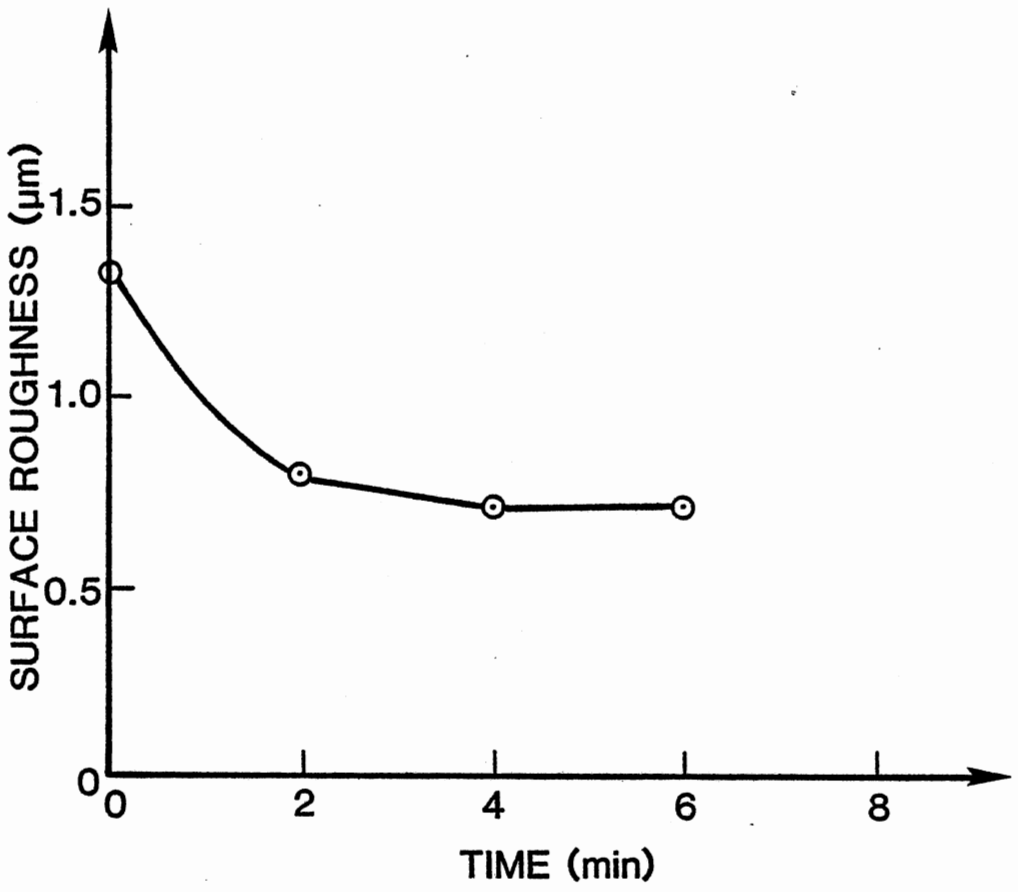

Figure 25. Gamma System Break-In Test Data

the surface roughness reaches a stable state after four minutes. Therefore, the choice of the break-in period of five minutes is sufficient.

The reason for running the break-in test at 500 rpm is mainly that under such rotating speed, the bearing operates in the mixed mode or in the boundary lubrication mode. Therefore, the asperities on the surfaces can be smoothed.

No wear can be observed in hydrodynamic lubrication condition providing that the lubricant is contaminant free since the bearing susrfaces are separated by a fluid film. Based on this concept, the lubrication mode can be distinguished. Six tests were performed to ensure the formation of hydrodynamic lubrication under the prescribed load condition.

From the calculation made in the previous section, it was found that a 0.5 lbs test load introduced a film thickness of 13.2 micrometers. Furthermore, a smaller test load results in a thicker fluid film. Thus, no wear occurs if the test load is less than 0.5 lbs. On the other hand, if the test load is larger than 0.5 lbs, it results in a thinner fluid film and brings the lubrication mode from hydrodynamic into the mixed or the boundary depending upon the film thickness ratio. From Figure 23, it is calculated that a 4.0 lbs test load forces the system into mixed mode. As a result, wear takes place. Therefore, test laods of 0.35 lbs, 0.5 lbs, and 4.0 lbs were imposed on the bearing respectively. And then wear behavior was monitored on the Gamma system by means of the teeth advanced on the ratchet wheel. It was expected that wear occurred at 4 lbs test load condition.

Each test was performed for twenty minutes and the difference of ratchet readings was recorded in a two minutes interval. Test results were

tabulated in Table V, and were illustrated graphically in Figure 26.

The test data revealed that there was a positive gamma slope, namely wear took place, at 4 lbs load. On the other hand, excluding the few initial points, it revealed a negligibly small amount of wear at both cases of 0.35 and 0.50 lbs load. It experimentally verified that the Gamma System is able to operate under different lubrication conditions. Moreover, the achievement of establishing the hydrodynamic lubrication has never been done by either the Falex tester or the Gamma Falex tester.

In order to assure the above findings, identical tests of different bearings were performed again. The test loads were 0.35, 0.50 and 4.0 lbs. However, at this time, the wear was detected by means of measuring the weight loss of the journal after a twenty minute test. The results were shown in Table V. As can be seen, no weight loss was observed at 0.35 lbs and 0.5 lbs condition. However, an amount of 120 micrograms weight loss appeared at 4 lbs condition. This again proves the validity of using the Gamma tester to investigate the hydrodynamic lubrication behavior.

Furthermore, abrasive particles were introduced into the Gamma System. The ACFTD was used as the abrasive particles. Eleven identical tests were conducted with mineral base fluid MIL-H-5606 at 2400 rpm and 0.5 lbs test load. The concentration of the injected ACFTD was 100 mg/L. This level is explained later. The purpose of these tests was to evaluate the repeatability of the Gamma System with respect to the abrasive wear. The weight loss of the journal was used to represent the amount of wear caused by the abrasive particles in the lubricating system. Test results were listed in Table VI, and plotted in Figure 27. It is observed that the mean value of the wear is 297.3 micrograms with a standard deviation of 13.5 micrograms.

TABLE V

TEST RESULT OF BEARING WEAR BEHAVIOR
UNDER DIFFERENT LOADS

Time(Min)	Load(LBS) 0.35	0.5	4
0	0	0	0
2	1*	0	1.5
4	2	1	2.0
6	2	1	3.0
8	2	1	3.5
10	3	1	4.0
12	2.5	1.5	4.5
14	3	2	5.0
16	3	2	5.5
18	3	1.5	6.5
20	3	2	7.0
Weight Loss	0	0	120**

* Number of gear teeth advanced
** Weight loss of journal after 20 min test, wunit in micrograms.

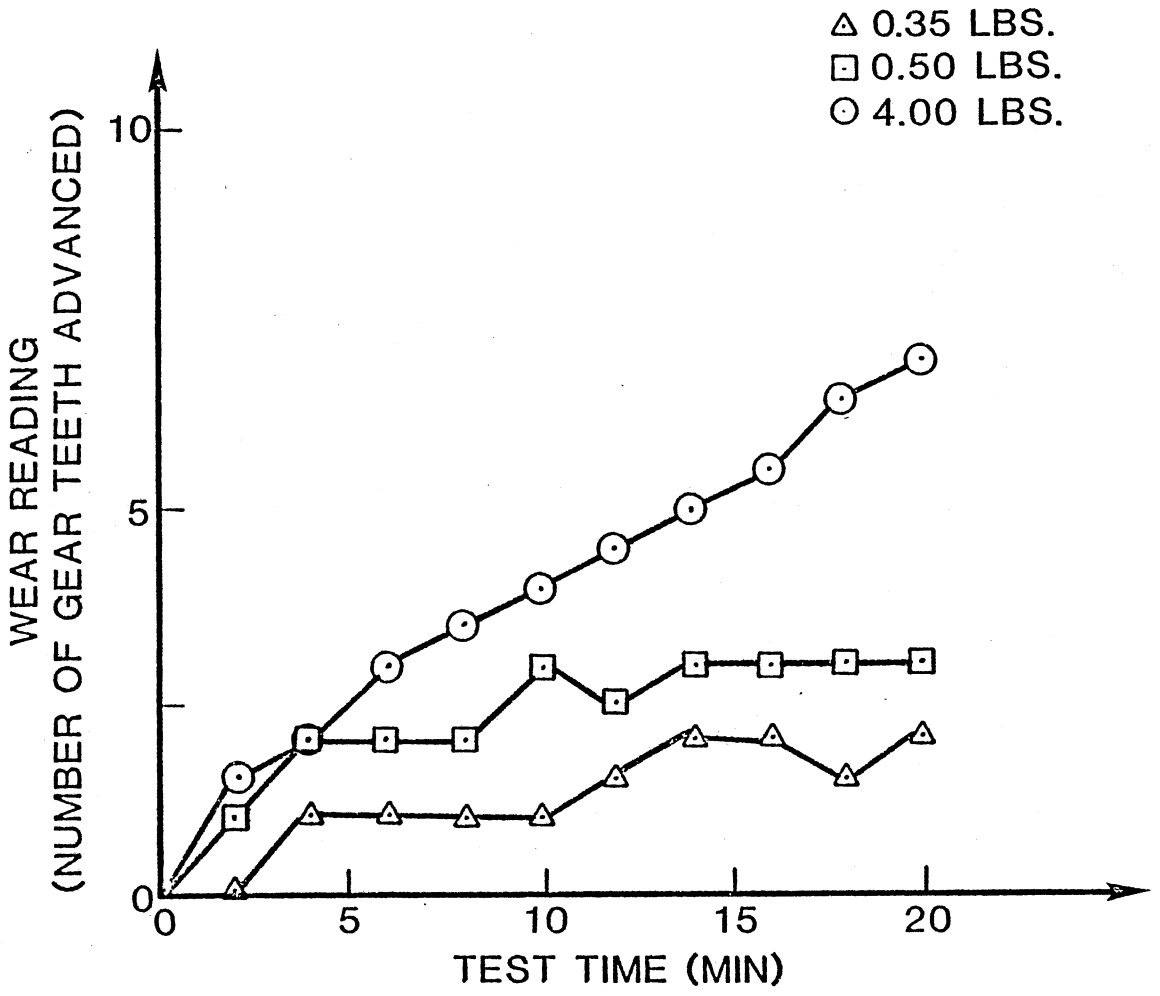

Figure 26. Gamma Wear Test Data of Different Loads

TABLE VI

GAMMA MACHINE REPETITION TEST RESULTS

TEST ID NO.	Journal Weight (grams) After Break-in	After Test	Weight Loss(μg)
WRP-01	7.42741	7.42713	280
WRP-02	7.43213	7.43184	290
WRP-03	7.40475	7.40445	300
WRP-04	7.43213	7.43184	290
WRP-05	7.40475	7.40445	300
WRP-06	7.42741	7.42713	280
WRP-07	7.44469	7.44439	300
WRP-08	7.42529	7.42500	290
WRP-09	7.71960	7.71928	320
WRP-10	7.36721	7.36689	320
WRP-11	7.42611	7.40743	300

Sampling Mean = 297.3 μg

Standard Deviation = 13.5 μg

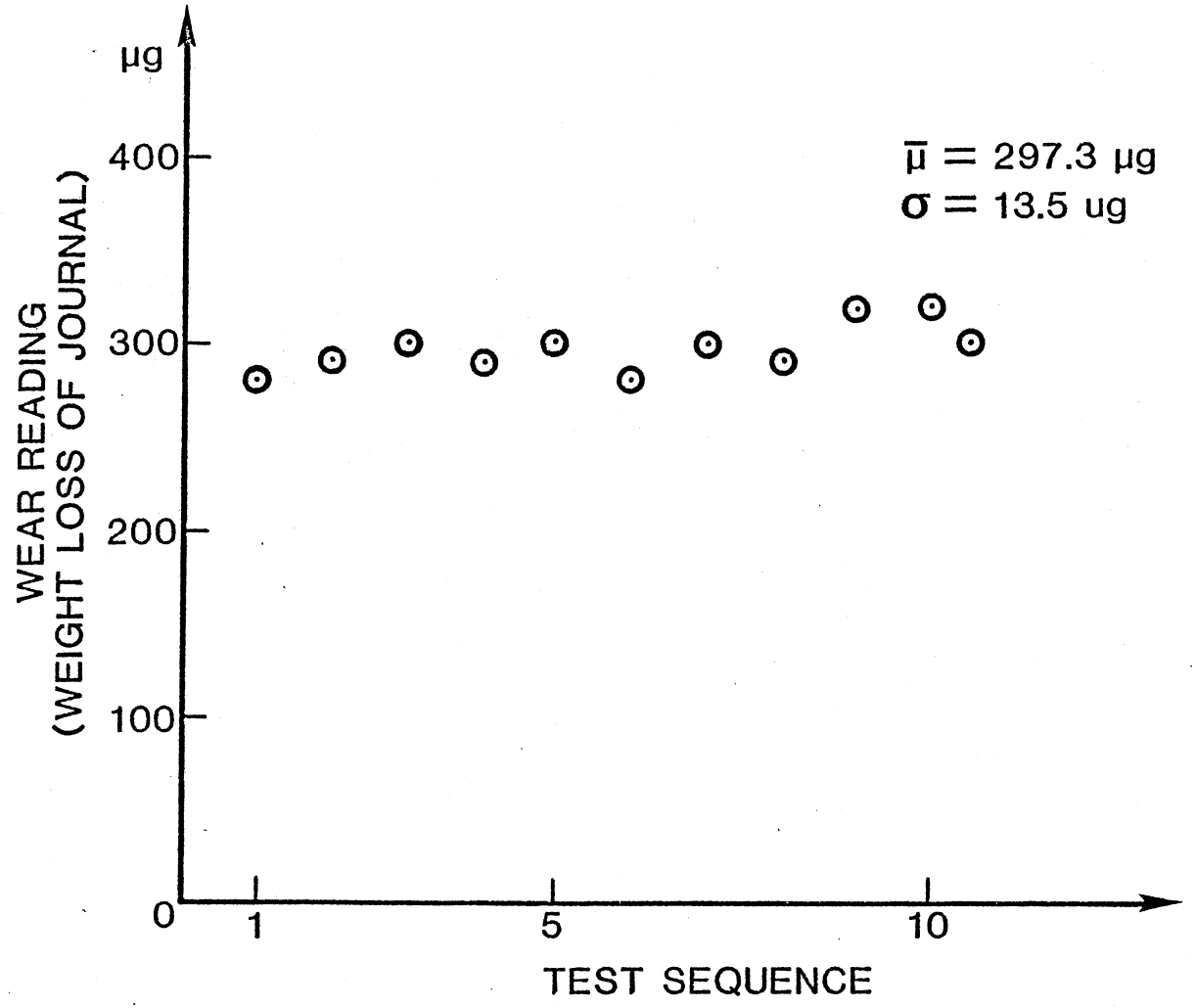

Figure 27. Repetition Test Data of Gamma Wear Tester

Tribological Wear Tests and Analysis

In Chapter III, it is noted that the tribological wear in a hydrodynamic lubricating system behaves as a three-body cutting mechanism. This section was intended to verify the wear model, Equation (4.2), experimentally. Furthermore, the three-body cutting process was investigated qualitatively.

The wear model states that the tribological wear rate of a rotating journal bearing is proportional to the entrained particle concentration if the fluid film thickness is constant for all the cases. Thus, tests were conducted under identical hydrodynamic lubricated conditions but at different contamination levels.

Primarily, eight tests were carried out with the mineral base fluid MIL-H-5606 at 2400 rpm and 0.5 lbs test load. The concentration of ACFTD injected were 40, 100, 200, and 300 mg/L for each test. And the identical tests were repeated. Eight sets of journal bearings were used and the weight loss of each journal was recorded and shown in Table VII.

The test data were plotted in Figure 28. It was found that the wear rate increased when the contaminant concentration increased up to a contamination level of 200 mg/L; from here it decreased. In order to ensure that data obtained at 300 mg/L concentration level were not due to the experimental error, two tests of 150 mg/L and 250 mg/L concentration level were performed individually. The results of these two tests (in Table VII) showed that the wear rate of 150 mg/L had the same tendency as those from 0 mg/L up to 200 mg/L. However, the wear of 250 mg/L followed the tendency from 200 mg/L to 300 mg/L. This phenomenon is not surprising. Figure 29 illustrates the mechanism that causes the decrease of wear rate at a high particle concentration level. As discussed in Chapter III,

TABLE VII

TEST RESULT OF WEAR SENSITIVITY TO
PARTICLE CONCENTRATION WITH
MIL-H-5606 OIL

Test ID No.	Particle Concentration (mg/L)	Journal Weight Loss (μg)
WCN-01	40	110
WCN-02	100	280
WCN-03	200	610
WCN-04	300	300
WCN-05	40	110
WCN-06	100	290
WCN-07	200	490
WCN-08	300	430
WCN-09	150	410
WCN-10	250	470

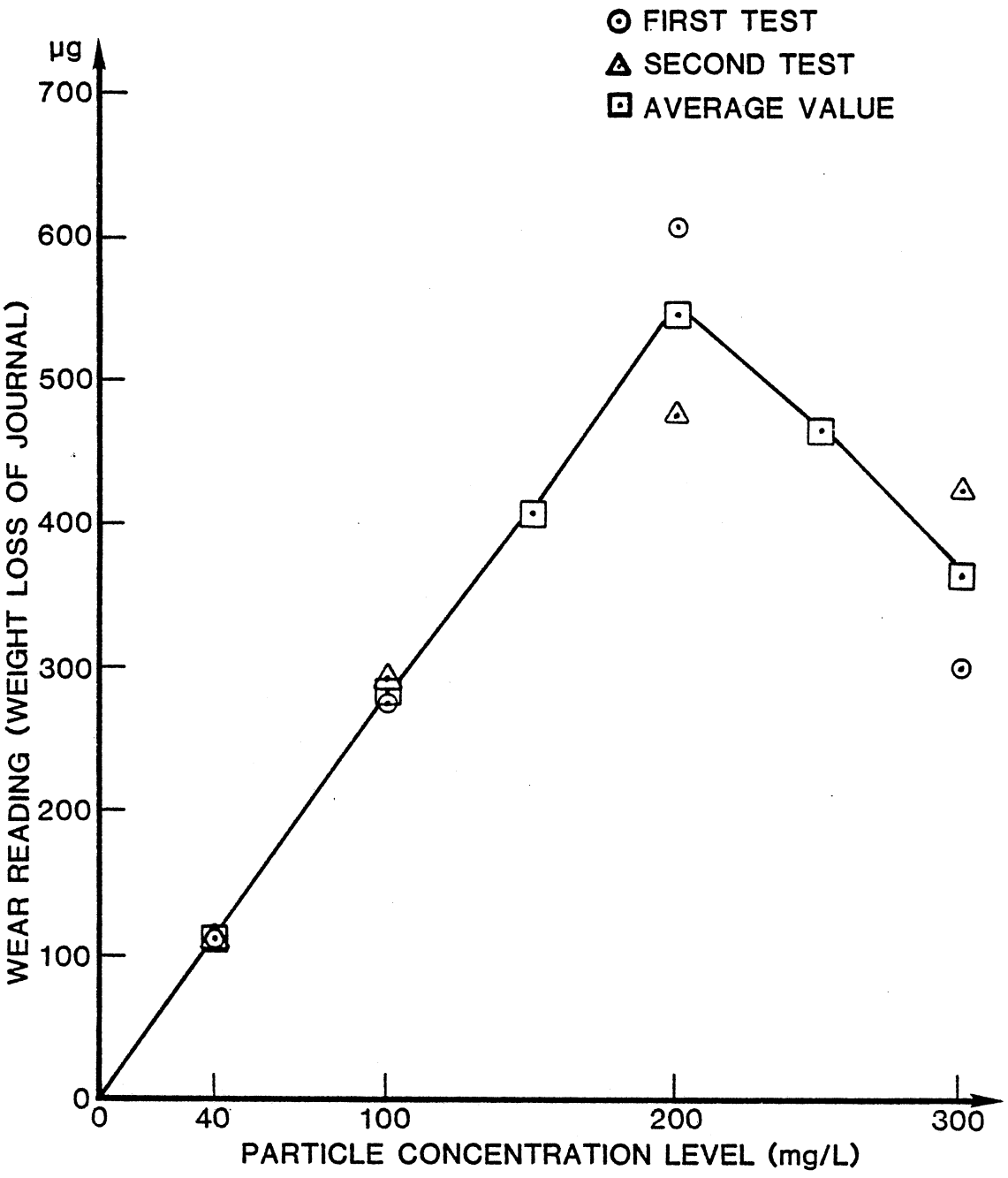

Figure 28. Concentration Test Data of Gamma Wear Tester

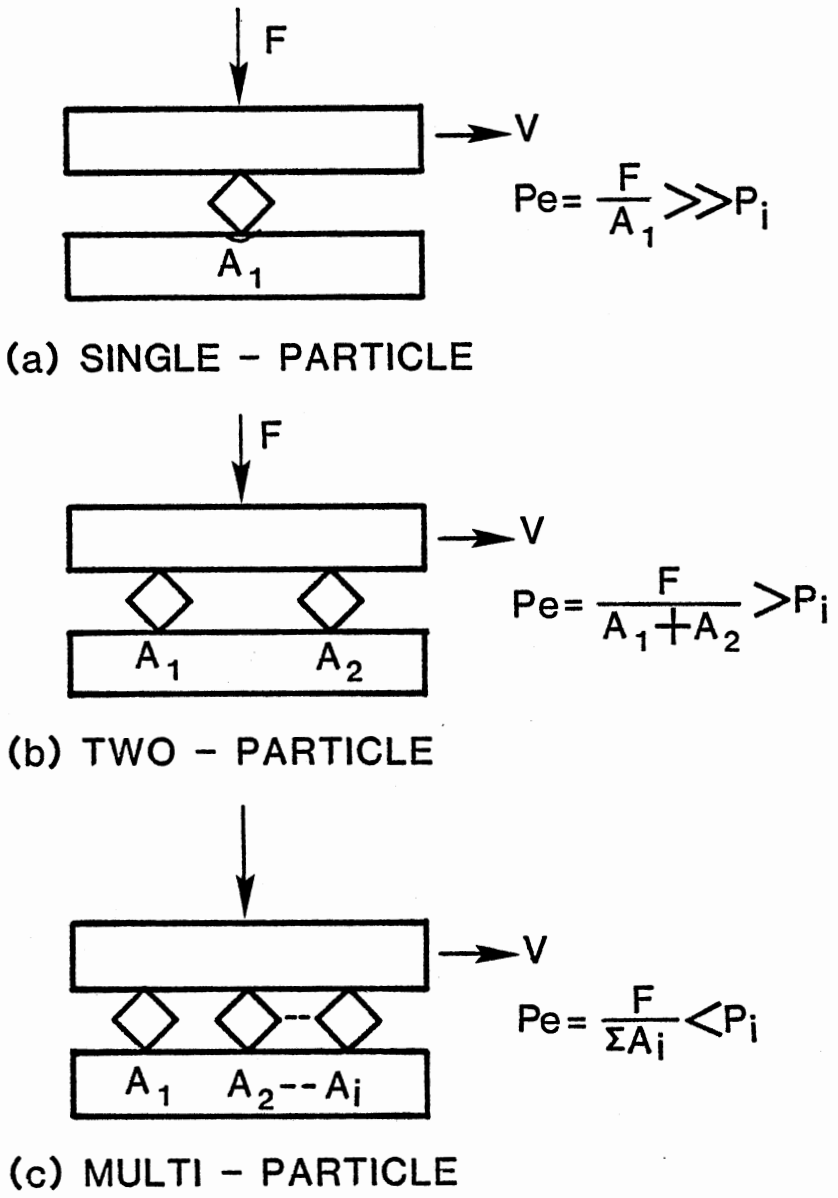

Figure 29. Wear Process Under Different Concentration Levels

the mechanism of a three-body wear is the abrasive particle embedded into the softer bearing surfaces and behaves like a cutter to abrade the hard surface. However, it requires a sufficient amount of load to press the particle. Thus it forces the particle to indent into the softer surface. Intuititively, the more particles between the bearing surface, the less the amount of load each individual particle can share if the total amount of the load is constant. Therefore, if the particle load on each individual particle is insufficient to cause indentation into the surface, no damage can occur. This is the limiting case and by virtue of a gradual reduction in indentation, wear reduces.

Figure 30 shows the data obtained that the point of saturation contaminant concentration level is less than or equal to 200 mg/L. The values used are taken from the average value of two test data for each concentration level. In order to compare these data with the developed wear model, the linear least square method is used to correlate these data points into a straight line. The equation is

$$w = 2.746 \cdot N + 2.876 \qquad (4.8)$$

when w = wear rate, μg

N = contamination level, mg/L

The coefficient of correlation is as high as 0.9995. This obviously indicates the validity of the developed wear model. The absolute Gamma slope of the mineral base oil MIL-H-5606 is 2.746.

The second test to verify the wear model was conducted with mineral base fluid MIL-L-2104. The purpose of using other test fluid is to ensure the Gamma System is valid for a change in fluid properties. The MIL-L-2104 oil has a different viscosity and antiwear property from the MIL-H-5606. The viscosity of the MIL-L-2104 oil is 40 centistokes at 40 degrees

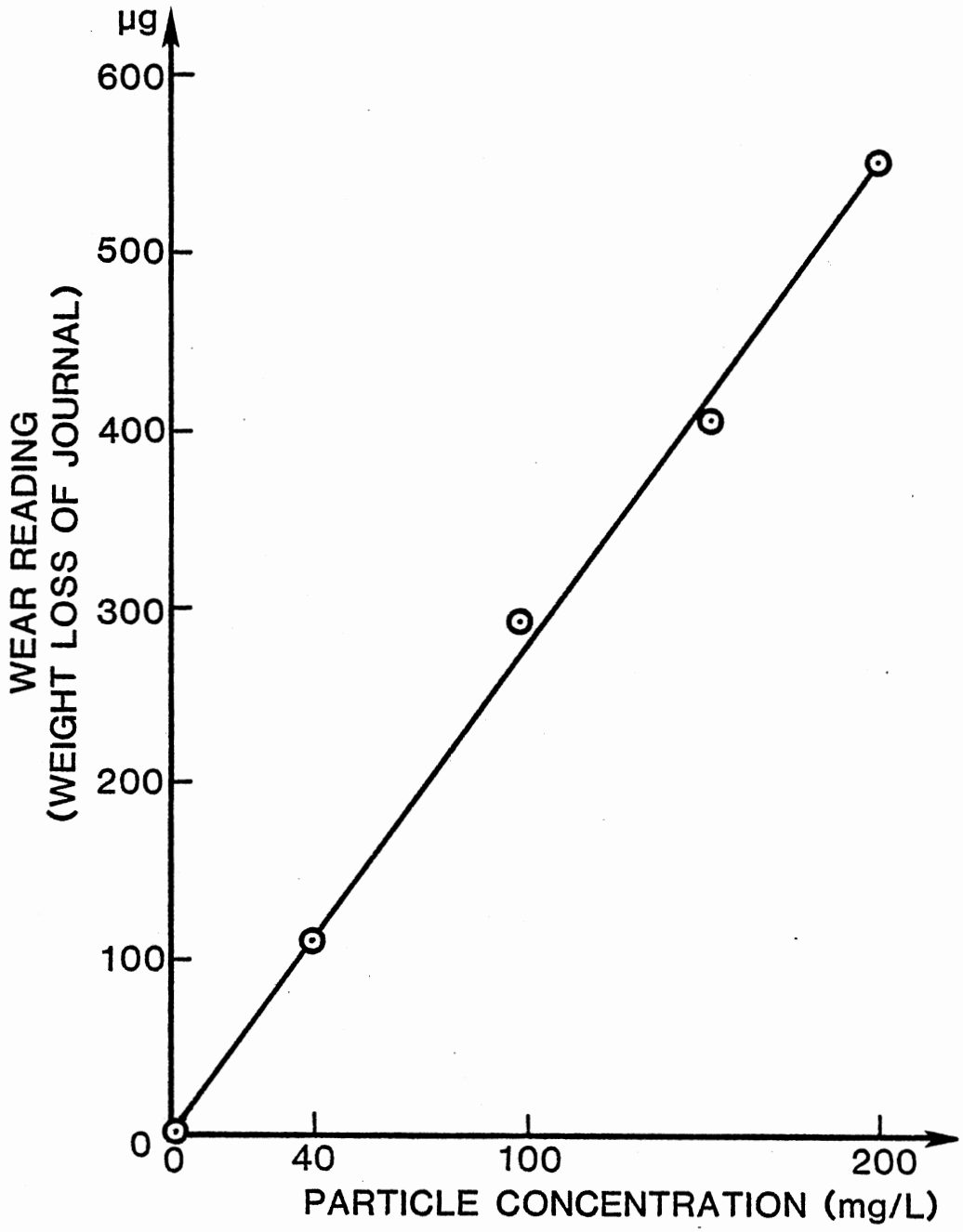

Figure 30. Abrasive Gamma Wear Test Data with MIL-H-5606

centigrade. This is about 2.8 times the viscosity of the MIL-H-5606. In other words, if the operating conditions are identical, then, a thicker film will be formed by using MIL-L-2104 oils.

As mentioned, the developed wear model can be applied to evaluate the abrasive wear severity reflected from fluid properties or entrained particle characteristic providing the fluid film thickness remains contant. Thus, in order to maintain a constant film thickness with MIL-L-2104 as that of using MIL-H-5606, the test load needs to increase 2.8 times to compensate the viscosity effect. This compensation factor is obvious from the definition of Sommerfeld number. As a result, the bearing characteristic number remains the same in both cases. From Equation (3.7), it is known that a test load of 1.4 lbs is required for using MIL-L-2104 to compensate the viscosity effect. Tribologically, under such an operating condition, the Gamma System still behaves as a hydrodynamic lubrication. Again, no wear can be observed. A test was conducted for this purpose, and the result was satisfactory. With the clean fluid no weight loss was found. Test data is shown in Table VIII.

Physically, if the bearing characteristic number is identical, then the wear behavior is independent of the fluid property. However, this is not the case, wear is also chemically affected by the individual anti-wear additive property. For example, the MIL-L-2104 oils have a better anti-wear characteristic than MIL-H-5606. Therefore, a lower wear rate is anticipated by using MIL-L-2104 oil subjected to the bearing characteristic number, is identical.

Four tests were carried out with MIL-L-2104 oils, at 2400 rpm and a test load of 1.4 lbs. The injected particle concentrations were 40, 100, 200, and 300 mg/L, respectively. Test results were tabulated in Table VIII

TABLE VIII

TEST RESULT OF WEAR SENSITIVITY TO
PARTICLE CONCENTRATION WITH
MIL-L-2104 OIL

Test ID No.	Particle Concentration (mg/L)	Journal Weight Loss (μg)
WCN-11	0	0
WCN-12	40	70
WCN-13	100	140
WCN-14	200	300
WCN-15	300	270

and plotted in Figure 31. The performance curve shows the same characteristic as observed with MIL-H-5606. The wear rate increases with particle concentration levels up to 200 mg/L and then decreases at 300 mg/L. The wear rate observed is lower than that with MIL-H-5606. In other words, MIL-L-2104 oil is more wear protective. This was as expected. The performance equation obtained is

$$w = 1.474\ N + 2.247 \qquad (4.9)$$

where w = wear rate (μg)

N = particle concentration (mg/L)

The coefficient of correlation is 0.9981, which again confirms the validity of the use of the Gamma tester. The absolute Gamma slope of MIL-L-2104 is 1.474. This is lower than that of MIL-H-5606. The degree of wear protection of fluids is therefore obviously revealed.

From the foregoing activities the wear model has been quantitatively approved. The following paragraphs describe the three-body wear mechanism qualitatively.

From the discussion made in Chapter III it is known that the ACFTD is embedded in the bearing and then cuts the journal under abrasive wear conditions. To insure this mechanism actually occurs, the test specimens were examined under a microscope before and after the test. Figure 32 shows the bearing surfaces after the test. The pictures were taken with a 100 magnification. It is observed that there are a great number of tiny particles embedded in the bearing surface. They slid along the rotating direction of the journal and eventually embedded in the bearing surface. To signify this process, one of the embedded regions was investigated under a SEM microscope with a 3060 magnification, Figure 33. The three-body cutting mechanism was revealed clearly. To insure the embedded

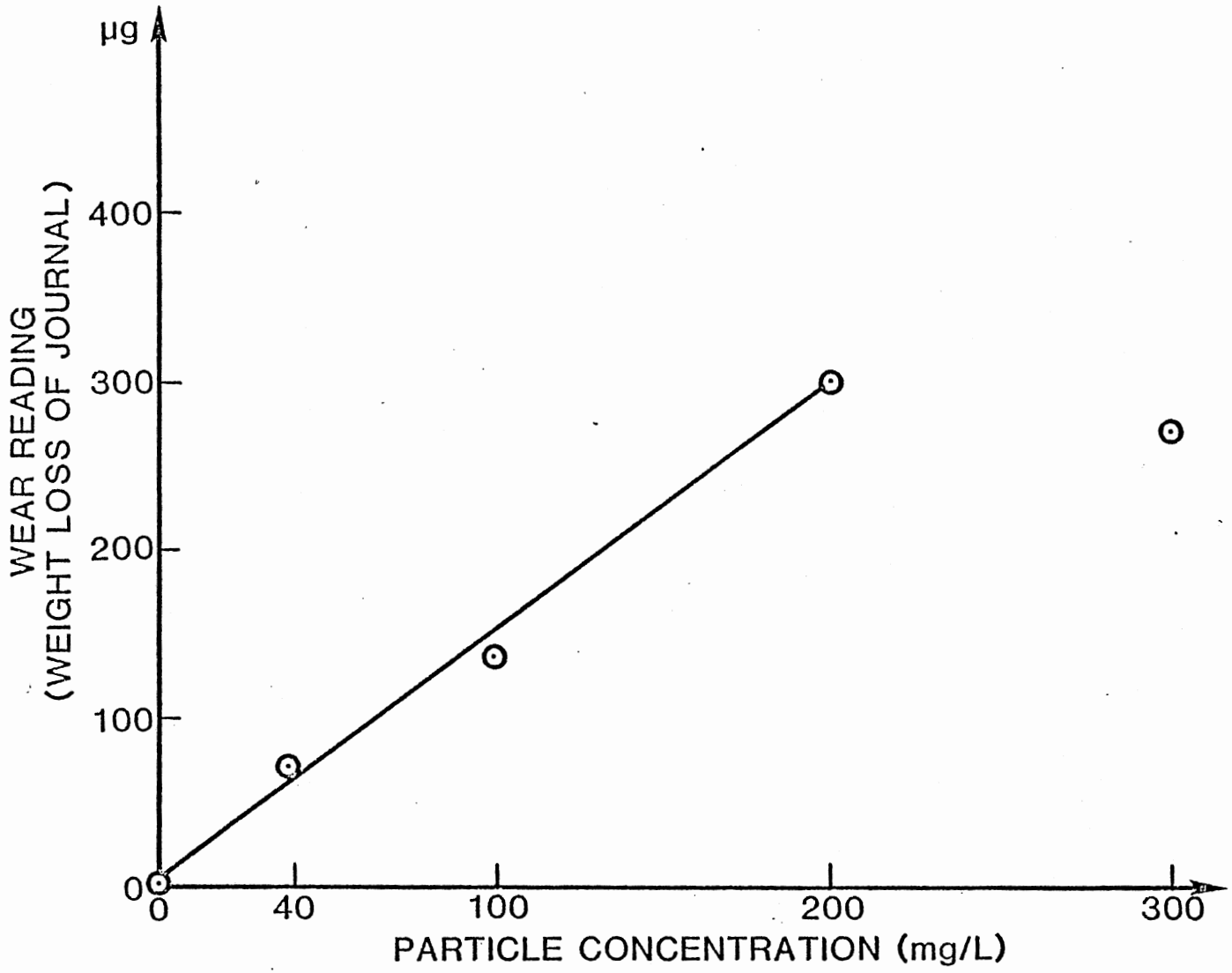

Figure 31. Abrasive Gamma Wear Test Data with MIL-L-2104

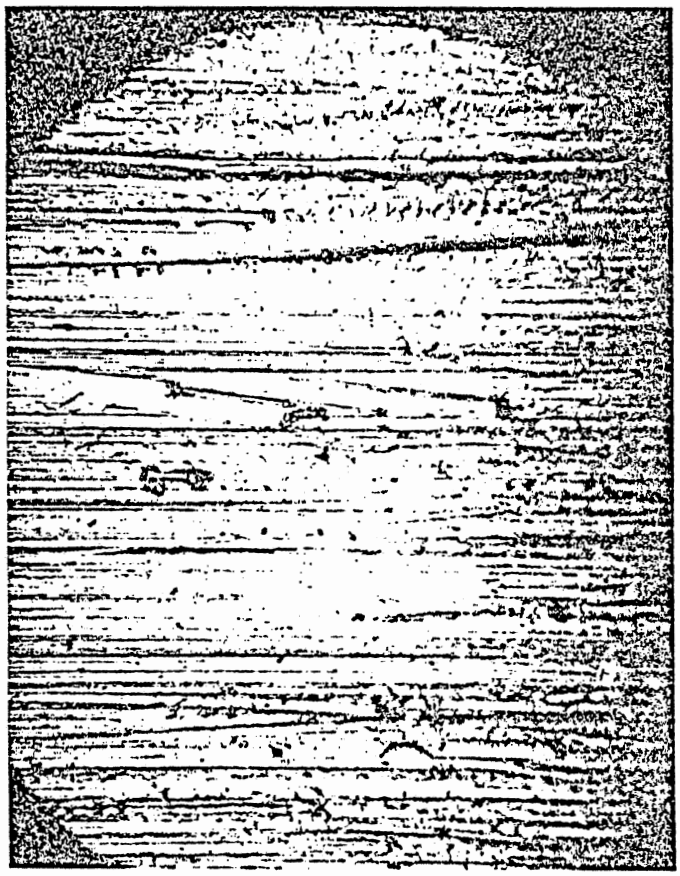

Figure 32. Indentation Phenomenon, ACFTD Embedded on the Bearing Surface, 100X

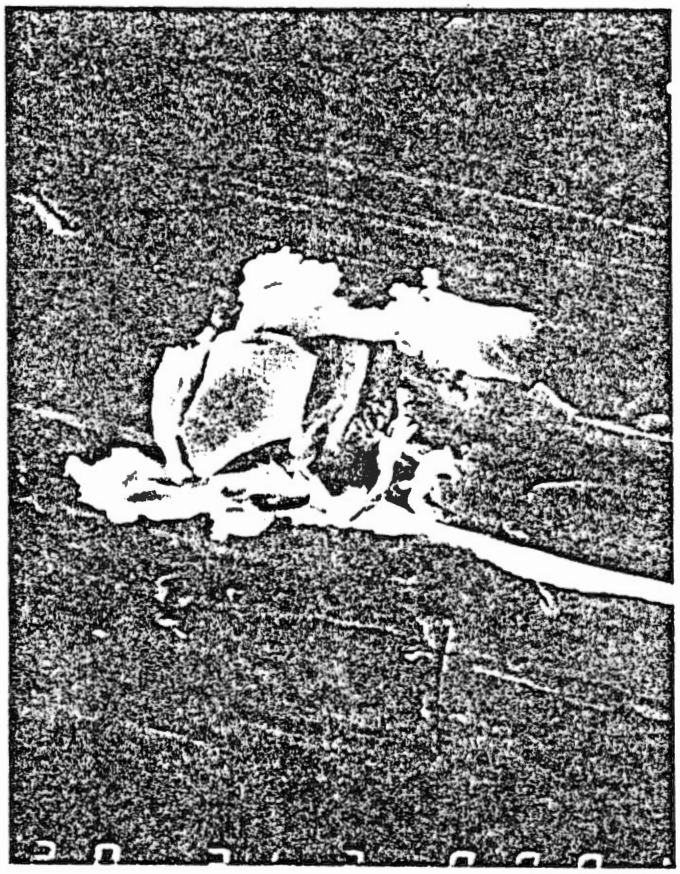

Figure 33. Indentation Phenomenon Observed by SEM, 3060X

particle is ACFTD, an x-ray spectrum analyzer was used to monitor the component of the region under study. Figure 34 illustrates the spectrum obtained. It is seen that copper (cu) and silicon (Si) are the predominant elements. The copper is the basis element of the bearing and the silicon is the ACFTD.

From Figure 35, it is found that there were no embedded particles on the journal surface, however, several cutting was observed. All this strongly supports the three-body wear mechanism used to develop the wear model for the rotating elements.

Furthermore, the cutting mechanism can be recognized by observing the wear index obtained conventionally from the Gamma tester. As mentioned, the cutting grooves that appeared on the journal surface do not change the overall profile of the journal, thus, the conventional wear detecting method fails to monitor the wear. Four tests were conducted to evaluate this phenomena. The tests were performed under a hydrodynamic lubrication condition. Different particle concentration levels of 40, 100, 200, and 300 mg/L were introduced to each test separately. Both the teeth advancement on the ratchet and the weight loss of the journal during the test were recorded. The test results are illustrated in Table IX and plotted in Figure 36. Obviously, the wear was not revealed by means of the ratchet change, (overall diameter change), but by the weight loss (abrasive cutting effect). Throughout the experimental verification of the Gamma System, the developed wear model has been well recognized.

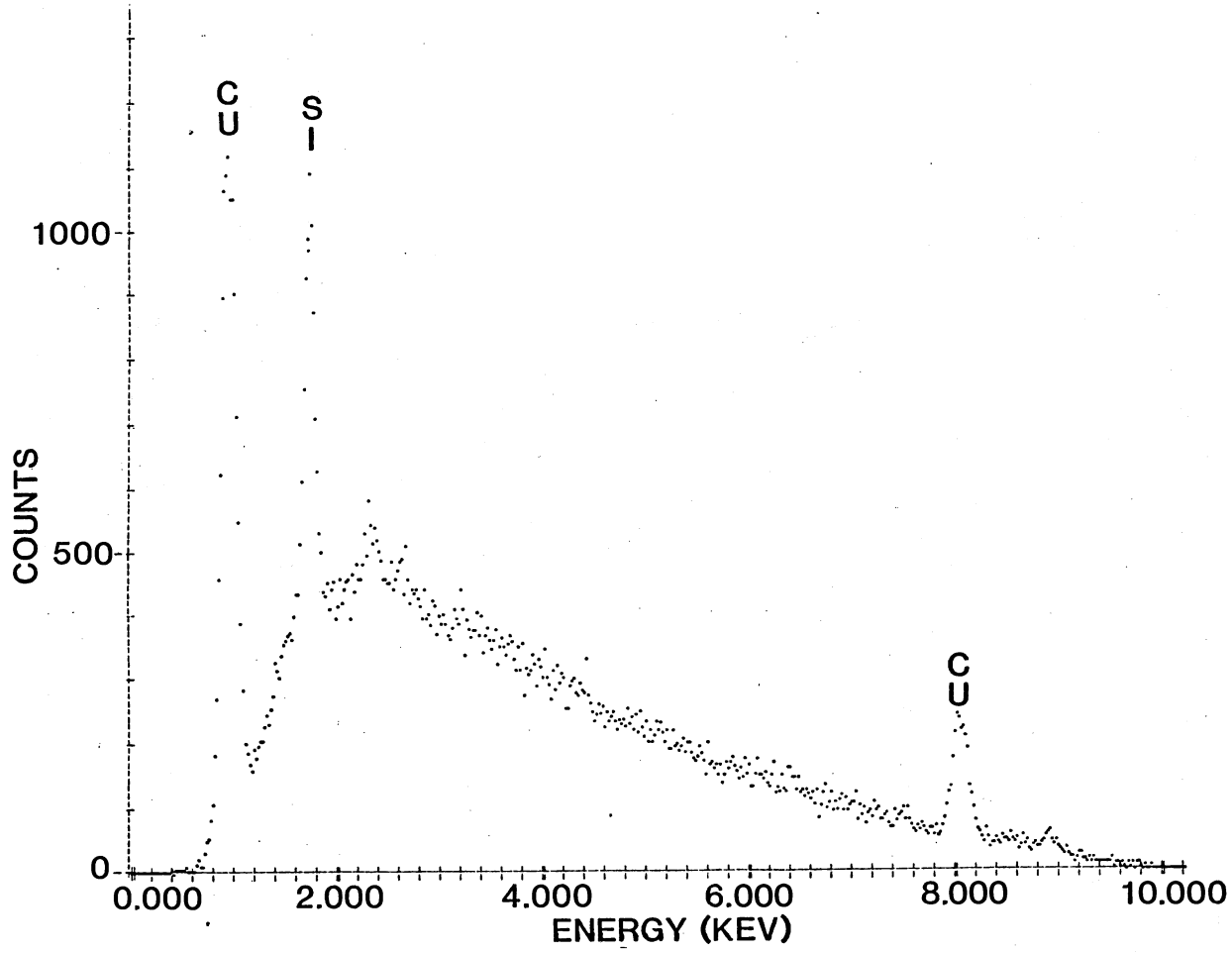

Figure 34. Indentation Phenomenon Analyzed by X-Ray Spectrum Analyzer

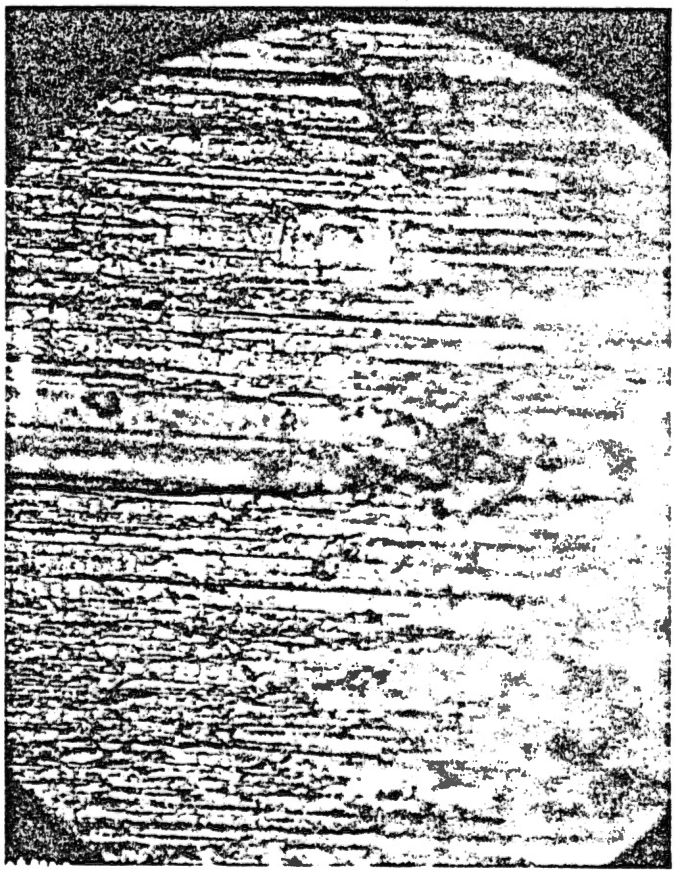

Figure 35. Abrasion Phenomena, A Cut on the Journal, 400X

TABLE IX

WEAR READING OF ABRASIVE WEAR TESTS USING GAMMA FALEX AND GAMMA METHODS

Time(min)	Particle Concentration Level (mg/L) 40	100	200	300
0	0	0	0	0
2	0	1.0*	1	1
4	0	1.0	1	1
6	0	1.0	2	1
8	0	1.0	2	1
10	0.5	1.0	2	1
12	1.0	1.5	2.5	2
14	1.5	1.5	3	2
16	1.5	1.5	3	2
18	1.5	1.5	3	2
20	1.5	1.5	3	2
Weight Loss(μg)	110	280	610	300

* Number of gear teeth advanced.

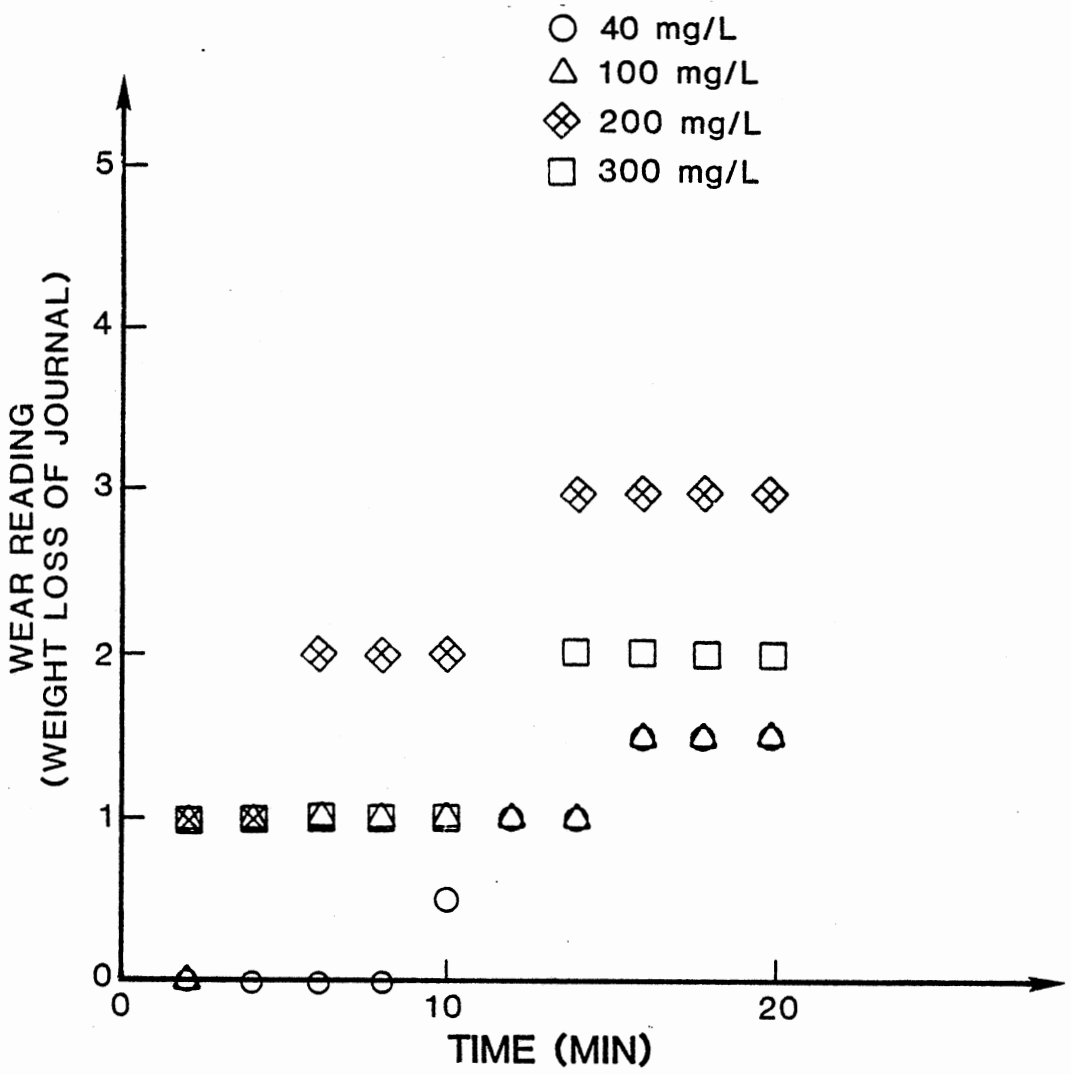

Figure 36. Wear Readings Obtained by Gamma and Gamma Falex Methods

CHAPTER V

EXPERIMENTAL VERIFICATION OF FILTRATION MODEL

General Considerations

This chapter details the experimental verification of the Beta Prime filtration model developed in Chapter III. The filtration model is expressed in Equation (3.45), and rewritten as follows:

$$Y = ax + b \tag{5.1}$$

where $Y = \ln(\ln(\beta'_{dp} (t))$

$x = \ln(t/T)$

$b = -a \cdot \ln S$

Accordingly, the Beta Prime can be correlated in terms of system operating parameters T, a, and s, and with a linear relationship on the x-y plane. The Beta Prime graph, Figure 37, schematically, illustrated the functional relationship of Equation (5.1). Because the Beta Prime filtration model is based on the concept of the draw-down test, the filtration ratio at any operating point is derived from the ratio of the initial particle concentration to that at that operating point. Theoretically, the filtration ratios obtained for a given filter must be a straight line on the Beta Prime graph.

In order to achieve the experimental verification of the filtration model, it required the test dust whose property and particle size distribution are known and controllable. In addition, it needs a feasible

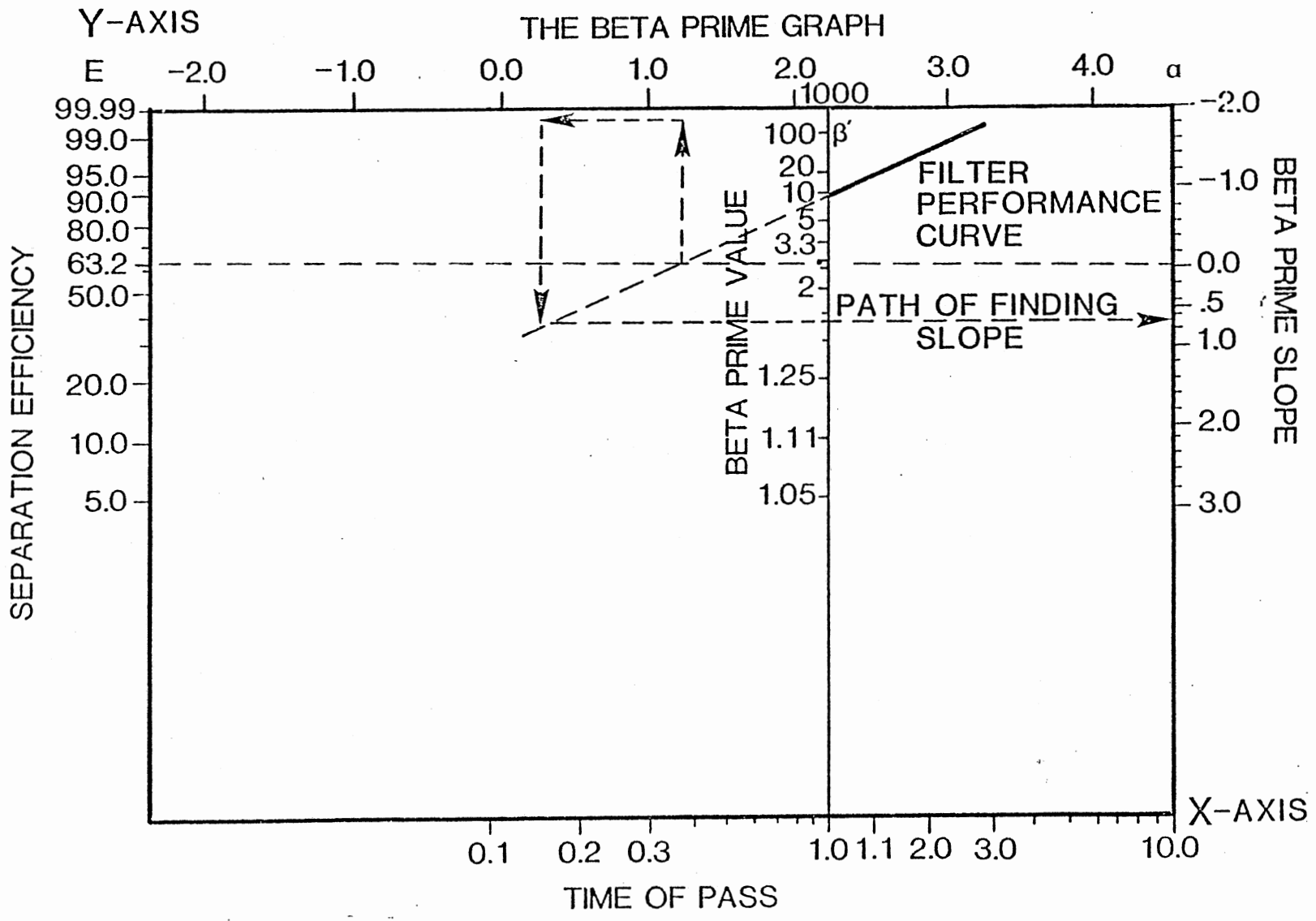

Figure 37. The Beta Prime Graph

particle counting device that may monitor the variation of particle size distribution throughout the entire test.

The ACFTD is selected as the test contaminant in the filtration test. This is because ACFTD has been approved both nationally and internationally (ISO 4402) as a standard for contamination control test. Specifically, it is mainly used in the multipass filtration test for evaluating filter performance.

The particle size distribution is the most important property of test dust for the use of filtration test. This property has been comprehensively studied by Bensch (53, 54). According to his work, the particle size distribution of ACFTD can be illustrated as

$$N = 10^{3.246 - 1.086(\log D)^2} \tag{5.2}$$

where N = the number of particles greater than D per 1.0 mg

D = particle diameter in micrometer

Normally, Equation (5.2) can be expressed as a straight line on the log-log squared scale paper. Figure 38 shows the characteristic curve of the particle size distribution of ACFTD. The ordinate represents the number of particles per millimeter greater than indicated size. And the abscissa is the particle size in micrometers.

Some researchers (45) reported that the value of the particle may deviate from that calculated by Equation (5.2) in the small particle size. However, according to a recent program (55), sponsored by the American Society of Testing and Materials (ASTM), in investigating the characteristic of the particle size distribution of ACFTD measured by different instruments, it is found that the difference is from the use of different instruments as well as operator error. Since the distribution expressed

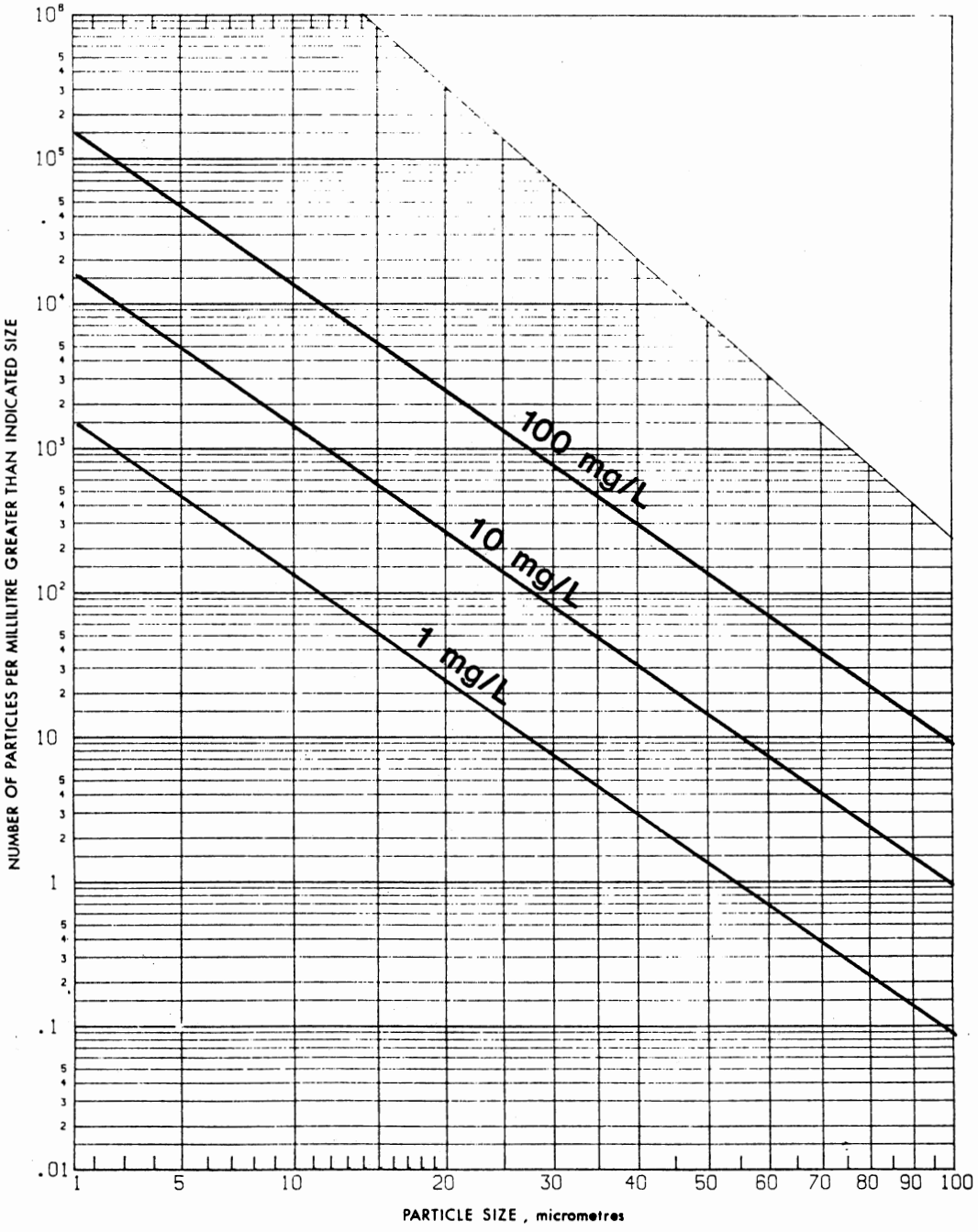

Figure 38. Characteristic Curve of ACFTD Particle Size Distribution

by Equation (5.2) has been accepted as the ISO standard (ISO 4402), it is used as the standard particle size distribution for the ACFTD in this study.

As noted the Beta Prime value derived from Equation (5.1) is a function of operating time. In practice, it would be more convenient if a reference Beta Prime is selected at a specific time. For example, the filtration ratio obtained at the time that the fluids have completed one circulating cycles.

It is worthy to review the basic principle used in the Beta system before specifying the reference operating point to define the Beta Prime value. The reason for this is because the Beta system has been widely used in engineering practice; there will be a need in the future to convert the Beta Prime value into the Beta value or vice versa. A proper determination of the reference operating system in the Beta Prime system may benefit this prospective necessity.

Figure 39 schematically illustrated the Beta filtration test system. Basically, it consists of two distinct systems: a filter test system and a contaminant injection system. According to the principle of particle balance in a test system, the theoretical relationship that describes variation of particle concentration is expressed as:

$$N_u(t)\cdot V = N_0\cdot V + \int N_i(t)\cdot Q_i(t)\ dt - \int (N_u(t)-N_d(t))\cdot Q(t)\ dt \qquad (5.3)$$

where N_u = cumulative particle concnetration of size greater than d_p at upstream of filter

N_d = cumulative particle concentration of size greater than d_p at downstream of filter

N_0 = cumulative particle concentration of particle size greater

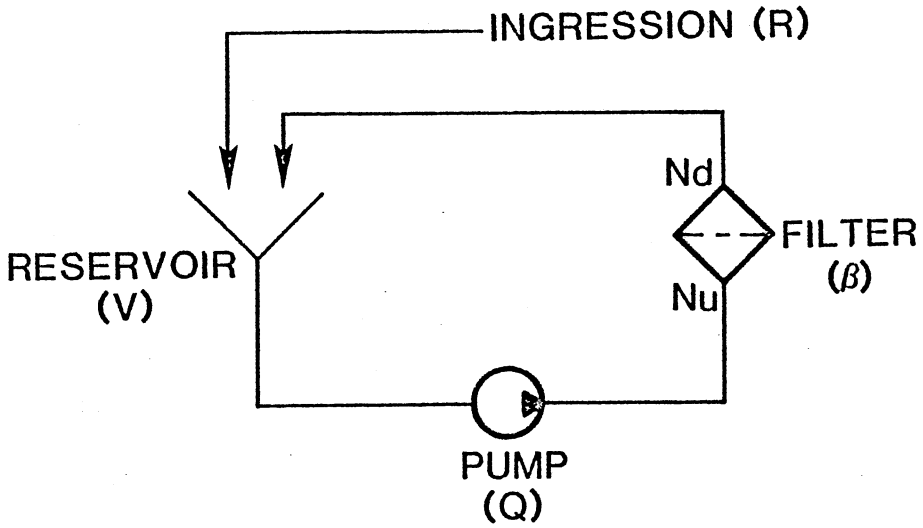

Figure 39. Schematic of Beta Filtration System

than size d_p originally in the system

N_i = cumulative particle concentration of size greater than d_p in injection flow

Q_i = injection flow rate

Q = filter flow rate

V = circulating volume of fluid in the system

The Beta filtration ratio is defined as

$$\beta(t) = N_u(t) \,/\, N_d(t) \tag{5.4}$$

Assuming the Beta filtration ratio is constant throughout the entire process, then Equation (5.3) becomes

$$\beta \cdot N_d(t) = N_0 + \frac{N_i(t) \cdot Q_i(t)}{V}\, dt - (\beta \cdot N_d(t) - N_d(t))\frac{Q(t)}{V}\, dt \tag{5.5}$$

Let the ingression rate be

$$R_i(t) = N_i(t) \cdot Q_i(t) \tag{5.6}$$

Consequently, Equation (5.5) is

$$\beta \cdot N_d(t) = N_0 + \frac{R_i(t)}{V}\, dt - (\beta \cdot N_d(t) - N_d(t))\, \frac{Q(t)}{V}\, dt \tag{5.7}$$

Furthermore, assume the ingression rate and flow are constant during the test, then the downstream particle concentration can be obtained by solving Equation (5.7). The result is

$$N_d(t) = \frac{1}{\beta} N_0\, e^{-(\frac{\beta - 1}{\beta})(\frac{Q}{V})t} + \frac{R_i}{Q}\, \frac{1}{\beta - 1}(1 - e^{-(\frac{\beta-1}{\beta})(\frac{Q}{V})t}) \tag{5.8}$$

Suppose that, originally, the system is clean, namely, N_0 is equal to zero. Also set the characteristic time constant, τ, as

$$\tau = \frac{\beta}{\beta - 1}(\frac{V}{Q}) \tag{5.9}$$

Thus,

$$N_d(t) = \frac{R_i}{Q} \frac{1}{\beta - 1} (1 - e^{-t/\tau}) \tag{5.10}$$

Figure 40 illustrates the functional relationship between the Beta and Beta Prime system. It is seen that if the initial particle concentration level of Beta Prime system set to be equal to the steady state value of particle concentration at upstream of Beta system, then the Beta value can be straight forward correlated with the Beta Prime value obtained at the time the fluids have completed the first circulation. Mathematically, it is expresses as

$$\frac{N_{u,s}}{N'_d} \Big|_{\beta} = \frac{N_0}{N_d(1)} \Big|_{\beta'} \tag{5.11}$$

where $N_{u,s}$ = steady state value of particle concentration at upstream

N_d' = downstream particle concentration at Qt/V = 1 subjected to no injection and initial value is $N_{u,s}$

N_0 = initial particle concentration

$N_d(1)$ = downstream particle concentration at the first pass.

From Equation (5.8), it is obvious that

$$N'_d = \frac{1}{\beta} \cdot N_{u,s} \cdot e^{-(\frac{\beta - 1}{\beta})} \tag{5.12}$$

Apparently, if the Beta Prime is defined as the filtration ratio of initial particle concentration to the downstream particle concentration at the first pass, and the initial particle concentration is equale to the upstream steady state particle concentration in the Beta system, then rearranging Equations (5.11) and (5.12) yields

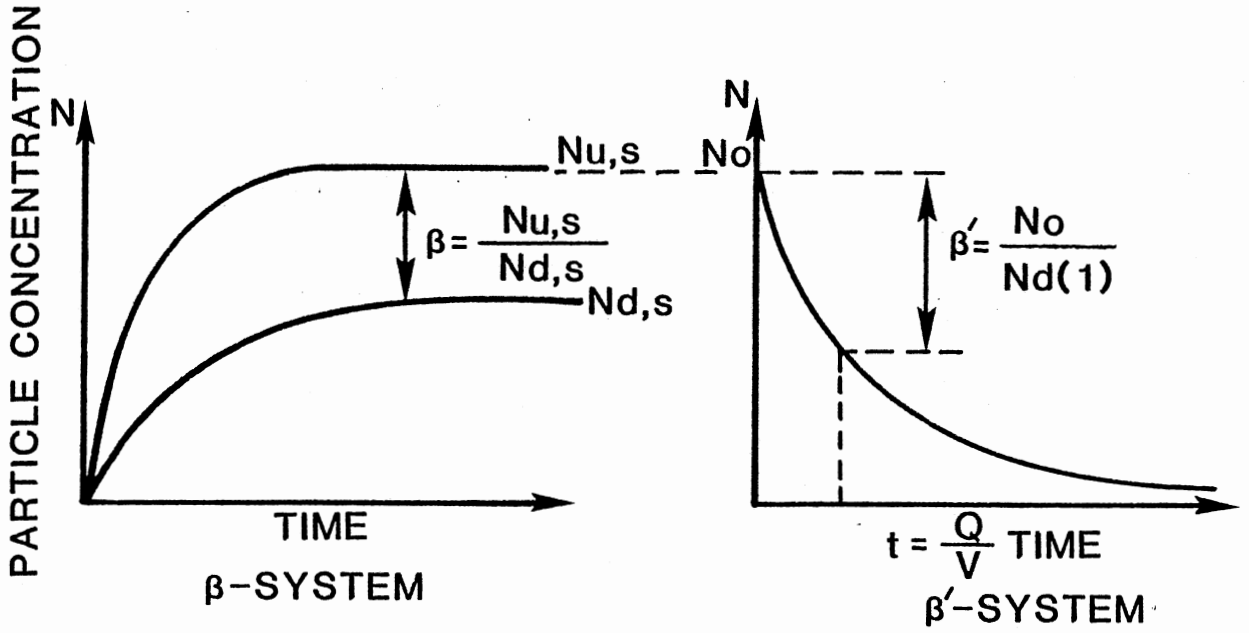

Figure 40. Functional Relationship Between Beta and Beta Prime System

$$\beta' = \beta \cdot e^{\left(\frac{\beta-1}{\beta}\right)} \tag{5.13}$$

Equation (5.13) provides the conversion between β and β'. From Equation (5.10), and the definition of Beta, the upstream particle concentration is

$$Nu(t) = \frac{Ri}{Q}\frac{\beta}{\beta-1}\left(1 - e^{-t/\tau}\right) \tag{5.14}$$

Therefore, the steady state value of Nu(t) is

$$Nu,s = \frac{\beta}{\beta-1}\frac{Ri}{Q} \tag{5.15}$$

According to the Beta filtration test procedure (ISO 4572), the injection particle concentration, namely Ri/Q, is 10 mg/L. Thus,

$$Nu,s = \frac{\beta}{\beta-1} \cdot (10\ mg/L) \tag{5.16}$$

Furthermore, in accordance with the Beta value obtained from more than 700 filter tests performed at FPRC/OSU, it is found that the average Beta ten value for most commonly used filters is around two. In other words, the steady state value of particle gravimetric concentration at upstream is about 20 mg/L.

Consequently, the initial contamination level set for the Beta Prime test is 20 mg/L and the Beta Prime value is defined as the filtration ratio of the initial system particle concentration to the downstream particle concentration of filter at the time that fluids have completed the first circulation.

Development of Test Facility

The Beta Prime filtration theory was developed based on the

"draw-down" test. The major predominant objective of the Beta Prime is to evaluate the performance of the low-flow, high beta type filter. Although the theory is applicable to analyze general type filters also, the test facility developed here was focused on the mentioned objective.

Normally, the average flow density of a hydraulic filter is about 0.06 gallons per minute per square inch (GPM/in^2). The low flow rate filters have a comparable small flow density to the average value shown above. In general, it is in the range of 0.002 to 0.02 GPM/in^2. To meet this requirement, the flow passes through the flat sheet filter with area of 22 square inches must be as low as 0.44 GPM.

The test system consists of a circulating system, a clean up system, a filter test system, a particle counting system and a temperature control system, Figure 41. The circulating system used to provide the required flow and power to the test system. The driver is a fixed displacement pump and the flow supplied to the filter is controlled by a flow control valve. The flow rate can be controlled within 0.05 to 0.37 gallons. This specification meets the low flow filter operating requirement.

The clean-up system is valved in and out of the circulating system by means of a four way valve. It is used to provide the system with a "clean" background whenever required. It usually requires a high beta filter.

The filter test system consists of a flat sheet filter and its housing. The flat sheet filter has a flow area of 22 square inches. Figure 42 shows a schematical diagram of the flat sheet filter housing assembly.

The particle counting system provides an in-line contamination analysis. The particle counter is used to monitor the downstream particle concentration level during the test. It is directly connected to the

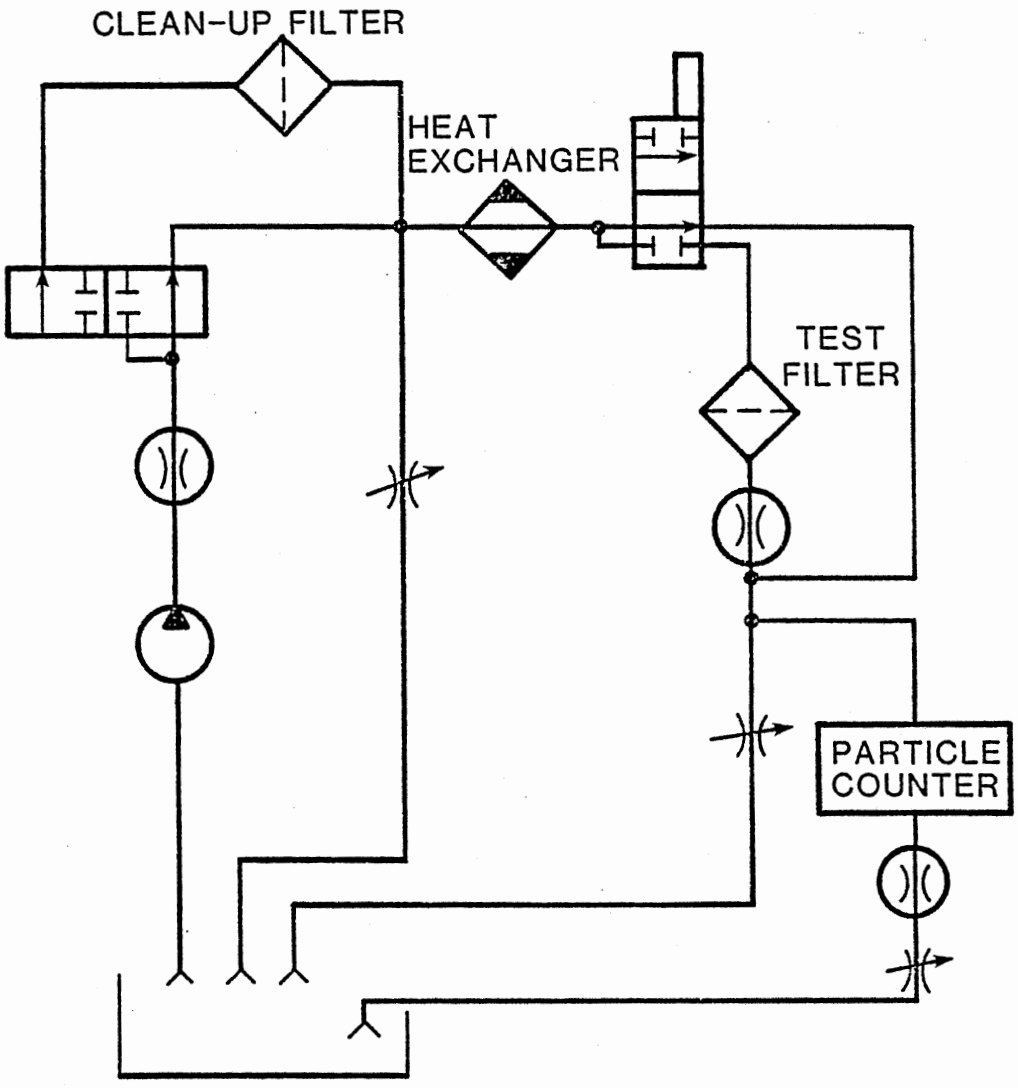

Figure 41. Schematic of Beta Prime Filtration System

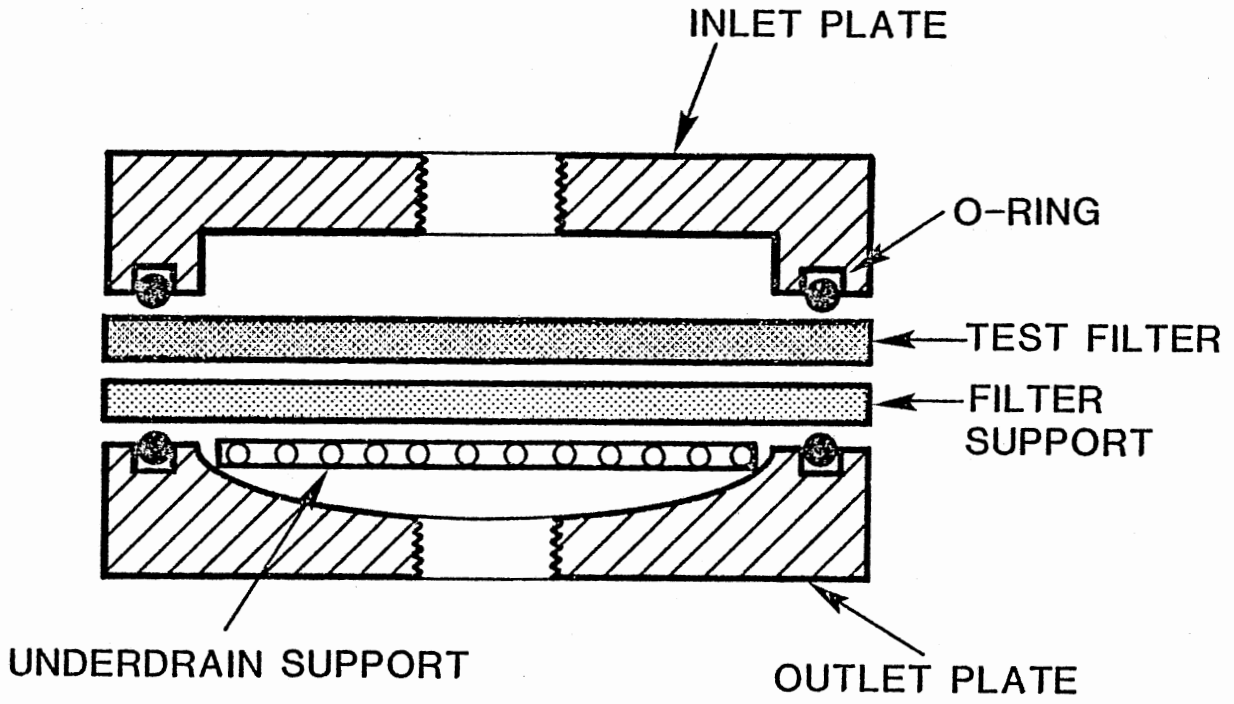

Figure 42. Schematic of Flat Sheet Filter Housing Assembly

circulating system to be analyzed. The use of the in-line particle counter minimizes the sampling error and thus improves the accuracy of measurement. This avoids the degradation of the performance credibility of high beta filters.

The temperature control system maintains the operating temperature constant such that the flow through the filter and the particle counter can be accurately controlled throughout the test.

Qualifying Experimental Facility

Three major aspects were considered in qualifying the performance of the developed Beta Prime test stand. They were the system clean-up characteristic, the establishment of a stable initial concentration level, and the test repeatability.

The system clean-up characteristic test was conducted by injecting the ACFTD with a concentration level of 10 mg/L into the Beta Prime system. Valve the cleanup filter into the circulating system after the ACFTD has mixed well and reaches a stable level. Record the concentration level of size 2, 5, 10, 20, 30, and 40 micrometers at the initial time and 2, 5, and 10 minutes. A clean background is established if there are less than 10 particles per milliliter greater than 10 micrometers in the system. The clean-up test result is tabulated in Table X and illustrated in Figure 43. As can be seen, the system reaches the cleanliness requirement at five minutes after the test began.

In contrast to the clean-up procedure, the establishment of a stable initial concentration level was initiated with a clean background. An amount of 20 mg ACFTD was injected into a two liter reservoir; namely, the particle concentration level was 10 mg/L; particle concentration level

TABLE X

CLEAN-UP TEST RESULT

Time (min)	0	2	5	10
Size (μm)				
5	5809*	2204	91.6	8.0
10	1762	650	6.8	2.4
20	352.2	36	1.2	0
30	105.2	4	0.4	0
40	24.0	0.4	0	0

* Particle number of size greater than given size per milliliter

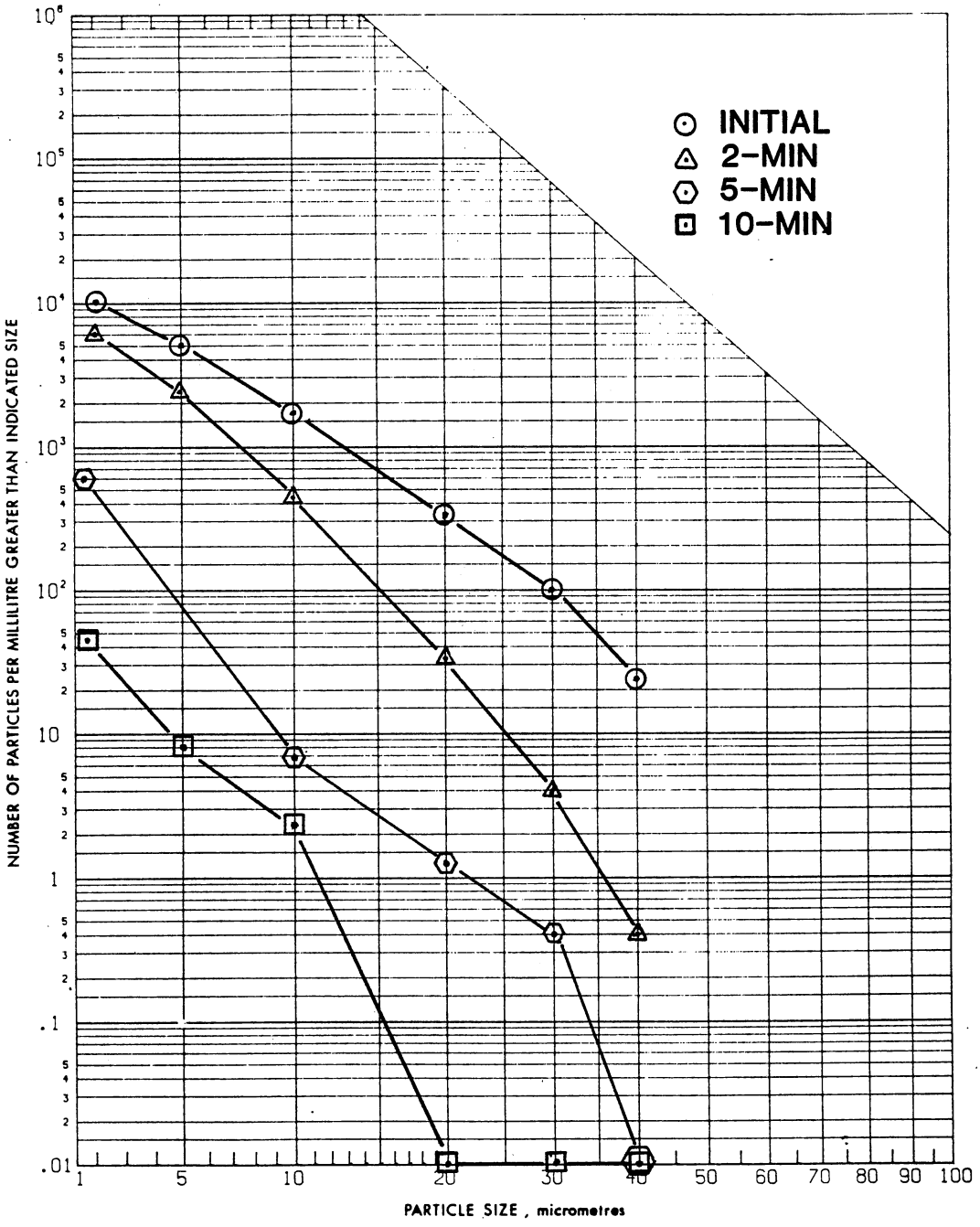

Figure 43. Clean Up Test Data of Beta Prime System

recorded at the initial, 5, 10, 15, 20, 25, and 30 minutes. The results were presented in Table XI and plotted in Figure 44. An identical test was carried out, and the results were shown in Table XII and Figure 45. From these test data, it is observed that the ACFTD mixed well and reached a stable concentration level 15 minutes after injection. The data also compared with the standard ACFTD distribution per ISO 4402. It revealed that the developed Beta Prime test stand is able to establish a stable initial concentration level for achieving the test.

Eight identical tests were conducted with mineral base fluid MIL-H-5606. The initial particle concentration level was established by introducing 40 mg ACFTD into a two liter reservoir. The filter flow rate was set at one liter per minute and the operating temperature was 40 degrees centigrade. Each test was operated for 16 minutes and particle concentration level was monitored and recorded every two minutes. The data are shown in Table XIII. From Equation (3.45), it is noted that the filtration data from the Beta Prime system have a straight-line characteristic. Therefore, the least square method was used to correlate the data point of each data set. The calculated Beta Prime value, the characteristic process constant, the time scaling constant, and the coefficient of correlation were tabulated in Table XIII. It is found that the average coefficient of correlation is as high as 0.9842. This signifies the linear characteristic of the filtration data on the Beta Prime graph. In addition, the validity of the developed model and test stand were assured.

Experimental Tests and Analysis

Two sets of tests were carried out with mineral base fluids MIL-H-5606 and MIL-L-2104 to validate the Beta Prime filtration model. Three

TABLE XI

PARTICLE CONCENTRATION BACKGROUND
TEST RESULT SET A

Time (min)	0	5	10	15	20	25	30
Size (μm)							
5	2.4*	3206	3919	5310	6270	6554	6692
10	0.4	792.8	1030	1532	1861	1448	2004
20	0	171.2	185.6	288.4	360.4	393.2	374.0
30	0	62.0	44.4	78.4	90.8	98.8	90.0
40	0	14.0	4.4	9.2	14.8	14.8	11.6

* Particle number of size greater than the given size per milliliter

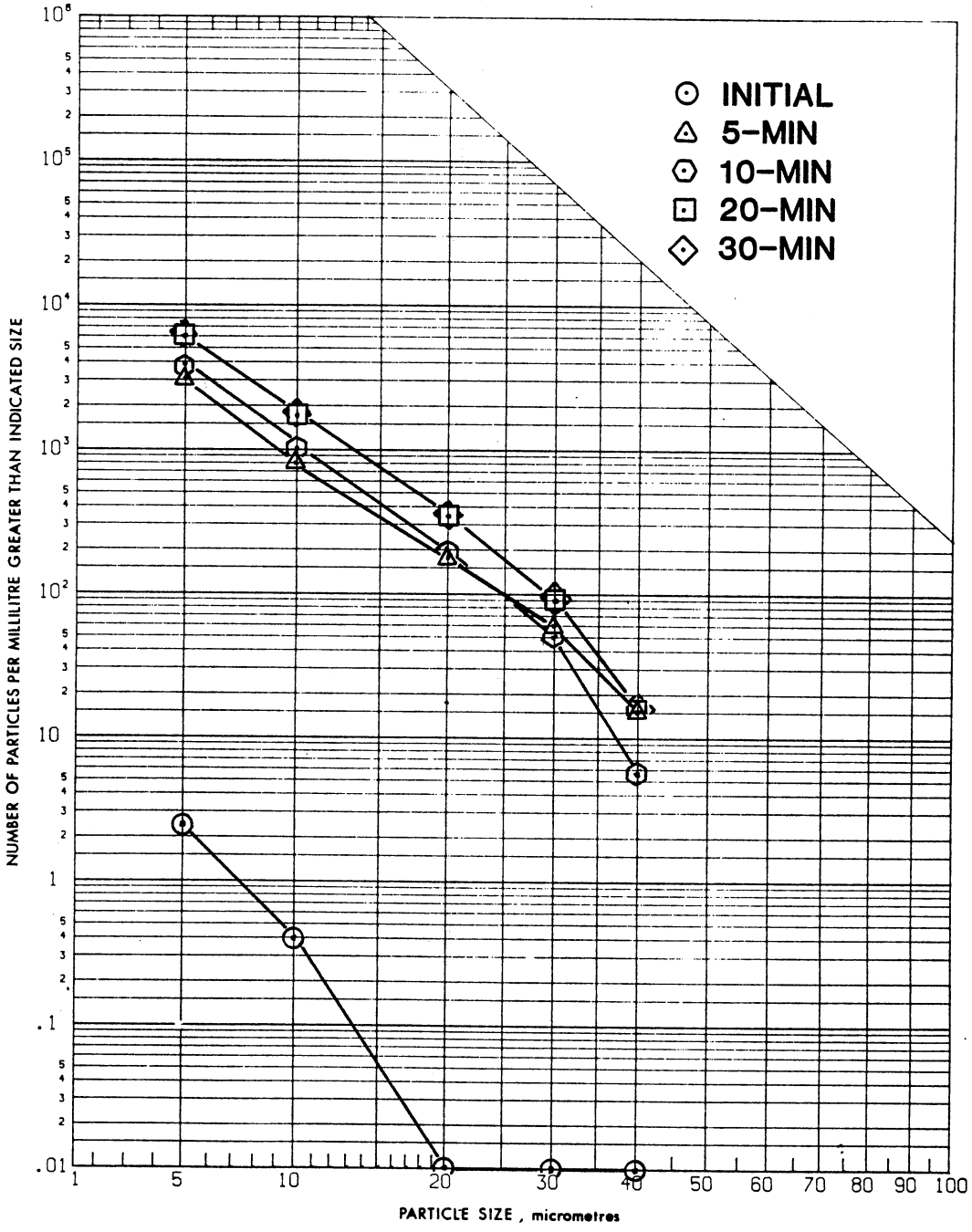

Figure 44. Concentration Test Data Set A of Beta Prime System

TABLE XII

PARTICLE CONCENTRATION BACKGROUND
TEST RESULT SET B

Time (min)	0	5	10	15	20	25	30
Size (μm)							
5	7.2*	5347	5924	6202	6323	6167	6468
10	2.0	1568	1693	1800	1796	1684	1733
20	1.2	303.2	322.4	304.0	278.8	258	253.6
30	0.4	79.2	71.6	73.6	51.2	48	42.4
40	0.4	25.2	16.8	13.2	6.8	4.8	4.0

* Particle number of size greater than the given size per milliliter

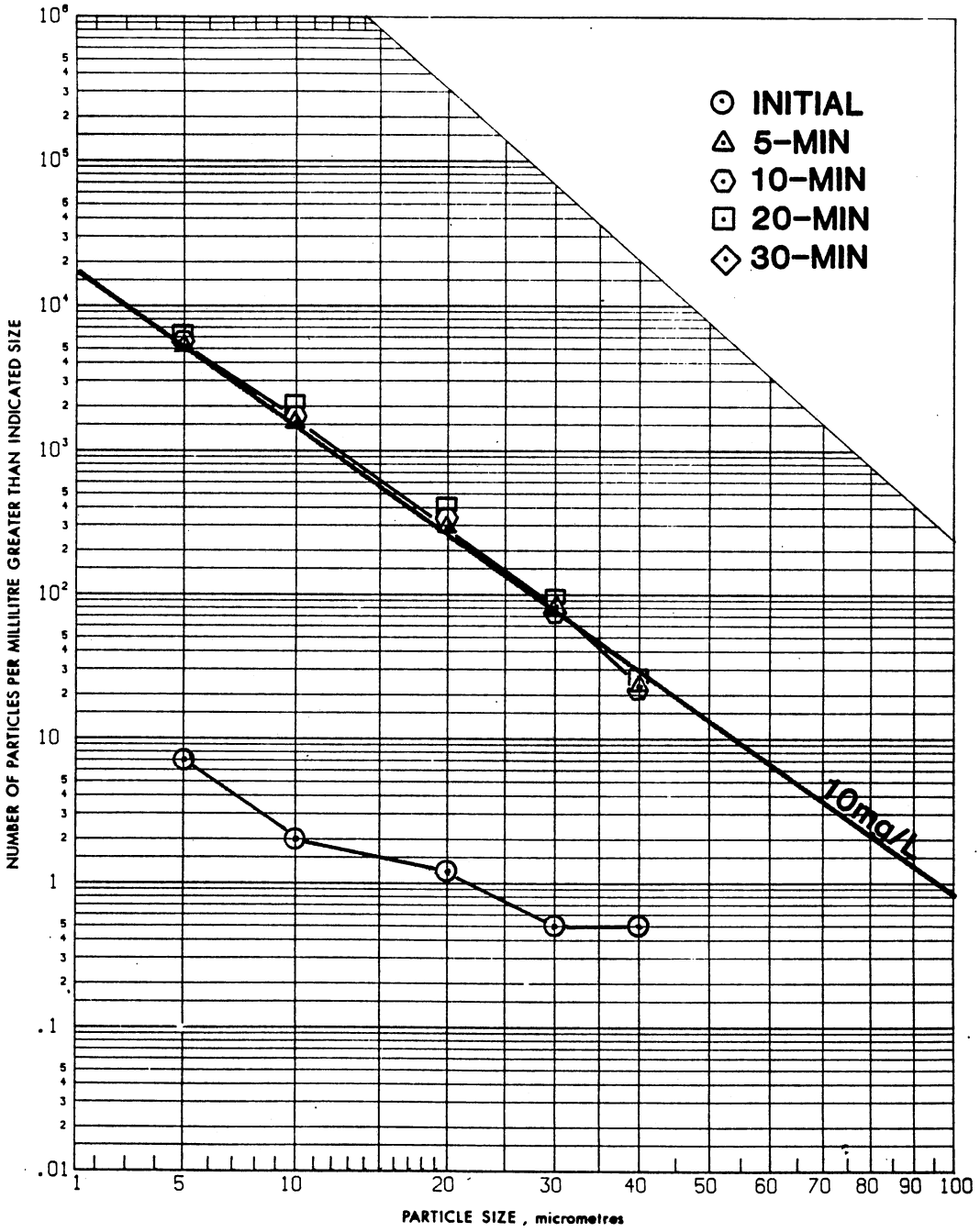

Figure 45. Concentration Test Data Set B of Beta Prime System

TABLE XIII

FILTER REPETITION TEST RESULTS

Test ID No.	Time (min) 0	2	4	6	8	10	12	14	16	Correlation Results β_{i0}	A	s	r
RT-1	3049*	738.4	426.4	232.4	156.0	118.4	99.6	76.4	60.4	4.215	0.4932	0.4784	0.9929
RT-2	2616	641.2	383.2	243.6	138.8	122.0	109.2	114.0	110.0	4.363	0.4156	0.3934	0.9474
RT-3	3036	728.4	685.6	232.0	185.6	168.0	121.6	117.4	77.2	3.786	0.4850	0.5543	0.9251
RT-4	3390	798.2	464.0	279.2	172.8	110.8	71.6	47.6	36.0	4.006	0.5643	0.5594	0.9954
RT-5	2951	558.8	324.8	201.2	151.2	111.2	61.2	45.2	32.0	4.969	0.4793	0.3734	0.9876
RT-6	3102	602.0	240.8	148.4	95.2	72.0	39.2	43.6	36.4	5.745	0.4790	0.3116	0.9795
RT-7	3554	954.8	572.8	355.2	230.8	201.6	140.4	124.8	106.8	3.787	0.4822	0.5521	0.9932
RT-8	3139	625.2	397.6	284.0	192.0	120.8	91.6	66.4	73.6	4.747	0.4413	0.3664	0.9847
Sampling Mean										4.4523	0.4800	0.4486	0.9757
Standard Deviation										0.6735	0.043	0.0945	0.0256

* Particle number of size greater than 10 μm per milliliter

filters with different filtration characteristics were selected for each set of tests. The filters were ranked as Excellent, Good, and Fair according to the individual degree of particle separation characteristic.

Following is the actual test procedure used to verify the Beta Prime theory:

1. Conduct clean-up of system by using a clean-up filter. The background particle concentration level should be less than 10 particles per milliliter greater than 10 micrometers as specified previously.
2. Inject the ACFTD into the system and allow to mix until a suitable initial concentration level is achieved. The initial gravimetric concentration level used is 20 mg/L.
3. Record the initial particle concentration level.
4. Valve test filter into the test circuit.
5. Record the downstream particle concentration at a predetermined increment. This increment is equal to the time of the fluid to complete a pass.

A filter flow rate of one liter per minute and a two liter circulating volume were used for each test. The corresponding test data and the theoretical correlation results with the MIL-H-5606 were presented in Table XIV and Figure 46. It can be seen that the test results behave very well on the Beta Prime graph, which confirms the validity of the developed filtration model. The calculated Beta Prime values are 27.19, 4.01, and 1.26 for excellent, good, and fair filters respectively. The credibility of filters is obviously revealed.

The identical test process was performed with MIL-L-2104. Test data were tabulated in Table XV and Figure 47. The corresponding Beta

TABLE XIV

FILTER TEST RESULTS WITH MIL-H-5606

Test ID No.	Time (min) 0	2	4	6	8	10	12	14	16	Correlation Results βi_0	A	s	r
PF-01	3425	2703	2480	2274	2196	2037	1887	1752	1690	1.256	0.5315	16.156	0.9895
PF-02	3390	798.2	464.0	279.2	172.8	110.8	71.6	47.6	36	4.006	0.5643	0.5594	0.9954
PF-03	3150	123.6	79.2	62.4	67.6	69.2	51.2	48.4	42.4	27.187	0.1205	0.0005	0.9016

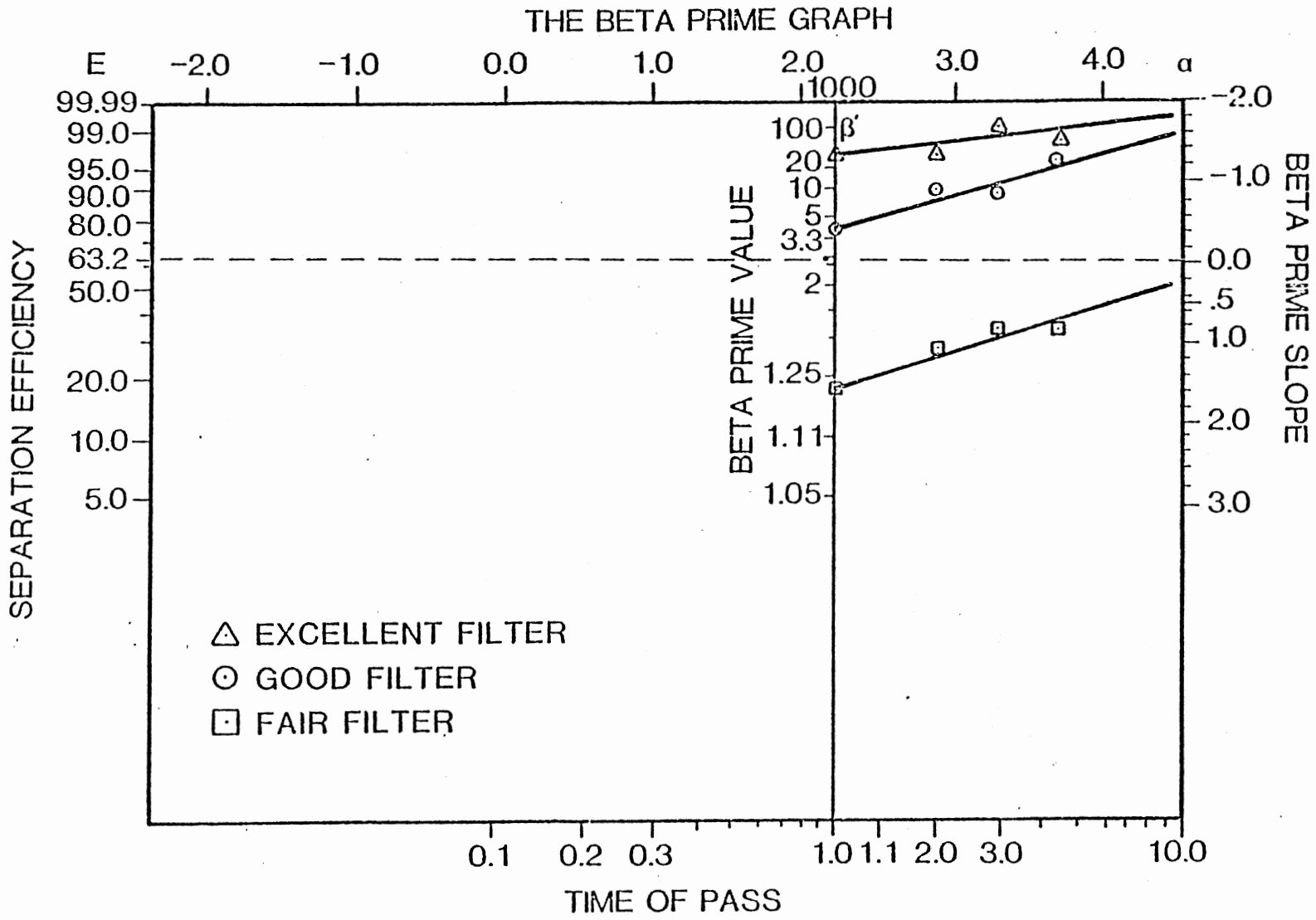

Figure 46. Filter Test Data with MIL-H-5606

TABLE XV

FILTER TEST RESULTS WITH MIL-L-2104

Test ID No.	Time (min) 0	2	4	6	8	10	12	14	16	Correlation Results β'_{10}	A	S	r
PF-04	2909	2526	1819	1780	1683	1433	1320	1191	1282	1.205	0.8031	8.097	0.9030
PF-05	2939	1208	520.4	262.0	140.4	90	86	74.8	55.2	2.741	0.7119	0.9882	0.9615
PF-06	3215	447.2	147.2	40.4	51.6	30.4	29.6	14.0	6.8	8.396	0.4956	0.2179	0.9447

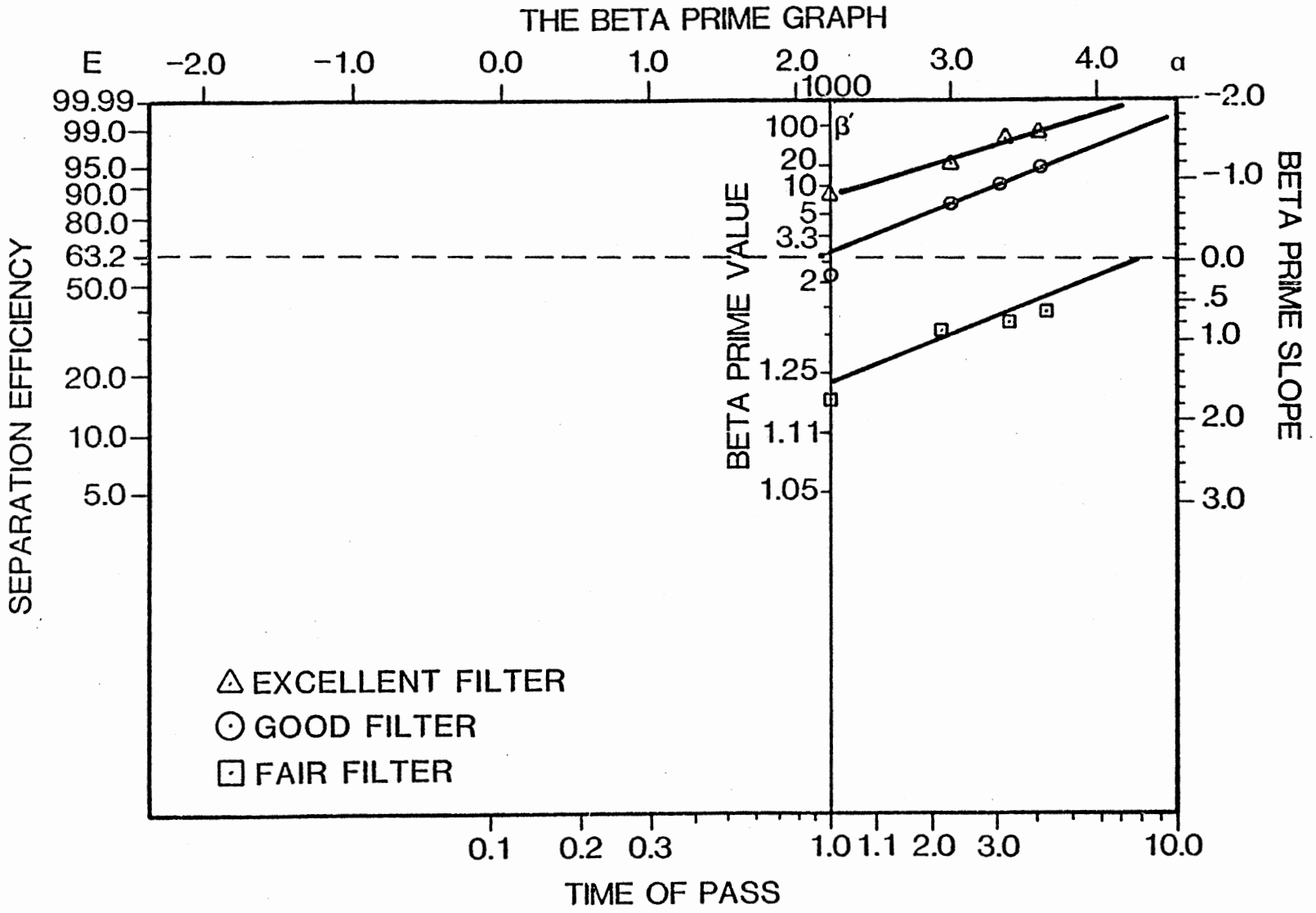

Figure 47. Filter Test Data with MIL-L-2104

Prime ten are 8.44, 2.74, and 1.27 for the excellent, good, and fair filters respectively. It is seen that the filtration performance of filters is degraded with the use of MIL-L-2140 oils. The reason for this degradation stems from the fluid viscosity effect.

The viscosity of MIL-L-2104 oils (40 centi-stokes at 100 degrees Farenheit) is higher than that of MIL-H-5606 (14.3 centi-stokes). Figure 48 illustrates the capture mechanism of a filter when a particle passes around it. For simplicity in motion analysis it is assumed that the Van-der-Waals force is the only force to attract the passing particle and the viscous force imposed on the particle is governed by Stoke's Law which has the following form:

$$Fu = 6\pi\nu\cdot\eta\cdot d_p \tag{5.17}$$

where Fu = flow force

ν = particle velocity

d_p = particle size

η = fluid viscosity

Consequently, referring to Equation (5.17) and the capture mechanism shown in Figure 48, it may be concluded that the higher the fluid viscosity, the lower the opportunity of particle capture. In other words, filters have a lower particle separation capacity if the working fluid viscosity is higher. This analysis also has been proven emperically by Ewbank (56). He carried out a series of tests by varying fluid viscosity from five centistokes to 108 centistokes to investigate the variation of filter separation efficiency by correlating test data. The result comfirmed the previous proposition. Accordingly, the filter has a worse filtration performance with MIL-L-2104 oils.

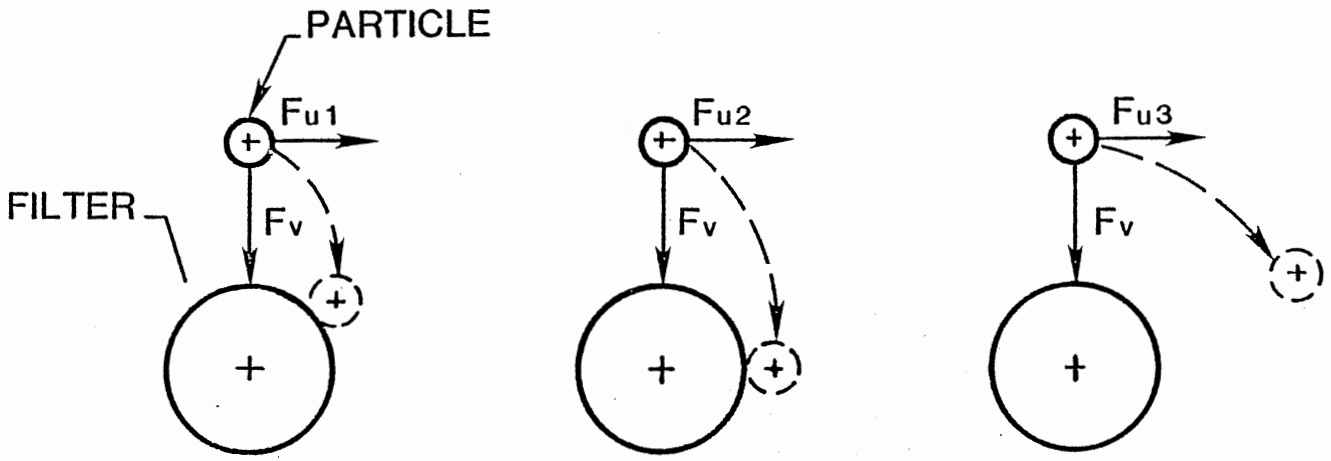

Figure 48. Filter Capture Mechanisms

CHAPTER VI

EXPERIMENTAL VERIFICATION OF THE TRIBO-FILTRATION MODEL

General Considerations

This chapter presents the experimental activities conducted to verify the developed tribo-filtration model, Equation (3.48). The model indicated that the accumulative abrasive wear rate of a rotating element is a function of system filter Beta Prime value, initial particle concentration level, and particle size. As mentioned previously, in the hydrodynamic lubricating condition, abrasive wear is caused by particles with a size within the two extremities of oil-film thickness. Moreover, the major part of the wear occurs at the location of minimum film thickness. In addition, particles with a size comparable to the dimension of minimum film thickness are the most damaging. As a result, Equation (3.48) can be rewritten as:

$$W(t) = \sum_{t=0}^{t} \left(\frac{N_{0,dp}}{\beta'_{dp}(t)} - \frac{N_{0,dp+1}}{\beta'_{dp+1}(t)} \right) \cdot K_d \cdot d_p^2 \Bigg|_{dp=h\ min} \qquad (6.1)$$

where $W(t)$ = accumulated wear rate up to time t

$h\ min$ = minimum film thickness

$N_{0,dp}$ = initial particle concentration of particle size greater than dp

$\beta'_{dp}(t)$ = the Beta Prime filtration ratio of size dp

K_d = wear coefficient depends on fluid property and material used.

The Beta Prime value of each individual particle size can be obtained, in terms of the reference Beta Prime value, by employing Equation (3.52) subjected to the particle size scaling constant. The particle size scaling constant can be obtained graphically or mathematically. Figure 49 schematically illustrates the functional relationship between the Beta Prime filtration ratio and the particle size scaling constant. The mathematical approach utilizes the following equation.

$$Sp = e^{(4.6052 - \ln(\ln(\beta'_{10})))/2} \tag{6.2}$$

where Sp = the particle size scaling constant

β'_{10} = the Beta Prime ten value

The initial particle concentration level can be calculated by using Equation (3.54). Further, the oil film thickness and wear coefficient are determined as long as the operating condition is set. Therefore, Equation (6.1) specifies the system tribo-filtration characteristic in terms of the reference Beta Prime value and the initial particle concentration.

Experimental Tests and Data Analysis

To validate the feasibility of the developed tribo-filtration model, a series of tests were conducted. Figure 50 schematically illustrates the tribo-filtration test system. Basically, it incorporates two distinct systems: the Gamma wear test system and the Beta Prime filtration system. Unlike the Gamma wear test system, in which the system contamination level

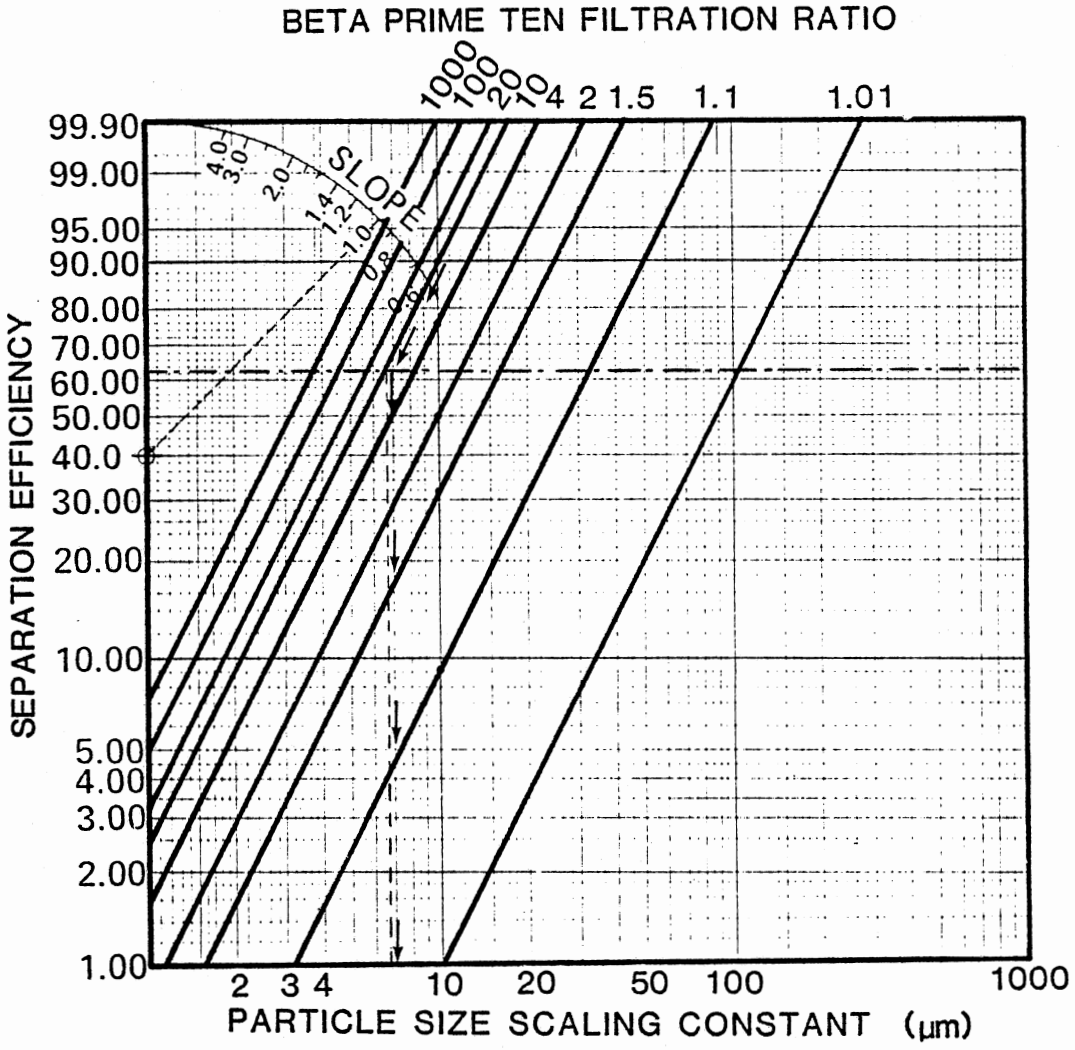

Figure 49. The Log-Normal Model of Beta Prime System

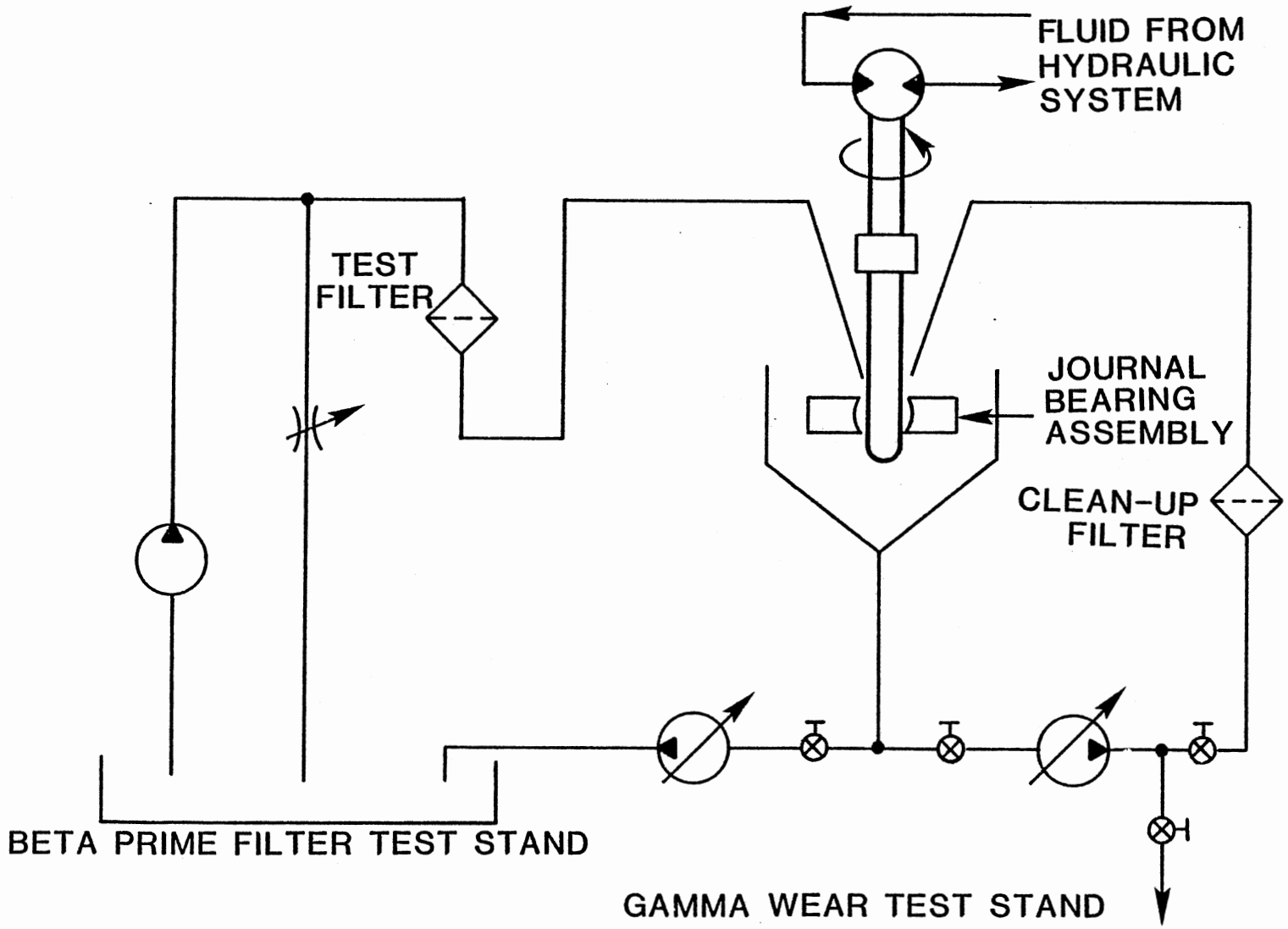

Figure 50. Schematic of Tribo-Filtration System

is governed by a self-lubricating circuit, the tribo-filtration system uses the Beta Prime filtration system to control the contamination level. By this arrangement, the wear phenomena can be directly monitored and investigated in terms of the correlation obtained between the wear rate and the filtration ratio.

Since the repeatability and accuracy of both the Gamma system and the Beta Prime system have been demonstrated in previous chapters, thus, no qualifying test for the tribo-filtration system were performed.

Two sets of tests were conducted with mineral base fluids, MIL-H-5606 and MIL-L-2104 respectively. Each set of tests includes two tests for each individual filter, and three kinds of filters were used. They were ranked as Excellent, Good, and Fair performance as used in Chapter V. In order to minimize the experimental error, the filters used in this chapter were from the same stoke of filters used in Chapter V.

All the operating conditions were kept the same as used in the Gamma wear system and the Beta Prime system. A gravimetric particle concentration level of 100 mg/L was introduced into the system. A circulating flow rate of one liter per minute with a two-liter circulation volume were maintained throughout the test.

The test results were tabulated in Table XVI and the average wear obtained from two identical tests, but with a new filter each time were shown in Figure 51. Thw wear test results, observed by using different filters, were compared with the wear results that were obtained in the contaminated condition without filter protection. It is found that a filter with a higher Beta Prime filtration value will provide better protection to the rotating element from contaminant induced wear. It is observed that the filter with a Beta Prime ten of 1.26 results in an almost

TABLE XVI

TRIBO-FILTRATION TEST RESULTS

Kind of Filter	MIL-H-5606				MIL-L-2104			
	Test 1	Test 2	Avg.	Simulated	Test 1	Test 2	Avg.	Simulated
Excellent	20*	20	20	23	20	10	15	15.2
Good	160	180	170	66.5	100	40	70	39.3
Fair	280	240	260	244	150	110	130	109.

* Weight loss of journal in μm

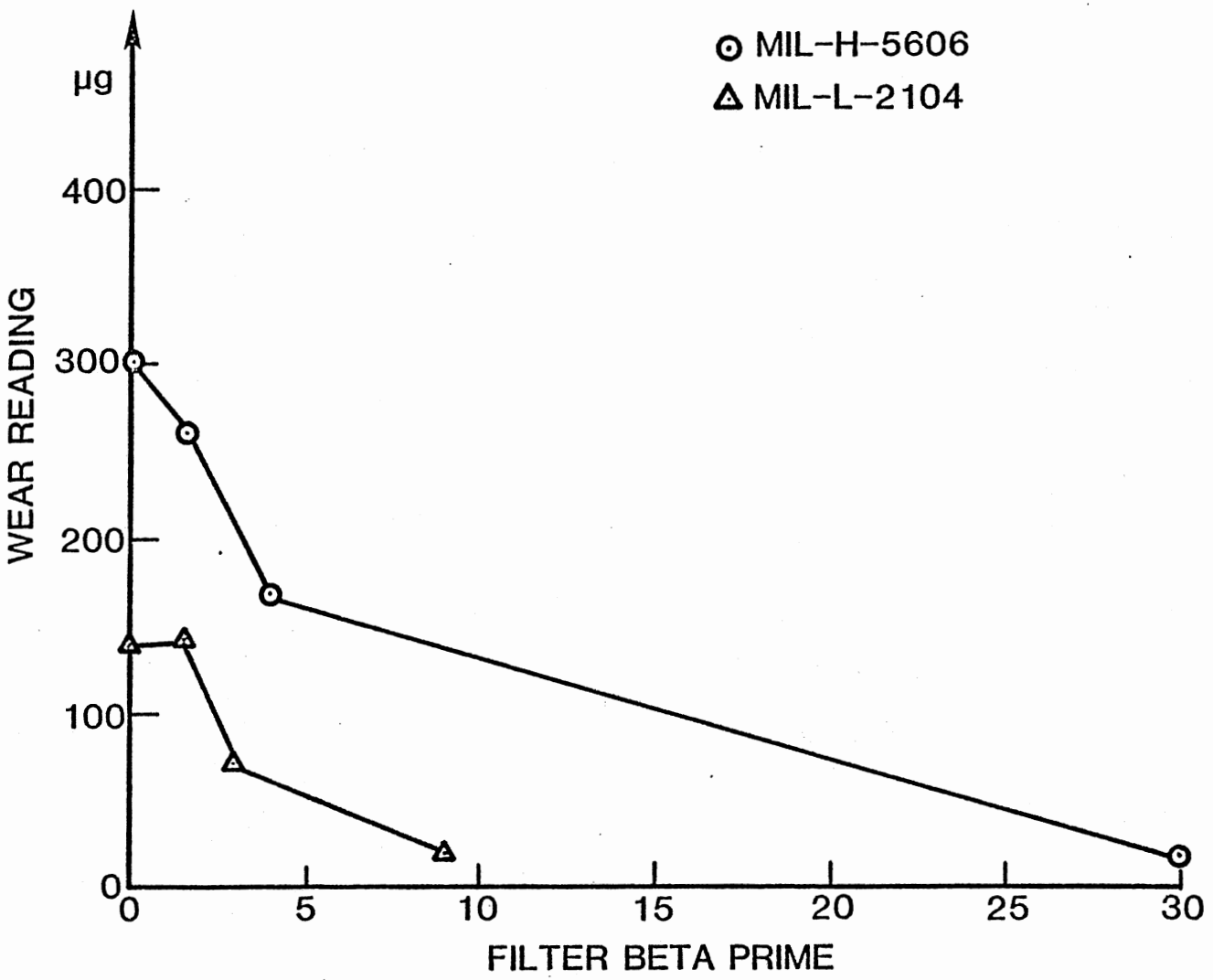

Figure 51. Tribo-Filtration Test Data with MIL-H-5606

equal amount of wear as that obtained in the no filter protection system. On the other hand, there is only a negligible amount of wear observed when the system is protected by the filter with a Beta Prime ten of 27.2. This confirms the performance of the tribo-filtration model, namely, the higher the Beta Prime of a filter, the better it protects the system from contaminant induced wear.

The tribo-filtration model, Equation (6.1), was simulated using the actual operating condition and the corresponding Beta Prime value of each individual filter. The simulation data are tabulated in Table XVII. The simualtion time is ten minutes. This is because most of the ACFTD particles lose their effectiveness of abrading the solid surfaces in this time period, if they are cutting the surfaces (27, 37). The simulation results are tabulated in Table XVI and plotted in Figure 52 for the case of using MIL-H-5606 oils. As can be seen the simulation results have good agreement with the test data for both excellent filters and fair filters. However, a discrepancy does occur in the use of good filters. This might be due to crush effect existing between the particle and the journal bearing, Figure 53. Larger particles were crushed into smaller particles when they entrained into the bearing. If the good filter could not remove the crushed particles effectively, then the higher wear rate was expected in the test. Nevertheless, the crushed particles do not affect the filtration performance of the excellent filters and the fair filters. The reason for this is evident since the excellent filter removes almost all the crushed particles. On the other hand, the concentration of crushed particles as compared to that of the same size particle in a system with fair filter is almost negligible. Thus, it does not change the filtration performance of the fair filter much. These results validate the model.

TABLE XVII

SIMULATION DATA FOR TRIBO-FILTRATION MODEL

Fluid	β'_{10}	A	S	SP
MIL-H-5606	1.26	0.5316	16.15	20.80
MIL-H-5606	4.0	0.5643	0.5394	8.4857
MIL-H-5606	27.18	0.1200	0.00005	5.5025
MIL-L-2104	1.20	0.8031	8.097	23.42
MIL-L-2104	2.741	0.7119	0.9882	9.9606
MIL-L-2104	8.396	0.4956	0.2179	6.8556

β'_{10} = Beta Prime Ten value

A = Beta Prime Slope

S = Time Scaling Constant

Sp = Particle Size Scaling Constant

hmin = 10 μm

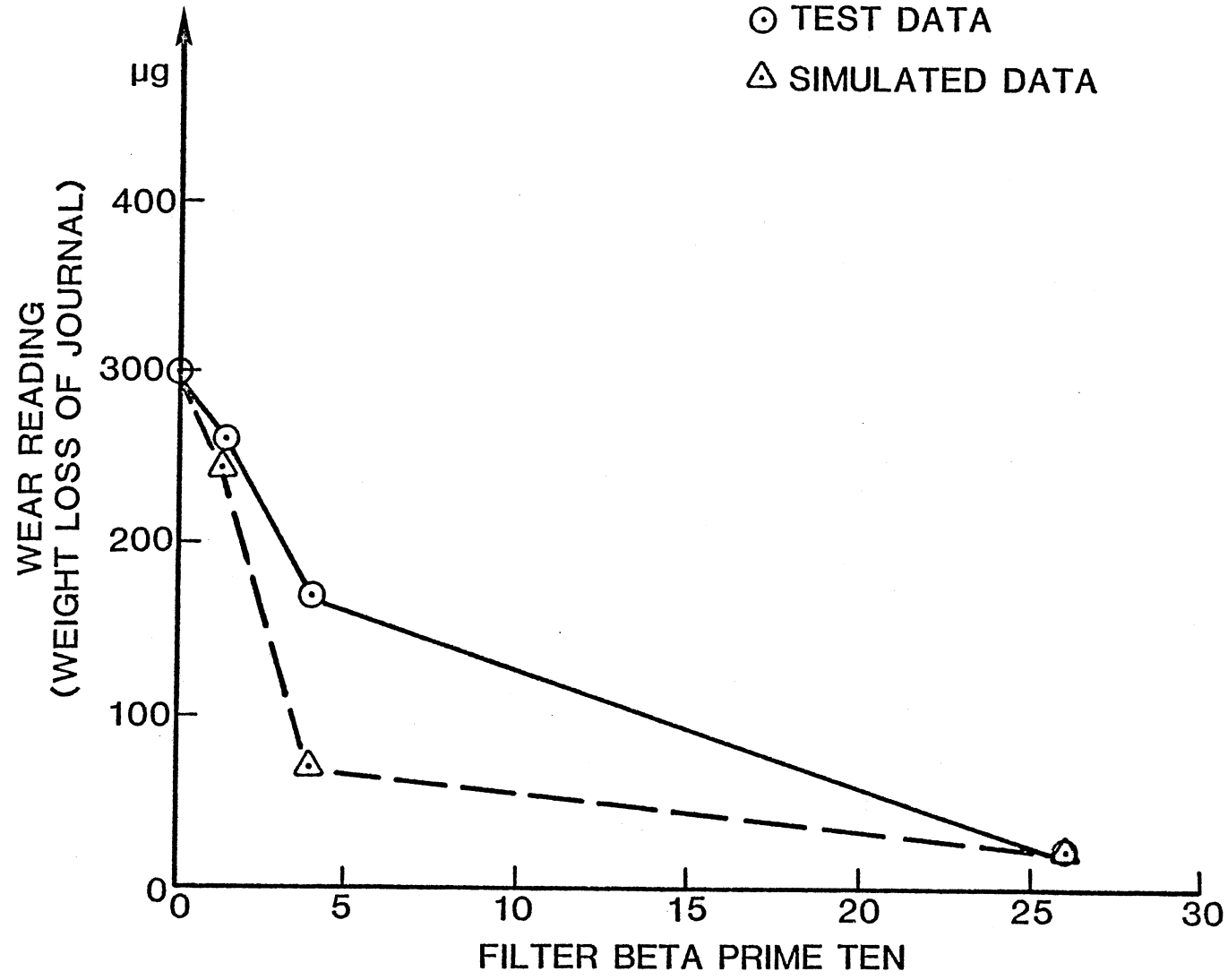

Figure 52. Tribo-Filtration Test Data with MIL-L-2104

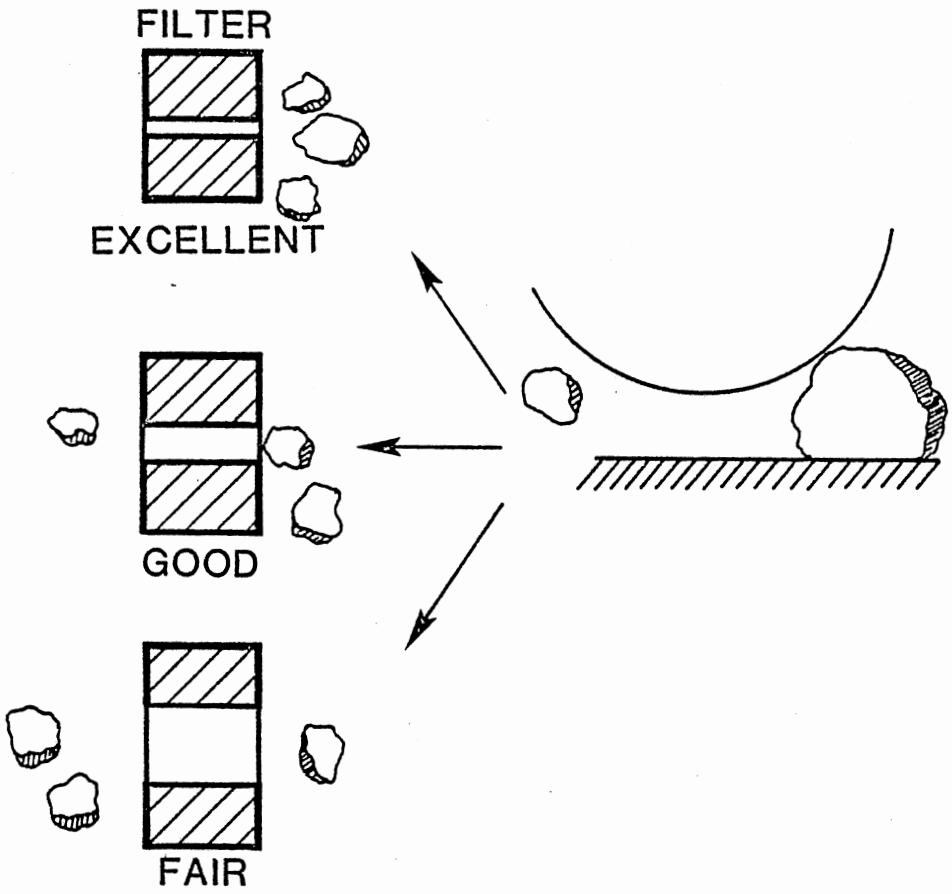

Figure 53. Particle Crush Mechanism in Tribo-Filtration Process

CHAPTER VII

APPLICATIONS AND EXTENSIONS OF THE RESEARCH

Contaminant Wear Control Through Filtration

The wear behavior of most lubrication systems normally depends on four distinguishing properties. They are filter performance (Beta), working fluid properties (Gamma), component material characteristic (Omega), and the entrained abrasive particle property (Zeta). All these parameters are also affected by environmental variables, for instance, temperature, pressure, flow rate, duty cycles, etc. Figure 54 illustrates the functional block diagram specifying the interference between each parameter. System tribo-filtration characteristics are essentially governed by these parameters.

The result of this research deals directly with Beta, Gamma, and Omega properties and only partially with Zeta. This section presents the application of the Beta Prime theory to control the tribological wear caused by the contaminants.

In practice, the designers and users of lubrication systems normally failed to answer questions such as: what level of cleanliness is required to protect a component from contaminant wear? and how to select a filter that meets the requirements? Answers to the above questions can not be

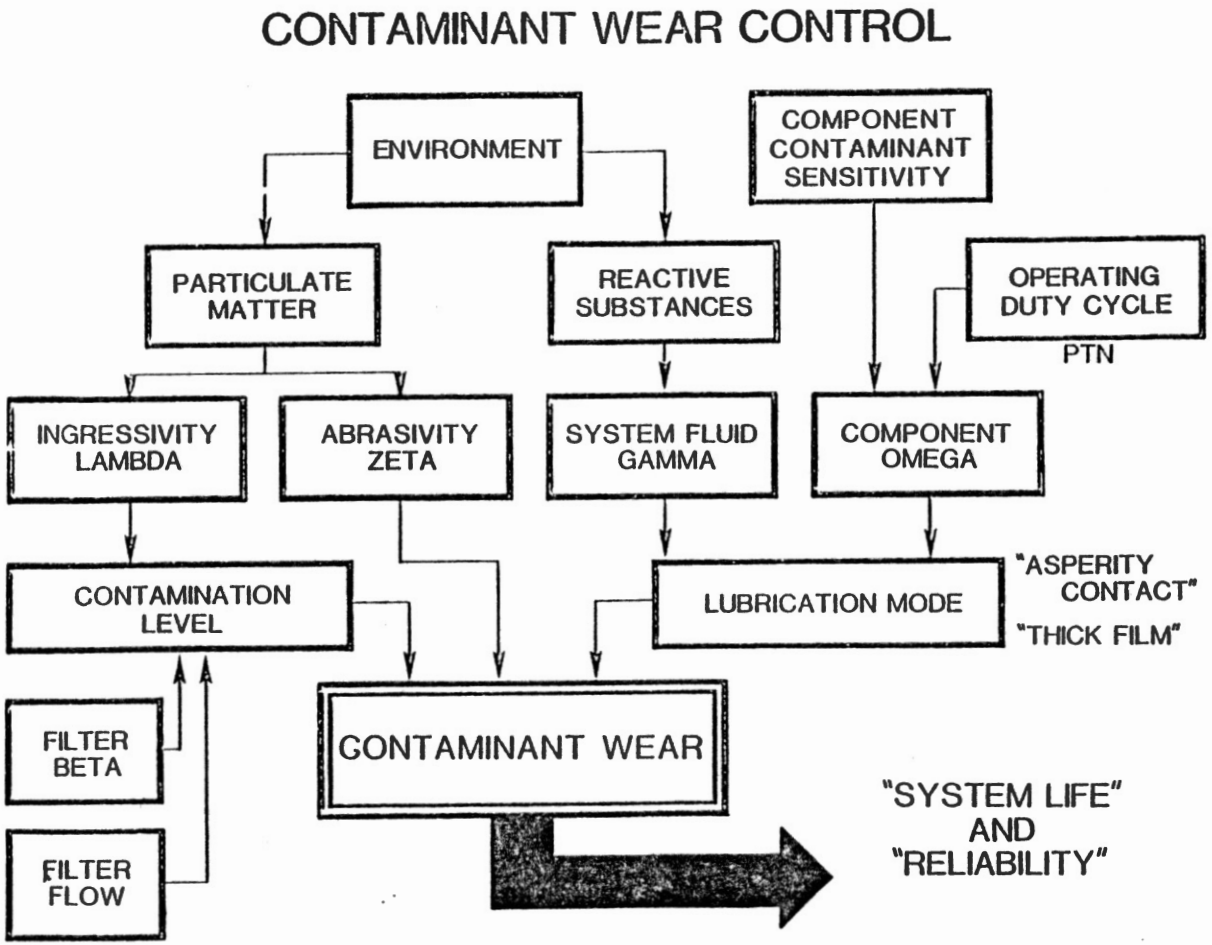

Figure 54. Contaminant Wear Control Chart

generally given due to a lack of technical knowledge. It is a practical question; however, it has deterred system designers from investigating it due to the lack of an effective filtration analysis technique and an adequate contaminant wear assessment method. The development of this study is intended to promote the state-of-the-art in tribo-filtration to practical applications.

The tribo-filtration model, Equation (3.48) developed in Chapter III and verified in Chapter VI stated that the particle concentration level and the minimum film thickness were two predominant parameters that governed the contaminant wear characteristic of a rotating element. Both the experimental results and the previous investigations also showed that particles with size less than the minimum film thickness were not significantly harmful to the critical element. Further, the wear increased as the particle concentration increased up to some critical point. Moreover, the particle concentration level is controlled by the filter used in the system. As a result, it is feasible, by using the proposed tribo-filtration theory, to select a filter to provide an environment that satisfies contaminant tolerance requirements or vice versa.

It is noted that the minimum oil film thickness can be obtained in terms of the Sommerfeld number and journal eccentricity ratio. Also, the Log-normal filter efficiency chart provides a graphical technique to correlate the Beta Prime with respect to each individual particle size with the reference Beta Prime value. Thus, it is conceived that a combination of the minimum film thickness chart and the log-normal filtration chart may enable the tribo-filtration theory to be applied to practical designs. Figure 55 shows the proposed tribo-filtration control chart. The following paragraphs present an example problem, and it is solved by the above

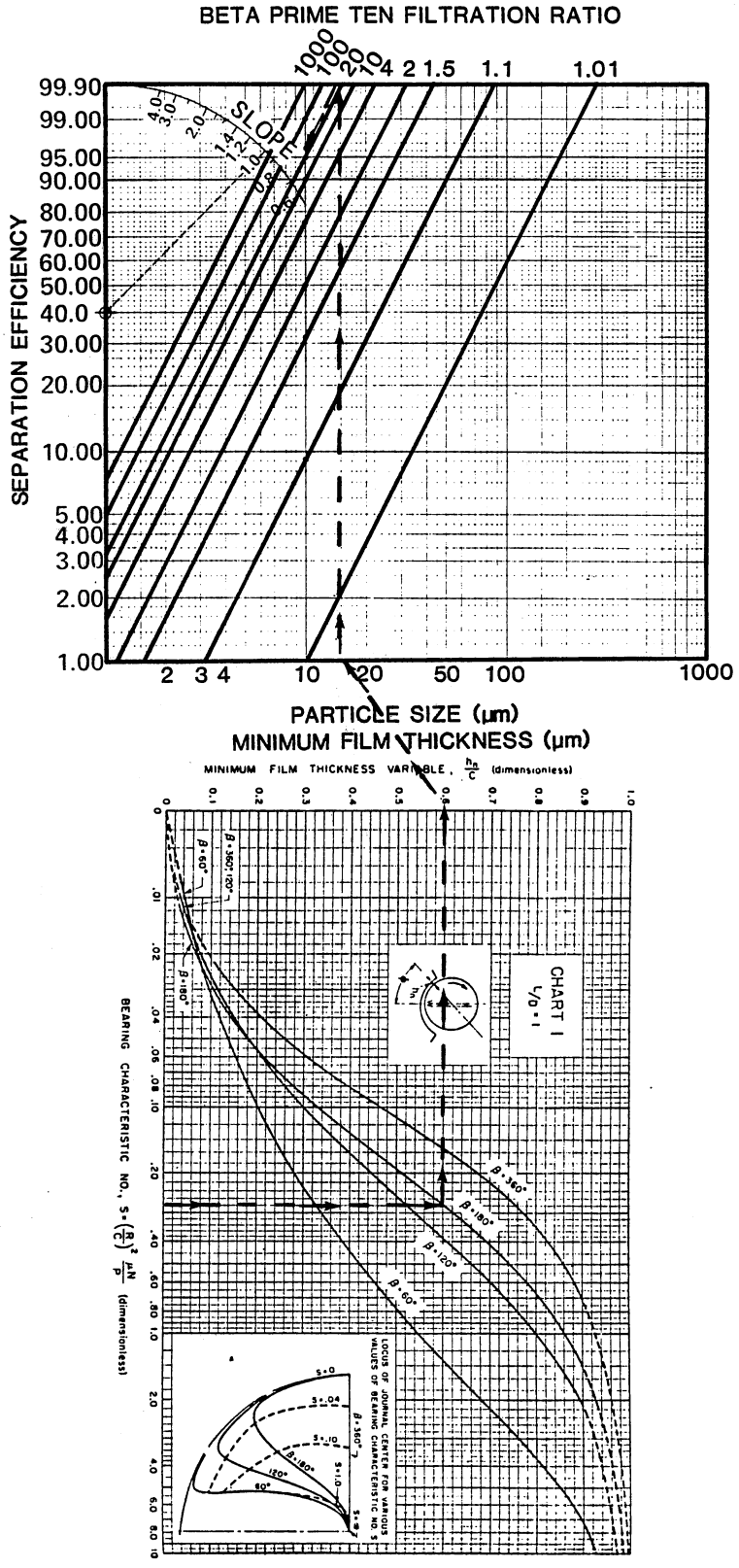

Figure 55. Tribo-Filtration Control Chart

described tribo-filtration rationale.

Suppose that a hydraulic pump bearing is designed to support an external load of 14,000 lbs. The bearing is a 180-degree partial journal bearing with a journal radius of 2 inches, the bearing length of 4 inches, and the radial clearance of 0.001 inches. The pump is working with mineral base oil MIL-H-5606 at 1800 rpm rotation speed. The operating temperature is 100-degree Farenheit. Assuming, in order to protect the pump from contaminant wear, it requires that 99.9 percent of the particles with a size greater than the minimum film thickness must be removed from the system. Therefore, the designers interest lies in specifying the performance of filters that meet the requirement. The Beta Prime ten value is normally given as the reference filtration ratio for a given filter. It frequently specifies the filter performance in terms of the Beta Prime ten value. This specification approach is adopted in the explanation of the filtration characteristic in the following example.

According to the given parameters the Sommerfeld number calculated is 0.2743. From Figure 55, it is found that the minimum film thickness is 0.59 times the radial clearance. This is equal to 15 micrometers. Then, the filtration chart shows that in order to remove 99.9 percent of particles with size greater than 15 micrometers, it requires a filter of Beta Prime ten of 25. Thus, the filter performance is specified.

Furthermore, if the operating condition changed, for example, the external load increased to 22,600 lbs, the filter used to protect the bearing from contaminant wear should be respecified to meet the new requirement. An external of 22,600 lbs results in a minimum film thickness of 12 micrometers. In this case, a filter of Beta Prime ten of 100 is required.

The above example demonstrates one of the applications of the results of this study. In addition to this application, the developed Beta Prime filtration system can effectively be used to evaluate the performance of a low flow, high beta filter. Furthermore, the developed thick film Gamma Wear test system can also be used to evaluate the anti-wear characteristic of fluid in hydrodynamic lubrication. Figure 56 illustrates the test results obtained from five different fluids. The wear behavior varies with different fluid. The significance of the application is obviously revealed.

Recommendation for Further Study

This research initiated the study of the tribo-filtration characteristic of a rotating element. This research provides valuable technical knowledge in the investigation of the properties of Beta, Gamma, Omega, Zeta as well as environmental factors. In order to promote the developed technology to complete the study of wear control in terms of Beta, Gamma, Omega and Zeta, the following recommendations are made:

1. The most obvious extension of the use of the Gamma machine is to include the tests of several different fluids, material combination of bearings, and different test dusts. Such comprehensive studies are deemed necessary to complete the wear control investigation.
2. In order to transfer the Gamma rating method into practical application, the use of a non-intrusive wear analysis technique, for example, the Ferrography technique is recommended. Currently, the direct measurement of the weight loss of the critical component is used.

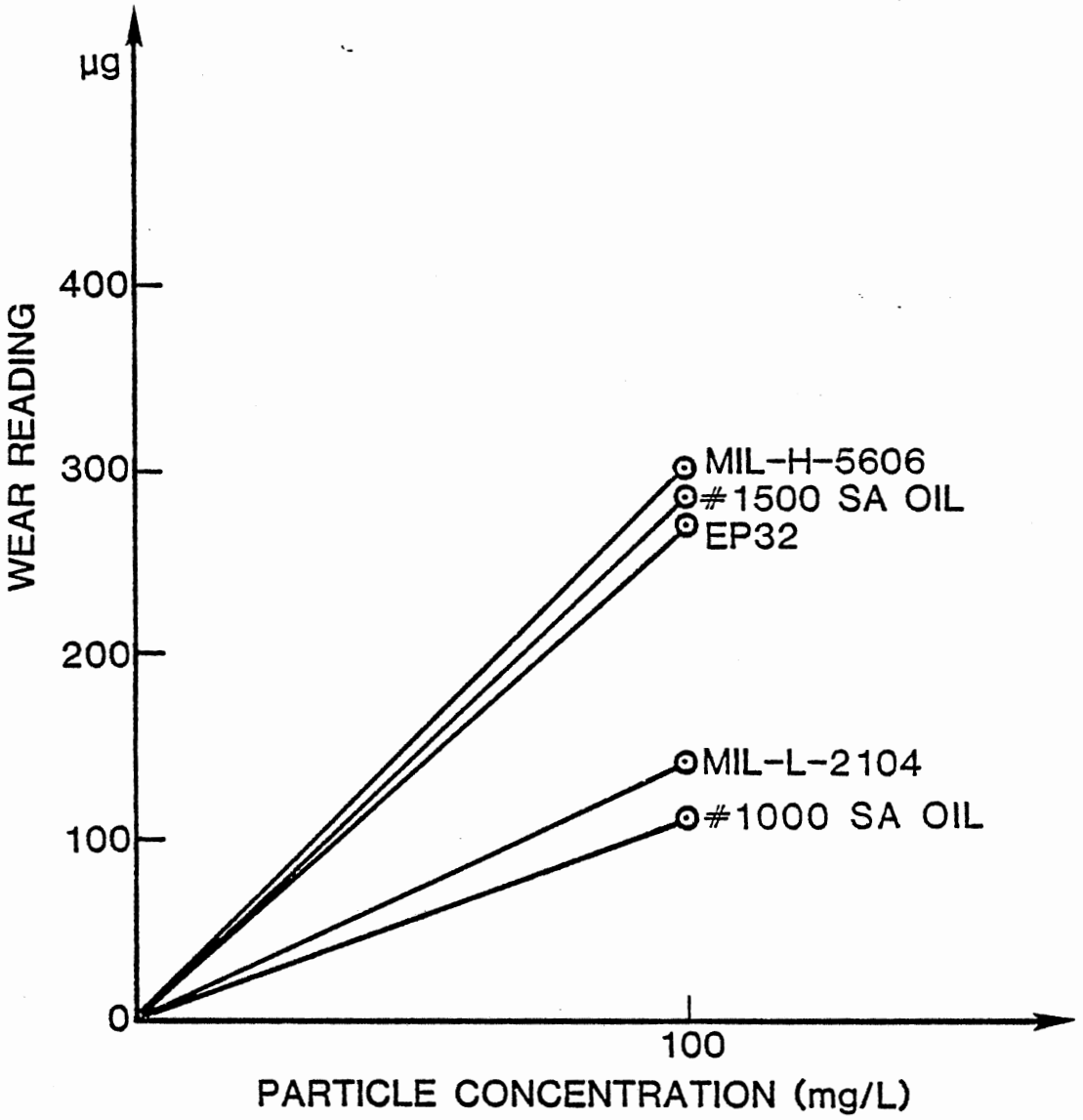

Figure 56. Gamma Wear Test Data with Different Fluids

3. As a result of the Gamma test, it was indicated that the minimum film thickness is a critical parameter affecting wear behavior. Thus, it is of interest to investigate the wear behavior by varying the film thickness.
4. Fatigue is the other failure mode in addition to the abrasion caused by the contaminant in the lubricant. It normally occurs in elasto-hydrodynamic lubrication condition and requires a considerable time (as compared to the abrasion) to fail the surface. This study did not cover the discussion of fatigue mechanism because the filtration theory proposed was based on the single injection concept. Further, the ACFTD lost its effectiveness of abrasion during short test period. These two factors inhibited the establishment of an ideal contamination condition to investigate fatigue effects. Although this topic was not discussed, it is recommended that the phenomena be investigated, along with the Beta system, which essentially includes the injection mechanism.
5. The Beta Prime filtration theory should be extended further to include the capacity pressure differential, flow rate and by-pass leakage factors. These are considered as important factors that may affect the performance and the service life of filters in practical application.
6. The extension, using the flat sheet medium as a test filter with the element type filter, is also recommended. The performance comparison between these two types of filters may provide valuable technical information for filter manufacturing application.
7. The concept of the Beta prime theory could also be extended to

investigate the performance of the water removal filter subject to the availability of an adequate water content measuring device.

CHAPTER VIII

SUMMARY AND CONCLUSIONS

Summary

This thesis investigates the problem of the tribological wear control of a rotating element through filtration. The overall objective of the study is to develop a contamination control theory for predicting the performance of a filter and its associated tribological wear degradation of rotating elements in a mechanical system.

Most rotating elements have a journal-form bearing and operate under hydrodynamic lubrication conditions. The external load imposed on the bearing is supported by the pressure generated due to the wedge action of the oil film formation. The lubrication condition is governed by the bearing characteristic number, the Sommerfeld number (which is a parametric group of the load pressure, rotation speed, fluid viscosity, and the geometric factors of the bearing).

In a hydrodynamic lubrication condition, the bearing surfaces are separated by the oil film and, therefore, no wear exists. Various bearing parameters can be investigated by solving the Reynolds equation, included in these parameters is the oil film thickness. If the entrained abrasive particles are of a size comparable to that of the minimum oil film thickness, the particle dramatically deteriorates the bearing surfaces.

The abrasive particles are part of a three-body cutting mechanism in a lubricated system. The particle embeds into the softer surface and

abrades the harder surface. With this in mind, the tribological wear model is derived based on both the cutting mechanism and the wedge indentation principle. The model is expressed in terms of the properties of lubricants, bearing material, and abrasive particles.

Filters are used in the lubrication system to remove harmful particles from the lubricant. No filter can completely filter out all the particles of the lubricant since there are flow passages in the filter to pass fluids. A multipass filtration theory, the Beta Prime, is developed to evaluate system filtration characteristic. The Beta Prime model is formulated in accordance with the concept of a draw down process. The filtration ratio is defined as the ratio of initial particle concentration of size greater than a given size to that downstream of the filter. The reference Beta Prime value is set as the filtration ratio obtained when the fluid has completed the first pass. The downstream particle concentration used to derive the filtration ratio is correlated by means of the least-square curve fitting method by using nine test data observed at the consequential operating points. Included in these nine data points is the initial concentration data point.

The tribo-filtration model is a result of the combination of both the wear model and the Beta Prime filtration model. The mathematical expression of the developed filtration model utilizes the standard ACFTD distribution (ISO 4402) as the contaminant concentration parameter and assumes a log-normal filter pore size distribution; although, the model is also generalized for other parameters.

The contaminants used in the development of the wear model and the filtration model are presumed to have the same material property and geometric characteristics as ACFTD. The particle shape is a square prism

in nature.

The wear model was validated by the Gamma machine which is a modification of the Gamma Falex Machine with the lower load capability and a partial bearing system. It is capable of establishing hydrodynamic lubrication conditions. The Beta Prime theory was verified by the draw down filter test stand which is specifically designed to test a low-flow, high beta filter. Finally, the tribo-filtration model was evaluated on the system which links the Gamma tester and the Beta Prime tester together.

Conclusions

From the research investigation described in the preceding Chapters, several noteworthy conclusions can be made. The major accomplishments and conclusions of this research are listed as follows:

1. A wear model was developed which emphasized the tribological interference between lubricant, abrasive particles, and the bearing surfaces of a rotating element. Classic hydrodynamic lubrication theory was reviewed and applied to formulate the three-body abrasion mechanism along with a cutting theory and a wedge indentation process.
2. A new multipass filtration theory, the Beta Prime, was developed based on a draw down process. The Beta Prime has a single figure of merit in evaluating the particle separation characteristic of an increasing family of low flow, high beta filters.
3. The tribo-filtration model signifies the effect of system filtration characteristics on wear control. It includes the concepts of lubrication, wear, and filtration theories.
4. Experimental activity was conducted to verify the developed wear

model by using a converted Gamma Falex machine. The results showed that the Gamma Falex machine was operated in an 'overload' condition. So much so that only boundary lubrication exists. No hydrodynamic lubrication was possible.

5. The Gamma machine is an improved version of the Gamma Falex machine. The loading mechanism was modified and the v-blocks were replaced by the 120-degree partial bearing with L/D of two. The modifications allow the establishment of hydrodynamic lubrication.
6. The wear index used in the Gamma system is the weight loss of the journal during a prescribed test time interval rather than the teeth advanced on the loading wheel. This is because abrasive wear behaves as a local cutting process instead of a surface adhesion. Thus, the Falex wear-monitoring principle is no longer applicable to the Gamma system.
7. Tests have been carried out to ensure the formation of the hydrodynamic lubrication according to the operating parameters specified by the bearing characterisitc number. No wear was observed under the prescribed load conditon.
8. ACFTD was introduced into the Gamma system. The abrasive wear was investigated both quantitatively and qualitatively. The test result indicated that for this bearing configuration, the wear rate is proportional to the injected particle concentration within a range from 0 to 200 milligrams per liter. The linear characteristic between particle concentration and wear rate validates the developed wear model.
9. The cause of a decreasing wear rate with the increasing particle

concentration after 200 mg/L is due to the pressure of each individual particle being lower than that required to indent the surface.

10. The qualitative examination of the journal bearing after the contamination test using an SEM shows that the ACFTD embedded on the bearing (brass) and cut the journal (steel). This confirms the proposed three-body cutting mechanism.
11. The results of the Beta Prime filtration tests showed that the better the particle separation performance a given filter has, the higher the Beta Prime value obtained.
12. The Beta Prime value can be obtained mathematically or graphically. The model has a linear characteristic on the Beta Prime graph.
13. The experimental tests with the use of the mineral base fluid MIL-L-2104 revealed a lower wear rate and a worse filtration characteristic than those using MIL-H-5606.
14. The results of the tribo-filtration tests revealed that the filtration characteristic can significantly affect the tribological wear behavior of a rotating element. The higher Beta Prime filter protects the system from wear more adequately.
15. The use of the Monte Carlo technique to simulate the tribo-filtration model has also been discussed. The simulation results showed the same tendency as the proposed tribo-filtration model.

BIBLIOGRAPHY

(1) Suh, N. P. and N. Saka. Fundamentals of Tribology. Cambridge: the Massachusetts Institute of Technology, 1980.

(2) Dowson, D. History of Tribology. London: Longman Group Limited, 1979.

(3) Szeri, A. Z. Tribology: Friction, Lubrication and Wear. New York: Hemisphere Publishing Co., 1980.

(4) Petrov, N. "Friction in Machine and the Effect of the Lubrication." Engineering Journal, 1 (1883), 1.

(5) Tower, B. "First Report on Friction Experiments." Proceedings Institution of Mechanical Engineers, 34 (1883), 10.

(6) Reynolds, O. "On the Theory of Lubrication and its Application to Mr. Beauchamp Tower's Experiment, Including and Experimental Determination of the Viscosity of Olive Oil." Phil. Trans. Royal Society, 177 (1886), 1.

(7) Czichos, H. Tribology, A System Approach to the Science and Technology of Friction, Lubrication and Wear. New York: Elsevier Scientific Publishing Co., 1978.

(8) Moore, D. F. Principles and Applications of Tribology. New York: Pergamon Press, 1975.

(9) Stribeck, R. "Die Wasentlichen Eigenschaften der Gleit - Und Rollenlager." VDI-Zeitschrift, 46 (1902), 1341-1342.

(10) Sommerfeld, A. "Zur Hydrodynamischen Theoric der Schmiermittelreibung." Z. Math. Phys., 50 (1904), 97.

(11) Lubrication. New York: Texaco Inc., 1980.

(12) Neale, M. J. Tribology Handbook. London: Newnes Butterworths, 1973.

(13) Cameron, A. The Principles of Lubrication. New York: John Wiley and Sons Inc., 1966.

(14) Raimondi, A. A. and J. Boyd. "A Solution for the Finite Journal Bearings and its Application to Analysis and Design." Transactions of the American Society of Lubrication Engineers, 1 (1958), 159-209.

(15) Peterson, M. B. "Classification of Wear Processes." Wear Control Handbook of the ASME, (1950), 9-15.

(16) Sarkar, A. D. Wear of Metals. New York: Pergamon Press, 1976.

(17) Kragelski, I. V. and E. A. Marchenko. "Wear of Machine Components." Journal of Lubrication Technology, 104 (January, 1982), 1-8.

(18) Moore, M. A. "A Review of Two-body Abrasive Wear." Wear, 28 (1974), 59-88.

(19) Sin, H., et. al. "Abrasive Wear Mechanism and the Grit Size Effect." Wear, 55 (1979), 163-190.

(20) Miller, N. E. "Three-body Abrasive Wear with Small Size Diamond Abrasives." Wear, 58 (1980), 249-259.

(21) Toporov, G. V. "The Influence of Structure on the Abrasive Wear of Cast Iron." Friction and Wear in Machinery, 12 (1958), 39-59.

(22) Rabinowicz, E., L. A. Dunn and D. G. Russell. "A Study of Abrasive Wear Under Three-body Conditions." Wear, 4 (1961), 345-355.

(23) Khrushchov, M. M. and M. A. Rabichen. "Investigation of the Resistance of Metal to Abrasion as Influenced by the Hardness of the Abrasive." Friction and Wear in Machinery, 11 (1956), 19-26.

(24) Murray, M. J. "Abrasive Wear Mechanisms in Steels." Journal of Lubrication Technology, 104 (January, 1982), 9-16.

(25) Rabinowicz, E. and A. Mutis. "Effect of Abrasive Particle Size on Wear." Wear, 8 (1965), 381-390.

(26) Inoue, R. Surface Contact Wear and Abrasive Wear in Lubricated Slinding Mechanism. (Unpub. Ph.D. Dissertation, Oklahoma State University, 1983.)

(27) Hong, I. T. The Effect of Particulate Contaminants on the Wear Rate of Sliding Mechanisms. Final Report, Contract No. Navy 68335-79-C-1171, Washington, D. C. : Command Air Sysytem, 1981.

(28) Larsen-Badse, J. "Influence of Grit Diameter and Speciment Size on Wear During Sliding Abrasion." Wear, 12 (1956), 35-53.

(29) Tessman, R. K. Non-Intrusive Analysis of Contaminant Wear in Gear Pump Through Ferrography. (Unpub. Ph.D. Dissertation, Oklahoma State University, 1977.)

(30) Wear in Fluid Power Systems. Final Report, Contract No. N00010-75-C-1157, Arlington, VA: Office of Naval Research, 1977.

(31) Tao, F. F., et. al. "An Experimental Study of the Wear Caused by Loose Abrasive Particles in Oils." Trans. of the ASLE, 13 (1969), 129-178.

(32) Roach, A. E. "Performance of Oil-Film Bearing with Abrasive Containing Lubrication." Trans. of the ASME, 73 (1951), 677-686.

(33) Broeder, J. J. and J. W. Heijnekamp. "Abrasive Wear of Journal Bearings by Particles in the Oil." Proc. Inst. Mechanical Engineers, 180 (1965), 21-31.

(34) Ronen, A., S. Makein and K. Loeng. "Wear of Dynamically Loaded Hydrodynamic Bearing by Contaminant Particles." Trans. of the ASME, 102 (1980), 452-458.

(35) Tallian, T. E. "Prediction of Rolling Contact Fatigue Life in Contaminated Lubricant: Part I - Mathematical Model." Journal of Lubrication Technology, (April, 1956), 251-257.

(36) Endo, K., Y. Fukuda and T. Kudo. "Wear of Steel in the Lubricating Oil Containing Abrasive Particles." Bulletin of Japanese Society of Mechancal Engineers, 9 (1966), 758-792.

(37) Fitch, E. C. An Encyclopedia of Fluid Contamination Control. Washigton, D. C. : Hemisphere Publishing Co., 1980.

(38) Tucker, R. H. The Development and Verification of Theoretical Models for the Performance of Wire Cloth Filter Media. (Unpub. Ph.D. Dissertation, Oklahoam State University, 1966.)

(39) Rosenfeld, L. "The Removal of Contaminant from Automotive Lubricating Oil -- Problems and Propects." Filtration and Separation, (March/April, 1969), 150-154.

(40) Stuntz, R. M. The Sieving Mechanism in Hydraulic Filtration. (Unpub. Ph.D. Dissertation, Oklahoma State University, 1971.)

(41) English, J. E. "A New Approach to the Theoretical Treament of the Mechanics of Sieving and Screening." Filtration and Separation , (March/April, 1974), 195-203.

(42) Payatakes, A. C., C. Tien and R. M. Turian "Trajectory Calculation of Particle Deposition in Deep-Bed Filtration." Journal of the American Institute of Chemical Engineers, 20 (1974), 889-900.

(43) Tichy, J. A. "A Model of Lubrication Filtration." Journal of Lubrication Technology, 103 (January, 1981), 81-89.

(44) Bensch, L. E. The Influence of Electrostatic Charge on the Filtration of Hydraulic Fluids by Fibrous Filters. (Unpub. Ph.D. Dissertation, Oklahoma State University, 1977.)

(45) Iwanaga, M. Contaminant Service Life and Cost Of Hydraulic System. (Unpub. Ph.D. Dissertation, Oklahoma State University, 1980.)

(46) Kroeker, B. A. "Air Cleaner Fine Test Dust, Kirnbauer's Counts vs. Weight Distribution." (Unpub. paper presented at the Society of Automobile Engineering A-6 Fall Meeting, Los Angeles, Oct. 13-17, 1980.)

(47) Oxley, D. C. B. "Mechanics of Metal Cutting." International Journal of Machine Tool Design and Research, 1 (1961), 89-97.

(48) Rubenstein, C "A Simple Theory of Orthogonal Cutting." International Journal of Machine Tool Design and Research, 5 (1965), 123-155.

(49) Sweeney, G. "The Consistency of Experimental Observation with a Model for the Metal Cutting." International Journal of Machine Tool Design and Research, 9 (1969), 309-391.

(50) Johson, W. and P. B. Mellor. Engineering Plasticity. London: Van Norstrand Reinhold Co., 1973.

(51) Grunzweig, J., et. al. "Calcualtions and Measurements on Wedge Indentation." Journal of Mechanics and Physics of Solids, 2 (1954), 81-86.

(52) Carter, A. D. S. Mechanical Reliability. New York: John Wiley and Sons Inc., 1972.

(53) Bensch, L. E. "Contamination Control." Basic Fluid Power Research Program, Stillwater, Oklahoma: Fluid Power Research Center, Oklahoma State University, (July, 1970), 10-16.

(54) Bensch, L. E. "An Investigation of the Variance of AC Test Dust." (Unpub. paper presented at the Fluid Power Research Conference, Stillwater, October 5-7, 1976.)

(55) Johnston, P. R. and R. Swanson. "A Correlation Between the Results of Different Instruments Used to Determine the Particle Size Diatribution in AC Fine Test Dust." Power Technology, 32 (1982), 119-124.

(56) Ewbank, W. J. "Factors Affecting the Efficiency of Absorption Oil Filtration at Constant Flow Rate." Filtration and Separation, (September/October, 1969), 576-583.

APPENDIX

TRIBO-FILTRATION USING MONTE CARLO SIMULATION

The filtration mechanism has been widely studied during the past three decades. Nevertheless, due to the complicated filter structure and the inherently random characteristics of particles, the formulated filtration model normally incorporated equations which could not be solved analytically. Until the use of the computer in research applications became popular, there was no means for using these models to explain system filtration characteristics satisfactorily.

In computer simulation, the numerical integration method and Monte Carlo simulation technique are usually involved in solving stochastic problems. Filtration is a typical stochastic process. Hence, these techniques have been used in analyzing filtration problems. Considering the programming simplicity, the Monte Carlo method is the most straightforward approach which can be employed. This appendix is intended to apply the Monte Carlo method to simualte the tribo-filtration process.

The Monte Carlo method is generally defined as representing the solution of a problem as a parameter of a hypothetical population, and using a random sequence of numbers to construct a sample of the population from which statistical estimates of the parameter can be obtained. Very often, in computer simulation practice, a procedure is required to generated random variables to satisfy certain conditions.

From the standpoint of the tribo-filtration process, several parametric groups can be treated as random variables to achieve the Monte Carlo simulation. These include filter pore size distribution, the contaminant particle size distribution, the particle motion characteristics, and the point where a given particle enters the journal bearing.

According to the discussions in the preceding chapters, it is reasonable to assume that the filter pore size distribution has a Log-normal shape. It is controlled by the mean pore size and the standard deviation of size. A uniform distribution is the best function to describe the particle motion attitude. In regards to the contaminant (ACFTD) particle size distribution, an emperical model is required since there is no commonly used standard function to represent the prescribed particle size distribution.

Mathematically, the uniform distribution on the interval (0,1) is the "seed" of other distributions. Normally, once the uniform random number generator is established, the other distributions can be derived and generated. The detailed discussion of the mathematical manipulation of generating a specific function is beyond the scope of this research; however, most of them can be found in the International Mathematics and Statistics Library (IMSL) package.

Figure 57 schematically illustrates the tribo-filtration process. It is noted that a square prism shape contaminant is randomly "generated" according to the ACFTD particle size distribution. The particle is randomly oriented in the space. In addition, one of the filter "pores" is then generated with a random size. The size of the pore is compared with the longest projected length obtained from ACFTD orientation. The mechanical sieving mechanism is applied to determine particle capture. Thus,

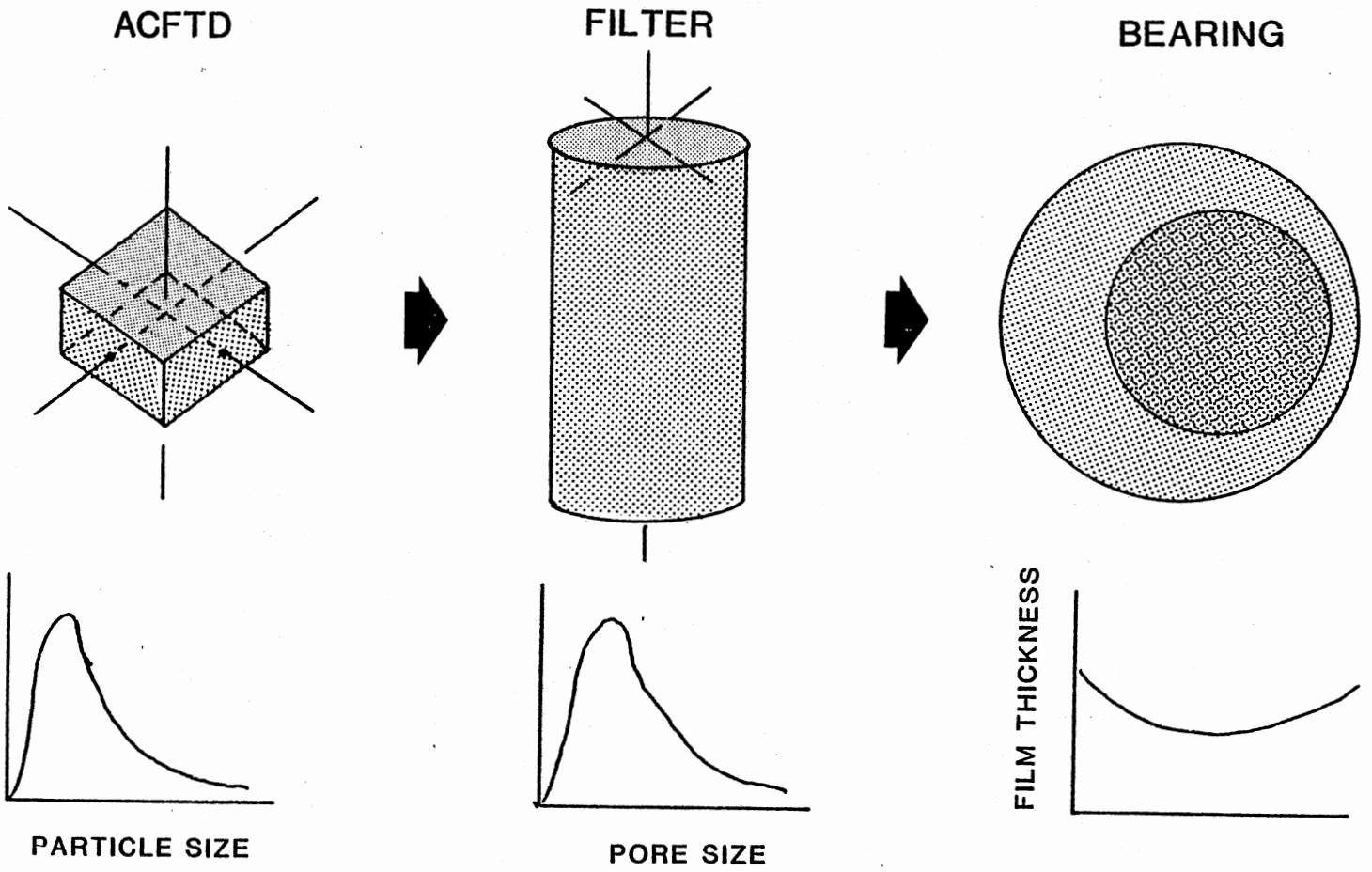

Figure 57. The Tribo-Filtration Process

if the particle projected size is larger than the filter pore size, the particle is caught, otherwise it passes through the filter. An escaped particle moves into the journal bearing and its size is compared with the inlet film thickness to determine the possibility of its reaching the critical bearing surfaces. If the particle size is larger than the minimum film thickness and less than the inlet film thickness, then wear occurs. Thus, it is feasible to simulate the tribo-filtration process by repeating this procedure. Figure 58 illustrates the flow chart for achieving such a simulation.

It is of significance to determine an adequate sampling size before conducting the tribo-filtration simulation. For this purpose, six sample sizes were tested. They were 500, 1000, 2000, 5000 and 10000, respectively. The corresponding filtration simulation results were tabulated in Table XVIII. It is seen that the Beta Prime filtration ratio raeches a stable value if the sampling size is greater than 5000. Consequently, the sample size of 5000 is used throughout the tribo-filtraion simulation in this study.

The following is an example problem to demonstrate the use of Monte Carlo method in the simulation of the tribo-filtration process. Assume that the filter has a mean pore size of 20 micrometers with a standard deviation of 3 micrometers. In addition, the bearing has an eccentricity of 0.5 and a radial clearance of 0.001 inches. This provides a minimum film thickness of 12.7 micrometers. The process was simulated sequentially for five passes, and randomly generated 5000 particles during each pass for a total of 25,000 particles. The simulation result showed that 421 of these 25,000 particles did damage to the bearing surface. If, however,

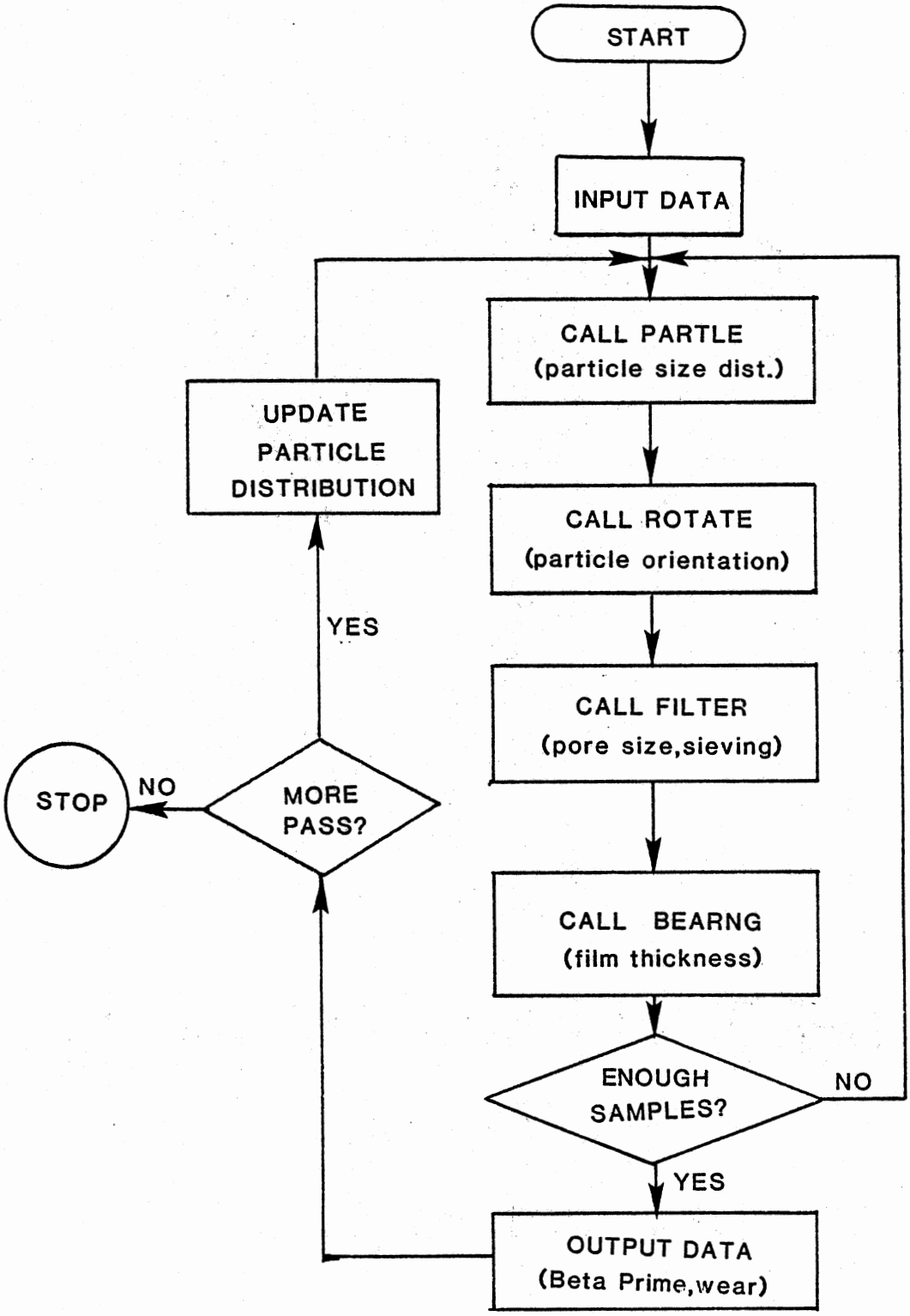

Figure 58. Monte Carlo Simulation Flow Chart

TABLE XVIII

FILTRATION SIMULATION RESULTS WITH DIFFERENT SAMPLE SIZES

Sample Size	β_5'	β_8'	β_{10}'	β_{12}'
500	1.39	2.09	3.12	∞
1000	1.42	2.35	3.70	28.2
2000	1.48	2.54	3.96	9.92
5000	1.45	2.44	4.03	8.63
10000	1.45	2.43	3.85	7.72

the filter mean pore size was reduced to 10 micrometers, only one of the 25,000 particles did damage. It is of significance that the simulated Beta Prime ten is 1.54 and 10000 for filters with mean pore size of 20 and 10 micrometers, respectively.

The simulation results confirm the validity of the proposed tribo-filtration model which indicates that a higher Beta Prime filter reduces the wear damage to bearing surfaces.

2

VITA

Ing-Tsann Hong

Candidate for the Degree of

Doctor of Philosophy

Thesis: EFFECT OF SYSTEM FILTRATION CHARACTERISTICS ON TRIBOLOGICAL WEAR OF ROTATING ELEMENTS

Major Field: Mechanical Engineering

Biographical:

Personal Data: Born in Taichung, Taiwan, March 7, 1952, the son of Mr. and Mrs. Y. S. Hong; married in Taiwan, July 19, 1980, to Li-Jane Lin. Beget Andrew Lynn Hong, November 10, 1981.

Education: Graduated from Taichung First High School, Taichung, Taiwan, in June, 1970; received the Bachelor of Science degree from National Central University in 1974 with a major in physics; received the Master of Science degree from Oklahoma State University in 1980, with a major in Mechanical Engineering; completed requirements for the Doctor of Philosophy degree at Oklahoma State University in December, 1983.

Professional Experience: Mechanical Engineer, Kung Hwa Arsenal, 1974-1976; Mechanical Quality Control Supervisor, TIMEX Watch Company Taiwan Branch, 1976-1977; Research Assistant, Chung-Shan Institute of Science and Technology, 1977-1979; Research Assistant, Fluid Power Research Center, 1979-1980; Research Engineer, Fluid Power Research Center, 1980-Present.

Professional and Academic Affiliations: American Society of Mechanical Engineers, National Society of Professional Engineers; American Committee Program of the Filtration Society.